CRANFIELD UNIVERSITY

School of Energy, Environment & Agrifood
MSc by Research

Academic Year 2016 - 17

Carly Jane Smith

Investigation of Transient Interactions in Centrifugal Pumps

Supervisor: Dr Joao Amaral Teixeira
May 2017

ABSTRACT

The quest for greater pump efficiency and improved reliability has focused research topics in the understanding of pump hydraulic and dynamic behaviours.

On-Design pump performance has been optimised utilising modern design strategies incorporating Computational Fluid Dynamics technology to predict and simulate the fluid flow in a pump.

The fluid conditions within the arrangement of an impeller and collector present a complex unsteady flow phenomenon, which give rise to fluid structure interaction. Periodic hydraulic excitation forces are generated as a consequence. The interaction forces increase as the flow recirculation grows; the flow becomes less uniform at the impeller periphery. Thus, the highest magnitude of forces is observed at low flow and high flow operating conditions. They are impacted onto the rotor and transmitted to the bearing housing, although the forces are not quantitatively known.

Lateral analysis of a pump rotor can demonstrate the rotor will not traverse or operate within a region of a critical speed, however, bearing housing vibration can be excessive and outside acceptable limits when operating at part load.

The rationale of the project was therefore to employ a numerical modelling technique to capture hydraulically induced vibration caused by the interaction of the rotor and stator. A series of transient numerical analyses were carried out to investigate the unsteady fluctuating pressure field within a single stage pump for five operating conditions. The hydraulic excitation forces were captured and incorporated into a rotordynamic model where the corresponding displacement vibration were evaluated. It was shown that the highest estimated displacement vibration was at the low flow operating condition and at the cutwater region. An experimental campaign of the single stage pump validated the unsteady pressure fluctuations within an acceptable margin of two percent for nominal flow and five percent for low flow operating point. Greater variations were found when comparing the numerical and experimental approximations to the displacement vibration.

Keywords:

Vibration, Computational Fluid Dynamics, Rotor-stator Interaction, Rotordynamics

ACKNOWLEDGEMENTS

I would like to thank my supervisor Dr Joao Amaral Texieira for his continued support throughout the research program.

I would like to express my gratitude to my mother and husband who have made part time research a possibility.

I would especially like to thank SPXFLOW for the sponsorship of this research programme and to Michael Homer for his mentorship.

TABLE OF CONTENTS

LIST OF FIGURES

LIST OF TABLES

LIST OF EQUATIONS

LIST OF ABBREVIATIONS

BEP	Best Efficiency Point
Q_n	Relative Flowrate: flowrate over nominal flow
BPF	Blade Passing Frequency
RMS	Root Mean Square
CFD	Computational Fluid Dynamics

1 Introduction

The sponsor of this research programme is SPXFLOW – Clydeunion pumps. The company provides an array of pumping technologies to the global market; the brand name represents 140 years of pump manufacturing heritage. Clydeunion pumps forms part of the SPX power and energy sector, the principal business market being oil and gas. Although the company specialises in the oil and gas application the capability does not stop there, mining, industrial, marine, nuclear are all established growing markets.

The performance and the application of centrifugal pumps are adaptable. The optimum efficiency is achieved by operating at a specific point, known as the best efficiency point BEP. It is desirable for a pumps duty conditions to coincide with BEP, however this is not always practical. In most cases duty conditions change to meet system demand, the pump performance can be modified to suit the new requirements, by means of a variable speed drive and control valves. A pump must therefore be capable of operating satisfactorily for a range of operating conditions.

In recent years the focus in the oil and gas industry has been towards enhancing productivity and reduced energy consumption. Refineries face constant challenges to remain cost effective and to meet strict environmental and safety standards. Machine operating efficiency is therefore increasingly more significant to end users.

Pump integrity is a key factor to end users and original equipment manufacturers. Machine failure is commonly caused by excessive levels of dynamic loading. The advancement of vibration monitoring equipment and predictive maintenance campaigns have prevented catastrophic failures by setting alarm and trip levels along with capturing a machines condition. The vibration is assessed at the bearing housing and is detected using accelerometers or velocity transducers. Rotor vibrations are commonly within acceptable limits however the bearing housing vibrations are occasionally excessive.

The quest for high efficiencies and low vibration is challenging as they are often associated as fundamental trade-offs. The internal clearances between the pump rotating and stationary parts are directly related to the efficiency a pump can achieve and the hydraulic vibration potential that will arise. The hydraulically induced vibration is chiefly responsible for reduced pump integrity. As the impeller vane passes the volute cutwater a destabilizing force is generated as the transient changes in pressure in the clearance result in dynamic forces and moments providing excitation.

Research efforts exploring the vane pass pulsation have led to sophisticated guidelines and recommendations being defined. Despite these investigations, expedient prediction methods of amplitudes of pressure pulsations are still absent today.

Furthermore, while the transfer mechanism of the hydraulic excitation is not entirely understood, it is accepted that a resultant vibration from the vane pass pressure pulsations is transmitted via the shaft to the bearing housing. However, this is not quantitatively known.

Mechanical and hydraulic forces are impacted onto the pump rotating element. The forces a rotor is subject to are steady and unsteady in nature. The steady forces are classified as mechanical in origin such as rotor weight and imbalance. Unsteady forces are generally hydraulic in origin. They are typically three-dimensional with major contributions in the radial and axial directions as the fluid flow in the impeller turns within the passageway, leading to an uneven pressure distribution at the impeller outlet. To estimate the radial load, two empirical methods exist given by Stepanoff and Hydraulic Institute, which are based on experimental data. The estimated radial load varies depending on which method is applied, providing little confidence in the accuracy of the prediction. San Andres (2006) concluded both methods are poor at predicting the radial load, as discrepancies in the load direction, as well as magnitude, are shown.

It is well understood the radial load is most detrimental to support bearings when operating at low flow or high flow regimes, where the bearings become more or less loaded as the hydraulic load changes.

The transient forces, either mechanical or hydraulic in origin, are always present independently of the rotor vibration, Gulich (2008). Mechanical transient forces can be due to mechanical unbalance. Hydraulic unsteady forces can in turn be either cyclical or random in nature. Stochastic forces are due to flow separation, recirculation and turbulence. Cyclic forces are generated by the interactions of the impeller with stationary components like the cutwater, diffuser blades and volutes and possibly by other events such as rotating stall and unbalanced blade forces.

1.1 Aims and Objectives of the Present Study

The aim of this project focuses on the quantification of the hydraulic interaction behaviour found within centrifugal pumps. The investigation seeks to describe the extent hydraulic forces that are generated by the rotor/stator interaction, are transmitted via the rotating element, to reaction forces at the bearing housings. A model representing the fluid interaction forces and rotordynamic elements is explored.

The objectives of this research provide a contribution to the following areas:

1. **Quantification of hydraulic excitation forces in a centrifugal pump** - The advancements in numerical modelling of unsteady flows has led to greater visualisation of the fluid behaviour through a centrifugal pump. Computational fluid dynamics (CFD) is proven to be a useful tool to simulate the fluid flow through a centrifugal pump and to predict the pump performance. To represent the interaction between the impeller and volute, a fully transient analysis is required to calculate the time dependent

terms in the equations. In order to capture the hydrodynamic excitation an entire pump model is required however for the present study a simplified model is employed neglecting leakage paths.

2. **Rotordynamic modelling of a pump rotor incorporating hydraulic excitation forces** - It is understood that the hydraulic excitation forces cause a mechanical reaction as a result. It is the aim of this project to go beyond the consideration of the hydraulic excitation forces within the pump and to account for the vibration these instabilities will cause and to the extend the forces result in excessive vibration at the bearing housing. To this end the hydraulic excitation forces extracted from CFD analysis are incorporated into a rotordynamic model.

3. **Hydraulically induced vibration at part load** – Operating a pump away from the BEP provides risk excessive vibration will occur. Advancing the characterisation of the transient fluid effects and resulting rotor response occurring at “off design” would lead to an improvement in reliability.

1.2 Structure of the Thesis

Following this introductory chapter and outline of the aims and objectives, Chapter 2 presents a background to pump fundamentals, vibration analysis and rotordynamics.

Chapter 3 presents a literature survey of published work relevant to the research themes. The review discusses principally the characterisation of the fluid flow through a centrifugal pump, rotor stator interaction and pump rotordynamics.

Chapter 4 presents a brief introduction to the commercial CFD package used for the numerical investigation and the appropriate theory to CFD is provided. Thereafter a numerical model of the single stage overhung pump at nominal flow is presented. Although a single stage pump configuration is not known for

hydraulically induced vibration, it has been chosen as it is a relatively simple model combined with the availability of a test pump, provided by the sponsoring company to carry out experimental testing for the purpose of validation.

Chapter 5 presents the experimental test campaign of the single stage pump. The series of tests focus on capturing the pressure fluctuations caused by rotor stator interaction.

Chapter 6 presents a numerical investigation into the transient effects within a single stage pump. The flow characteristics are discussed and method for modelling rotor stator interaction forces in a rotordynamic model is explored.

Chapter 7 discusses the results obtained and starts with a comparison between the numerical and experimental results followed by a review of the robustness of the numerical method explored in chapter 6.

Chapter 8 concludes with a summary of the research conducted and recommendations for further work is discussed.

2 Background

This chapter is written to provide an induction to pump fundamentals and to praise readers not conversant with the terminology and physics of centrifugal pumps employed in this study. The chapter is divided into three sections, pump characteristics, pump vibration and pump rotordynamics.

2.1 Introduction

Centrifugal pumps are essentially the most adaptable in performance and application in comparison to all other rotating fluid machines. At design conditions they can achieve up to and beyond 90% efficiency, although this is dependent on application. It is not always feasible to operate at design conditions therefore it is a necessity for the operating range of centrifugal pumps to be flexible. A pump must be capable of operating satisfactorily within the stated operating range. In many applications the operating conditions change, such as incoming flow, system demand and reservoir levels. By means of a variable speed drive or a discharge control valve the pump can be modified to suit system requirements. Along with operating range other performance parameters which are required to have an adaptable range are pumping fluid, temperature and pressure. In order for pump manufacturers to achieve such varying operating parameters it is essential to fully understand the fluid flow within a centrifugal pump. This has been a keen area of research with numerous experimental investigations and in recent times advancement in Computational Fluid Dynamics (CFD) technology has sparked interest in numerical investigations. CFD allows one to simulate and predict the fluid flow within a centrifugal pump. An advantage in CFD investigations is the reduction in time and construction costs when compared with experimental testing. Therefore, CFD is used in industry as a practical tool as well as a research method.

CFD simulations and analyses are extensively used in the pumping industry in order to further the understanding of the fluid flow through a pump. Numerical methods are becoming indispensable tools in the development of hydraulic components. Previous to CFD tools it has been down to the ability of the hydraulics engineer to have a mental picture of the fluid flow through a pump. At optimization stages of a new impeller, diffuser or volute, CFD allows design modifications to be evaluated without the need to manufacture and test. This process of combining CFD analyses along with historic test data then enables the designer to proceed towards an optimum design solution. This type of development process can be incorporated without the necessity for expensive computer processing. Quite complex hydraulic components may be optimised with minimal effort.

2.2 Centrifugal Pump Characteristics

The purpose of a centrifugal pump is to raise the specified volume flow to a specified pressure level. This is accomplished using a centrifugal force from liquid rotation induced by an impeller, which is enclosed within a casing. The impeller is mounted on a shaft and is coupled to a motor. The pump absorbs the transmitted motor power and converts it to the kinetic energy of the pumping fluid. The energy transfer is a hydrodynamic process as the pressure and energy differences are dependent on the rotational speed of the shaft. The energy transfer is delivered to the pumpage through changes in velocity as the fluid flows through the impeller. The flow exiting the impeller periphery is at a higher velocity creating a rise in static pressure. This is fairly complex due to the flow following a curved path and is therefore associated to pressure gradients, which provides the necessary centripetal acceleration. The flow is then decelerated upon exit via a volute or diffuser to utilise the greatest element of kinetic energy in order to increase static pressure. The casing and impeller are separated by an annular seal; this allows leakage back from the impeller outlet to the inlet. A shaft seal such as a stuffing box or mechanical seal prevents the pumping fluid from leaking

to the environment and bearing housing. Figure 1 shows a single stage over hung centrifugal pump with a volute illustrating all main components and mechanical construction.

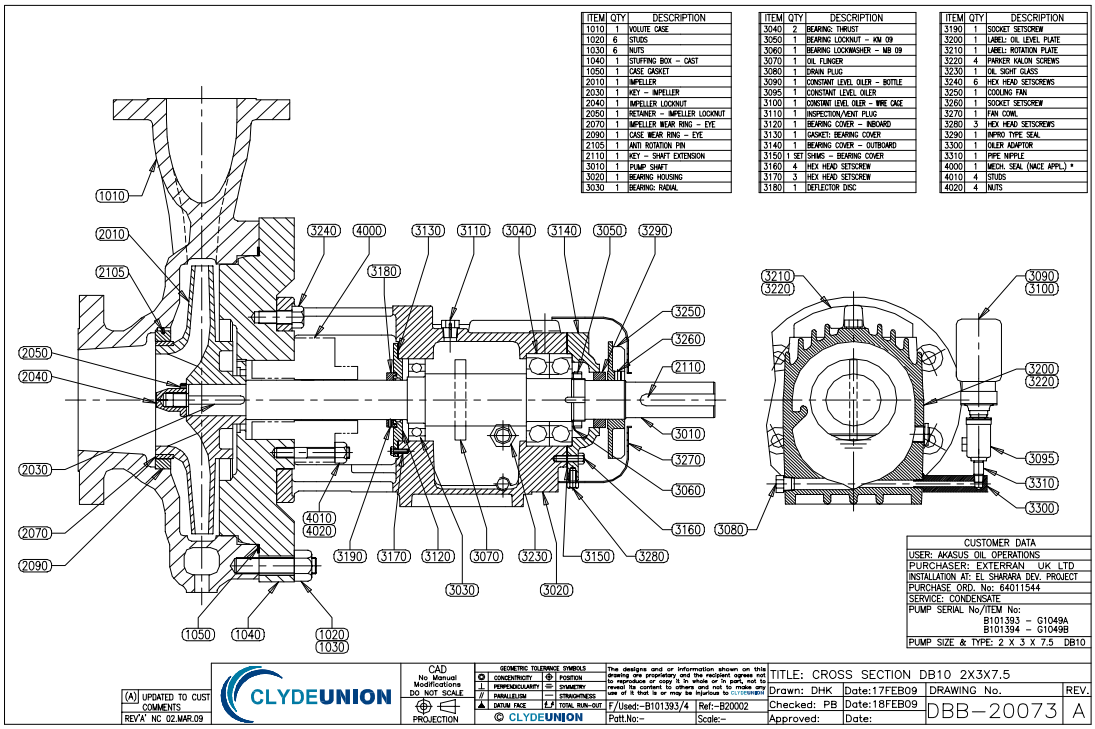

Figure 1 Single stage overhung centrifugal pump SPXFLOW Clydeunion pumps

The common rotordynamic pump types which are widely distributed fall into three main categories. They are radial flow, mixed flow and axial flow. The majority of rotordynamic pumps are of the radial flow type. They cover an extensive range of flow rates for a variety of applications.

The radial flow category consists mainly of single stage and multistage pumps. They can be horizontal or vertical, each type with many different arrangements,

such as single entry, double entry impeller arrangements or the layout of the suction and discharge nozzles.

There are a number of options and arrangements to the hydraulic components in centrifugal pumps which contribute to their classification. There are three impeller types, closed (shrouded), semi open and open. The flow characteristic is governed by the flow direction at the impeller outlet being either radial, semi radial or axial. The description of an impeller is referred to as the hub, blades, rear shroud and front shroud (unless semi open or open impeller). The collector type can either be a diffuser type machine, Figure 2, or a volute type machine, each has varying arrangements. The volute may have a single path or a double path, (Figure 3) where the liquid is expelled into two passages which then join at the discharge. A double volute is chosen for higher flow applications and is common in single and multi-stage pumps. An important geometrical parameter which requires careful consideration in volute machines is the cutwater diameter, the cutwater is shown in Figure 3. The cutwater clearance is the radial gap between the impeller vanes and the outlet cutwater and is calculated using equation 1. It is widely recognised that this parameter contributes to pressure pulsations due to the interaction effect of rotating and stationary parts. The clearance is expressed as a percentage and may be calculated by equation (1). A diffuser is either radial or semi axial in terms of flow direction. The diffuser and impeller form multiple blade rows and must be carefully designed due to the interaction of rotating and stationary parts. They are generally used for high head applications.

$$\text{CutwaterGap} = \frac{(D_3 - D_2)}{D_2} \text{x} 100\% \qquad \textbf{Equation 1}$$

Where D_3 is the diameter of the volute lip

D_2 is the diameter of the impeller

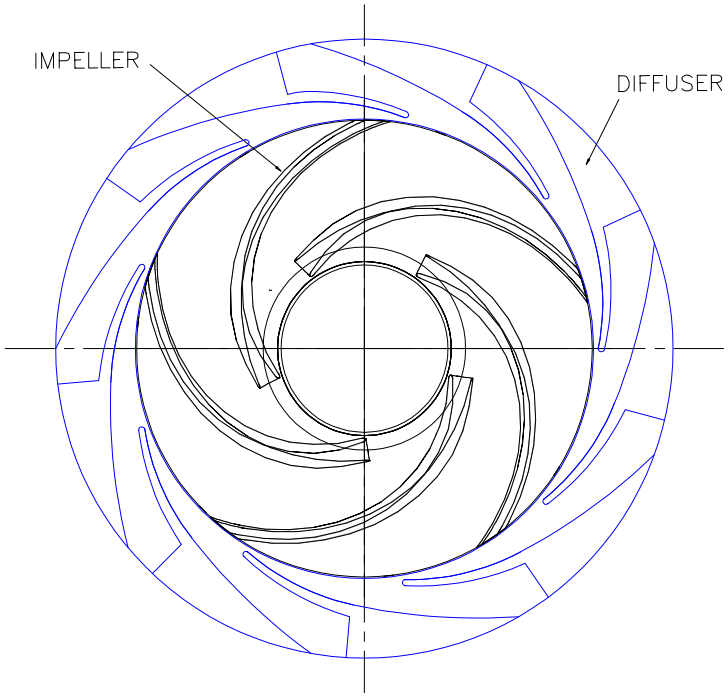

Figure 2 Impeller and diffuser

a

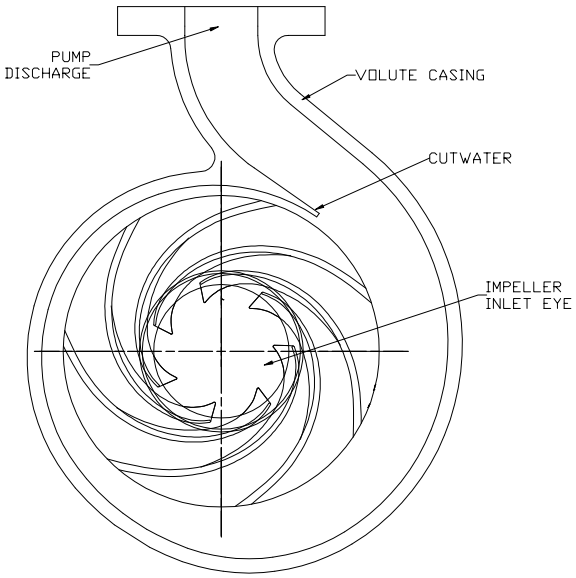

b

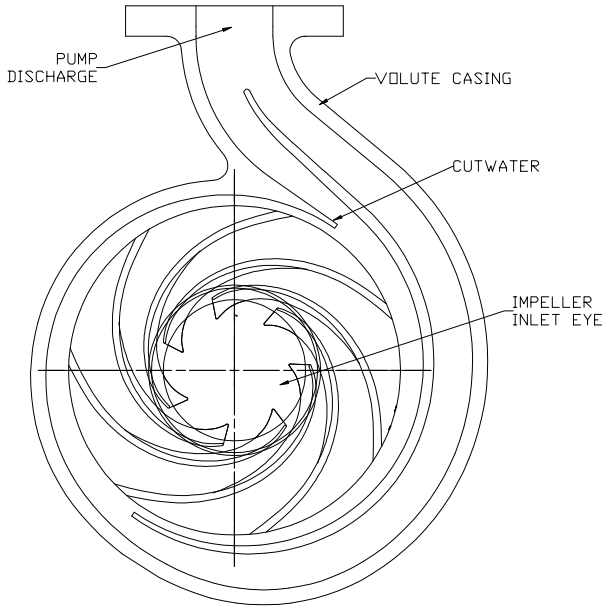

Figure 3 Volute machine with a) single volute b) double volute

The design of both the impeller and collector are complex. There are a number of geometrical parameters along with general arrangements that need to be specified. These are evaluated using flow calculations. The geometrical parameters dictate the hydraulic efficiency of a pump. Idealised one dimensional flow theory is employed for the basic understanding and initial design of an impeller, volute or diffuser. In order for the energy transfer to the fluid to be efficient, design features such as blade number, inlet and outlet blade angles, blade sweep, meridional profile, leading and trailing edge, blade thickness and eye diameter must be carefully engineered.

The fluid conditions within the arrangement of an impeller and collector present a complex unsteady flow phenomenon. The flow is three dimensional and turbulent in character. The analysis of flow through a centrifugal pump is based around classical fluid dynamic principals and physical laws. These are the conservation of mass, momentum and energy equations. Understanding boundary layers and their control is also important as these determine to some extent the losses and velocity distributions over a component. However, the main concern is to avoid recirculation and flow separation, which give high hydraulic losses. Accelerated flow gives a decreased boundary layer thickness and results in reduced hydraulic losses. With decelerated flow the opposite occurs, the boundary layer thickness increases and the wall shear stress will eventually reduce to zero. At this point the flow separates completely from the wall, a stall condition occurs and results in recirculation further downstream. Under this condition the reduced main stream accelerates and interacts with the wake due to change in momentum. Unsurprisingly a designer seeks to design so the flow does not decelerate in order to prevent hydraulic losses. Hydraulics losses can account for up to 60% loss in efficiency.

A flow may be described as inviscid if there is a “no friction” condition and the relative velocity at the walls is zero. The “no slip” inviscid flow condition is generally used in classical fluid dynamics. In a centrifugal pump where the main flow is turbulent in nature, there is a slip condition. The laminar boundary layer at the inlet becomes turbulent further downstream. The velocity distribution when

modelling turbulent effects accounts for the wall roughness and Reynolds number.

A pumping systems performance characteristic are shaped in terms of

- Flow rate, Q
- Head H
- Power consumption at the pump coupling, P
- Efficiency at the pump coupling, μ
- Net Positive Suction Head (NPSH) at the pump inlet

A centrifugal pump is designed to raise the height of the liquid flowing through it to a specific height which is known as head. Head is not associated with the density of a fluid; therefore, this parameter does not change with pumping fluid. It allows the performance of a pump to be analysed without the need to involve fluid properties. Pressure differences, stresses and powers are all associated with density and would vary with fluid type.

The differential head or total dynamic head is defined in the following expression:

$$H_{tot} = H_d - H_s \qquad \text{Equation 2}$$

Where H_d is the discharge head

H_s is the suction head

The Head produced by a pump is solely achieved by the impeller. The casing and other contributing components only determine the losses in the final value.

The performance curves of a pump are presented as a function of flow rate. An example is shown in Figure 4. The triangle indicates the locus of the Best Efficiency Point (BEP). It is the flow rate at which the pump produces its greatest efficiency. The nominal operating range is from shut off which is zero flow, to maximum flow, usually corresponding to 120% of the BEP. The impeller and collector are designed so that at the best efficiency point, there will be no recirculation or separation effects. Operating below the BEP is known as part load operation, typically below 70% of BEP, recirculation can exist in the impeller inlet and outlet. If part load operation is sustained, it can cause damage to components. In Figure 4, the red line indicates the minimum continuous stable flow (MCSF) point. The pump should not be run below this flow in operation. The HQ curve is presented for maximum and minimum impeller diameter.

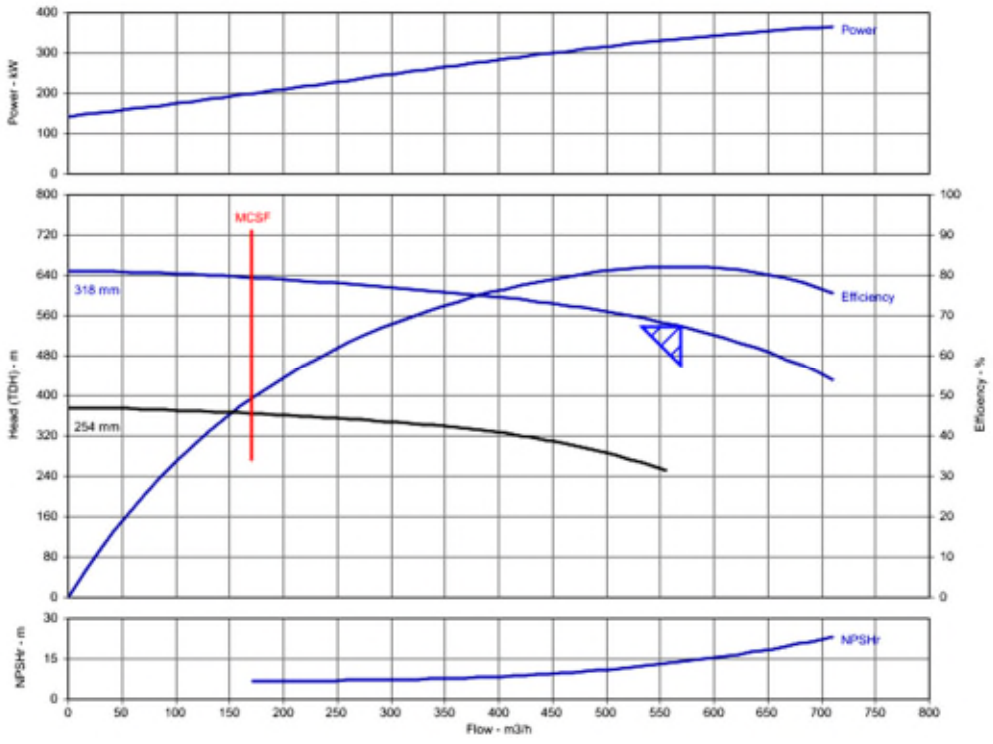

Figure 4 Pump performance curve SPXFlow Clydeunion Pumps

2.3 Vibrations in Centrifugal Pumps

Vibration analysis plays an important part of condition monitoring and is used extensively to assess the running integrity of centrifugal pumps and other rotating machinery. Vibration is generally the most common symptom of operational problems in centrifugal pumps industry wide. Efficient condition monitoring is therefore a useful tool to proactively monitor a pumps condition. Sophisticated vibration monitoring techniques and industry standards having tighter limits on allowable vibration mean furthering the understanding of pump vibration is ever more important.

All pumps vibrate due to response from excitation forces. Common causes are turbulent flow, pressure pulsations, cavitation and rotor imbalance. It is the assessment of the vibration magnitude that is indicative of whether the level of vibration will actually cause damage. High levels of vibration have a direct effect on pump performance which leads to wasted energy, pump failures and environmental harm.

When measuring the vibration response of a pump or any rotating equipment a time waveform is obtained. Figure 5 shows the amplitude of vibration vs. time. In order to evaluate the vibration signature, the data in the time waveform is transposed into a frequency spectrum, Figure 6, which is amplitude of vibration vs. frequency. This is done due to the time waveform consisting of many simple periodic waves and when arithmetic added they produce a complex wave. Each vibration gives a vibration signature at different frequencies. Therefore, by displaying the information in a frequency spectrum each wave can be separated and easily associated with a physical mechanism in the machine. The most common methods for regenerating the information are by either Fast Fourier Transform (FFT) or Power Spectral Density (PSD).

The general measurement location of pump vibration analysis is at the bearing housing, taken in three planes. It is the vibration velocity which is measured as this is the energy of a vibration and is the best account for the severity and

condition of a machine. Whereby a design of the bearing housing is non-isotropic, it is expected that vibration amplitudes will vary in each measurement plane. This is also influenced by the baseplate and foundation. In “between bearing” pumps it is common to have a large variation in drive end (DE) and non-drive end (NDE) vibrations due to variations in mass, stiffness and force transmission path. For pumps with hydrodynamic bearing arrangements, shaft displacement is measured as it senses the relative motion of the shaft in relation to the bearing.

The frequency spectrum can expose specific machine faults. Examples of common faults are imbalance, mis-alignment, mechanical looseness and a bent shaft. They are identified at characteristic frequencies as a function of the fundamental frequency, which is the rotational speed of the shaft. This is synchronous vibration. These are vibration peaks that are multiples of the fundamental frequency. Non synchronous vibrations are peaks that are not integers of the fundamental frequency. They correspond to faults such as rolling element bearing defects relating to the ball, cage, inner race and outer race defect frequencies. Hydrodynamic bearings produce a sub synchronous vibration peak at 0.48 times the fundamental frequency which relates oil whirl and instability of the rotor.

The onset of mechanical vibration problems may be corrected through precision alignment, balancing, good piping practices, etc, whereas hydraulic vibration issues involve detailed re-design of hydraulic components this greatly relies on the ability of a hydraulics engineer to compromise between the performance and high vibration “trade off”.

Vibration-based techniques have been developed and refined to cost-effectively monitor pump operation and the onset of failures. Mechanical sources of vibration, for example imbalance due to operational reasons (damage on impellers leading to imbalance), shaft misalignment, base plate design, etc, are all significant but outside the scope of the project.

It is not only mechanical vibration which can be identified using vibration analysis techniques. Flow induced vibration caused by recirculation, cavitation and acoustic resonance present themselves at certain frequencies.

The most common flow induced vibration is the blade passing frequency (bpf). It is the vibration caused as the impeller blade passes the cutwater or diffuser blade. It can be easily identified as it is usually fairly dominant within the frequency spectrum of a centrifugal pump. It has a synchronous frequency response corresponding to the number of vanes of the impeller as a function of the rotation of the shaft. Hence, a five vane impeller has a frequency of five times the running speed. Minimum cutwater clearances are dictated in standards to prevent high bpf vibration. High level of bpf vibration can be particularly damaging if it coincides with a natural frequency of a bearing housing and results in highly destructive amplitudes and damage to seals and bearings.

A method of measuring a structure's natural frequency is by performing an impact test. This is a simple technique which excites resonances and measures the mechanical natural frequencies of a unit. It is used in conjunction with spectrum analysis to evaluate if a machine is resonating. Any external force which is within 20% of a natural frequency of a pump, foundation and piping, can result in amplification of the magnitude of a vibration.

The "allowable" and "preferred" operation range for vibration amplitudes are heavily dictated by the International Standards Organisation (ISO) and specific industry standards such as the American Petroleum Institute (API). Vibration limits are stated which pump manufacturers must comply to. These are given in unfiltered velocity amplitude with unit's mm/s Root Mean Square (RMS) or for shaft displacement with units µm. The vibration limits are of course dependent on pump type, rotational speed and absorbed power.

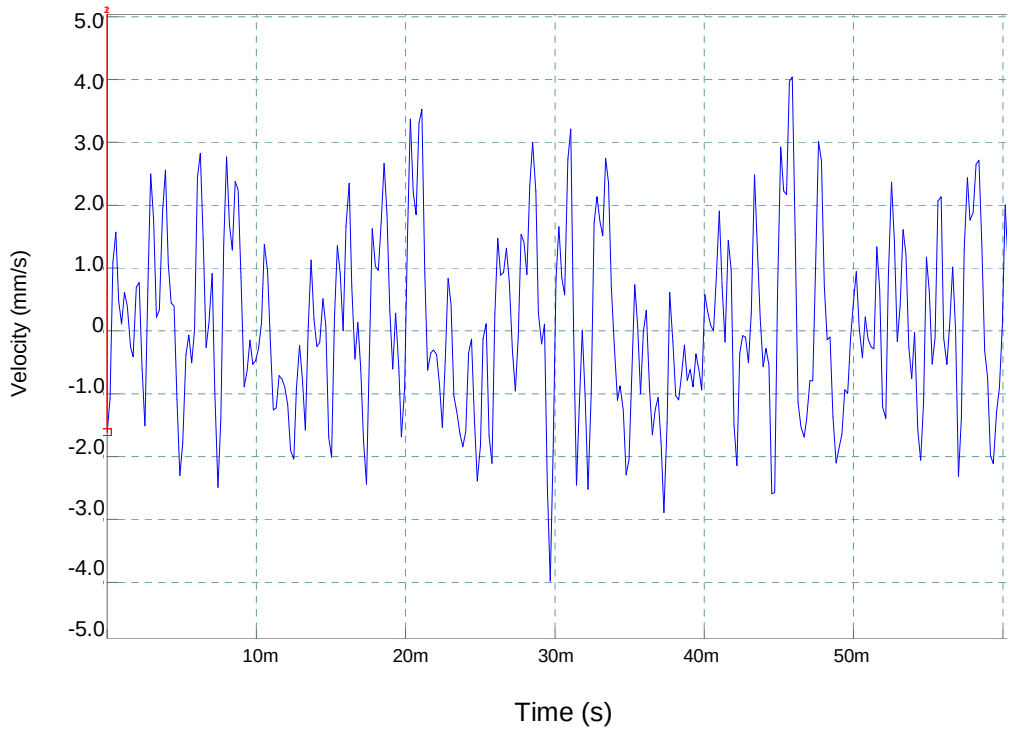

Figure 5 Sample time waveform

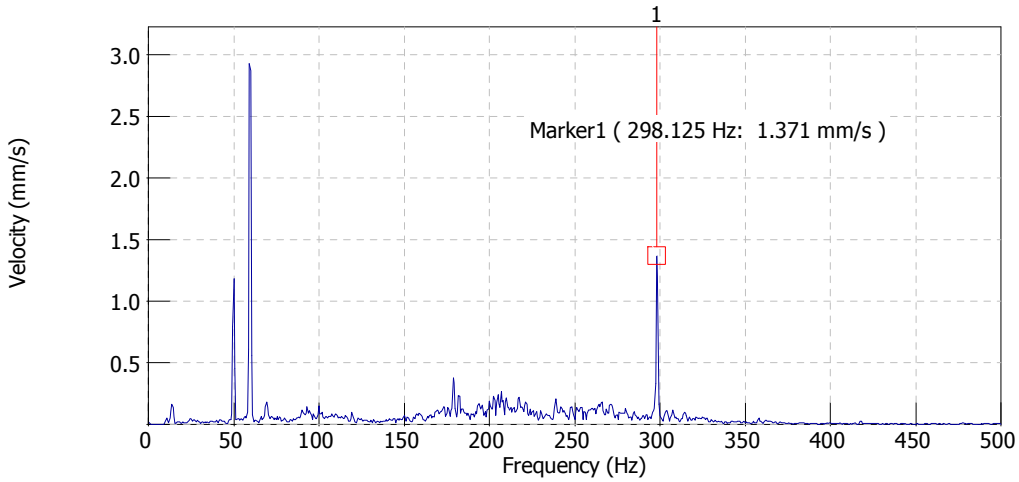

Figure 6 Sample FFT Frequency spectrum

2.4 Hydraulically Induced Vibration

The main source of unsteady flow within centrifugal pumps is a response to a rotating component passing a stationary component. This is the cutwater in volute machines and diffuser blades in diffuser machines. The interaction has consequential effects which are primarily seen when operating at off design conditions. Pressure pulsations present themselves as discrete frequencies in a spectrum at multiples of the rotational frequency, relating to the blade passing frequency.

The pressure fluctuations are particularly concerning when operating at part load where recirculation's at the impeller inlet provoke strong rotor stator interaction. Vortices are generated due to shear layers and flow separation between the re-circulating flow and the main flow. The turbulent separated flow results in broadband pressure pulsations.

Strong interactions that lead to component loadings under transient flow conditions result in the stresses on the impeller shroud to become excessive. The stress alternates as the force direction reverses. A pressure wave enters the impeller sidewall gap and is reflected towards the annular seal as it passes through the impeller channels. The impeller shroud therefore experiences pressure fluctuations. The fluctuations are the differential pressure between the impeller channels and the sidewall gap, which give rise to the alternating stress and reduce component life.

By taking a multistage pump as an example, the axial thrust is in the forward direction to the impeller inlet. As the reflected wave travels back into the pump from the discharge piping, the axial thrust is reversed, causing the last stage impeller to be axially displaced. Figure 7 shows the effect of pressure waves on the pressure distribution on the impeller shrouds which determines the axial thrust: the forward wave the axial force does not change much because the rear and front shrouds are subject to the same loads (figure 7a). However, the reflected wave causes a momentary pressure peak at the impeller inlet whereas

the impeller outlet and the impeller sidewall gaps are still in the trough of the wave (figure 7b). The impeller can then come into contact with the casing. For multi-stage pumps with a back to back impeller arrangement, the standing waves exist in the long cross over passage resulting in acoustic resonance. These events are largely determined by the discharge piping or passage way cross sectional changes for a reflection to occur.

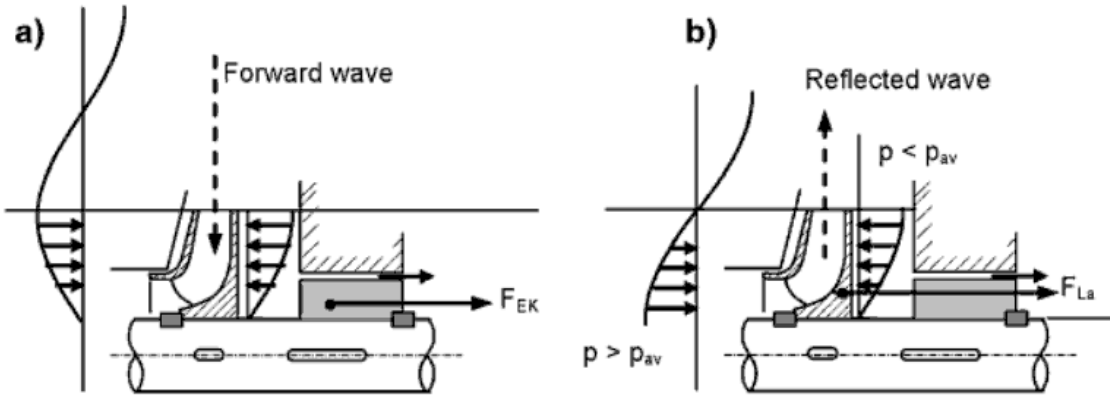

Figure 7 Pressure waves on pressure distributions and forces a) excessive loading with forward wave b) axial thrust reversal with wave reflection (Gulich, 2008)

Hydraulic excitation forces such as pressure pulsations interact with mechanical vibrations leading to the reduced mechanical integrity of a pump. The excitation forces generated at the impeller outlet which are transmitted via the shaft to the bearing housing are not quantitatively known. There are a number of factors which must be first considered such as running clearances, rotor damping and the oil film damping coefficients.

Measurement of pressure pulsations is challenging both numerically and experimentally. Gulich (2008) provides guidelines for evaluation of pressure pulsation measurements. It is stated that the measurements can be subject to uncertainties due to influence of the system and are dependent on location of the pressure transducer. It is indicated that values can be distorted by up to a factor of ten.

Pressure pulsations can be shown in the following representation

- Peak to peak
- Peak
- Root Mean Square (RMS)

Equation 3

$$\Delta pRMS = \frac{\Delta p_{p-p}}{2\sqrt{2}}$$

Where $\Delta P_{p\text{-}p}$ = pressure pulsation peak – peak

Pressure variation is unavoidable but excess causes component fatigue fractures and radiation of solid-borne noise. The hydraulic vibrations transmit to the bearing housings, baseplates and piping. The interaction of the system is also important when considering acoustic resonance in the piping. These standing waves in the piping system can interrupt control systems and even break instrumentation via excitation of the mechanical components.

Pressure pulsations can be classified as acoustic or hydraulic. This is defined by the mechanism of their generation and propagation within the fluid. The speed in which the wave is propagated can be used to differentiate between the two.

The physical mechanisms that lead to the generation of pressure pulsations are outlined as

- The finite thickness of the blade trailing edge of the vane
- The boundary layers on both sides of the vane
- The difference in the velocity distribution between suction and pressure side of the vane inherent to a vane which transfers work from an impeller to a fluid.
- The wake flow gives rise to pressure pulsations by two mechanisms; the unsteady vortex flow and impingement of the wakes on the diffuser vanes or the volute tongues (Guelich and Bolleter 1992).

There have been many attempts to reduce pressure pulsations. The current recommendations to reduce pulsations are to increase the clearances between the diffuser and impeller vanes or increasing the cutwater clearance, oblique trimming of the impeller blade trailing edge and profiling of the impeller blades. However, by changing geometrical features of the impeller there is an influence on the characteristics of the pump. The method of increasing clearances has the greatest effect; yet there is a penalty on efficiency.

Other popular methods which have been employed by most pump manufacturers is staggering blades and having a twisted blade profile at the impeller outlet as shown in Figure 8. Staggering vanes reduce the amplitude of the blade passing frequency as each pressure pulse, as the blade passes the volute tongue is offset from the next. The volute cutwater can also be modified to have an oblique correction. For multistage pumps clocking of impellers on the shaft is a common practice employed to have the same effect of staggering vanes and reduce hydraulic forces.

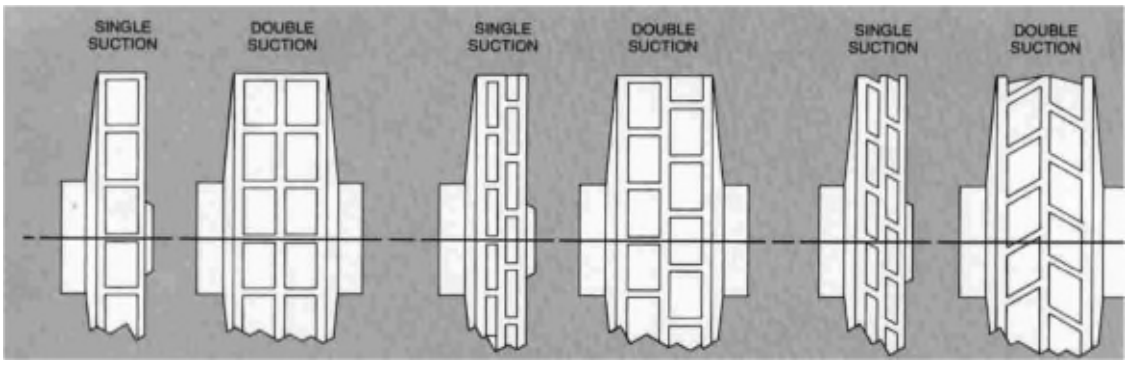

Figure 8 Enclosed impellers with a) straight vanes b) staggered with straight vanes c) staggered and skewed vanes (WARREN PUMPS)

2.5 Pump Rotordynamics

In order to produce lighter pump packages with higher efficiencies rotordynamics of pumps has formed an essential role in determining pump integrity. The pump rotating element is the origin of energy transfer and therefore is the source of all vibrations which are excited by the pump (Gulich 2008). The adequate operation is therefore defined as the ability to tolerate vibrations levels without significantly affecting the overall performance of the pump (San Adres 2006).

Rotordynamic analysis in the pump industry is particularly important in the design of multistage pump rotors or pumps which have a high impeller tip speed. Today a large amount of centrifugal pumps has high shaft speeds up to 6000 rpm, which produce high energy densities and flow rates. This presents challenges with high inertial loads, vibration and rotor dynamic instability.

Rotordynamic analysis of a pump differs to that of pneumatic turbomachinery. The mass of the fluid entrained within the impellers and in the volute passage ways is significant when compared to the mass of the rotor. When evaluating a pumps critical speed, the “wet” and “dry” conditions are considerably different. Key factors which give rise to the significant difference is close running clearances of annular seals, wear rings and impellers where by fluid-structure interaction forces are generated.

A pump rotor is subject to certain forces which can be noted as

- Excitation forces- synchronous mechanical and periodic hydraulic forces
- Steady forces- rotor weight and hydraulic forces within bearings.
- Hydraulic reaction forces- orbital movement of the rotor induces changes in pressure distributions.

Mechanical forces acting on the pump rotor are calculated fairly easily whereas hydraulic forces are highly dependent on the hydraulic design and operating conditions. For this reason, the hydraulic contributions are commonly assessed by empirical data. Collating empirical data relevant to a new pump design is not

always possible; the emphasis is on the design engineer to make a number of assumptions, this can lead to discrepancies in the results. Lateral rotordynamic analysis of a pump is a complex process, in order to obtain an accurate evaluation of a pump design, factors such as the interaction forces in annular seals, impeller interaction forces, hydraulic imbalance and dynamic effects due to case deformation must be accounted for.

Rotordynamics is voluminous topic covering both torsional and lateral aspects of vibration potential. For the purpose of this work lateral rotordynamic method is discussed in section 2.5.1. The annular seal effects and representation of hydraulic forces are discussed in sections 2.5.2 and 2.5.3 respectively.

2.5.1 Rotordynamic Lateral Analysis Method

The main objectives in a rotordynamic assessment listed as follows:

- Undamped Critical speed analysis
- Synchronous response analysis
- Damped natural frequency/stability analysis

2.5.1.1 Undamped Critical Speed Analysis

The first step in a lateral rotordynamic analysis is to establish the undamped critical speeds and corresponding mode shapes.

Critical speed is the theoretical value which excites a natural frequency of a rotating object. Every rotor has discrete natural frequencies and each natural frequency has a corresponding mode shape. A mode shape is a snapshot of the greatest deflection at maximum strain during a vibration. The distribution of mass and stiffness and the bearing support stiffness have a direct influence on the

mode shapes. As the mode shape corresponds to the undamped condition, the value produced for absolute displacement is unimportant as it is theoretically infinite; the mode shape is to reveal the relationships of the displacements of the disk element, with respect to each other.

Firstly, a mathematical model consisting of parameters of lumped masses of disks and shaft elements is generated, example shown in Figure 9. This model includes all significant masses; impellers, coupling hub, mechanical seal as well as bushes and stage pieces which are mounted to the shaft. In the model, moments of inertia are to be included for each disk element so gyroscopic effects can be included in the analysis.

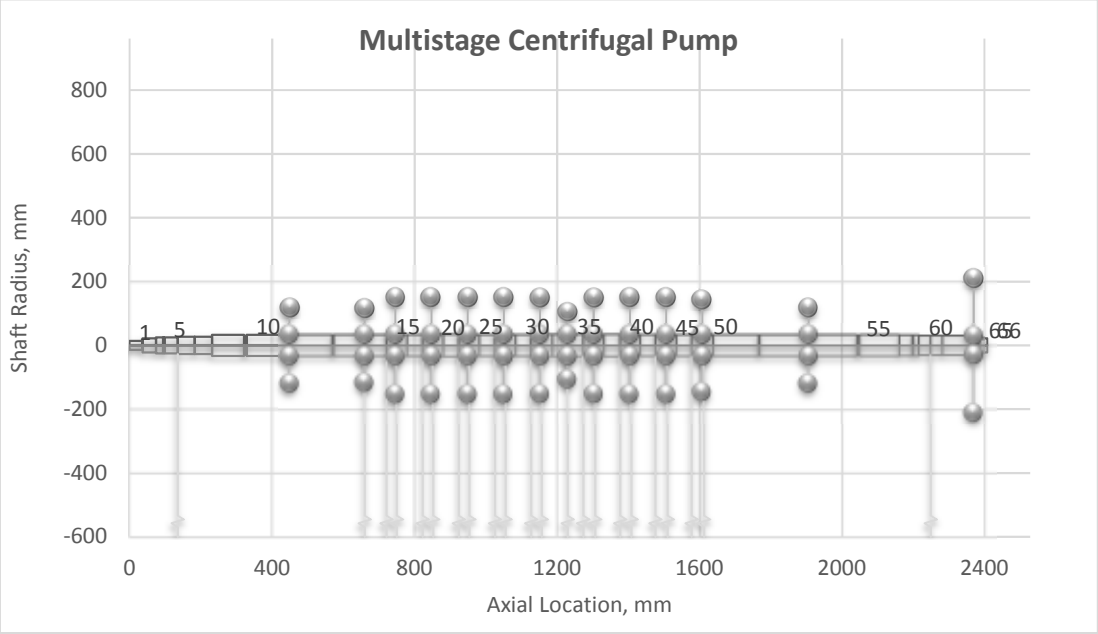

Figure 9 Geometry plot of shaft elements, disk elements and bearings/seals shown as springs (SPXFLOW Clydeunion pumps)

Varying parameters such as increasing shaft stiffness or adding mass will raise and lower natural frequencies, respectively. Natural frequencies are also dependant on bearing stiffness's. They are described by the conventional stiffness and damping coefficients. Journal bearings are represented by all eight

coefficients shown in a linearized model in accordance to Taylor's theory, equation 4. For rolling contact bearings the direct stiffness is relevant only.

$$\begin{pmatrix} F_x \\ F_y \end{pmatrix} = -\begin{pmatrix} K_{xx} & K_{xy} \\ K_{yx} & K_{yy} \end{pmatrix}\begin{pmatrix} x \\ y \end{pmatrix} - \begin{pmatrix} C_{xx} & C_{xy} \\ C_{yx} & C_{yy} \end{pmatrix}\begin{pmatrix} \dot{x} \\ \dot{y} \end{pmatrix} \qquad \textbf{Equation 4}$$

F_x = Force in x direction

F_y = Force in y direction

K = Stiffness coefficient

C = Damping coefficient

Subscript xx, yy correspond to the direct terms x, y and the subscript xy, yx correspond to the cross coupled terms

Once the mathematical model is generated and the natural frequencies and corresponding mode shapes are calculated a critical speed map is created to present the findings. It is a useful lateral analysis tool as it provides visibility of the systems undamped natural frequencies in rpm as a function of bearing stiffness. The critical speeds in relation to the operating point can be approximated and the mode shape sensitivity to bearing stiffness is indicated by the gradient of the natural frequency curve.

The analysis may be deemed complete if the first critical speed is approximated to be much higher than the operating point; this is classified as being a rigid rotor. In this regime the rotor appears rigid in that the critical speed is not influenced by the stiffness of the rotor. Thus the rotor will not operate on or transverse a critical speed. Generally, most rotor critical speeds are impacted by both rotor and bearing stiffness effects and therefore classified as a flexible rotor design. In this regime a rotor critical speed will situate below operating point for "dry" running conditions.

2.5.1.2 Unbalance Response

Unbalance response analysis predicts a rotor systems response to an unbalance loading that is strategically placed at critical speed locations, uncovered in the undamped critical speed map described in section 2.5.1.1. This type of analysis provides insight to whether a critical speed located in the operating range of a machine, will be problematic.

As the actual distribution of unbalance in a system is unknown, a common approach for response analysis is to assign an unbalanced force to the disk elements at locations where a mode shape reveals a displacement maximum. The impact of loads on the system will only be significant if applied in this region of higher amplitude. The analysis seeks to quantify the synchronous vibration amplitudes at critical stations such as bearings, impellers and seals.

The unbalance response is run for a speed range spanning the undamped critical speed to obtain the location of the peak response. The results to the unbalance calculation for a given speed consist of displacements and phase angles at each point in a system. The dynamic loads at the bearing housing are also revealed. A plot of the dynamic amplitudes as a function of speed illustrates the findings.

2.5.1.3 Damped Natural Frequency and Stability Analysis

Using the same mathematical model for lumped masses of disks and shaft elements, damped critical speeds can be evaluated. At these frequencies damped free vibrations can occur.

The widely used method for this type of analysis is the damped eigenvalue method (Lund 1973). The method includes damping and is therefore complex; it involves extracting damped natural frequencies through the eigenvalue analysis of a system for a given speed. As values obtained for the damped natural frequencies are for a specified operating speed and the bearing stiffness and

damping coefficients are dependent on speed, there is a variance between the damped critical speed and the damped natural frequencies.

A Campbell diagram is utilised to determine the synchronous damped critical speed.. Figure 10 provides an example of a Campbell diagram. It can be seen from the diagram that the positively sloped line corresponds to forward procession and the negatively sloped line respresents the backward precession. All modes have two damped natural frequencies. Gyroscopic effects usually raise the natural frequencies of forward modes and has the opposite effect on backward whirling modes.

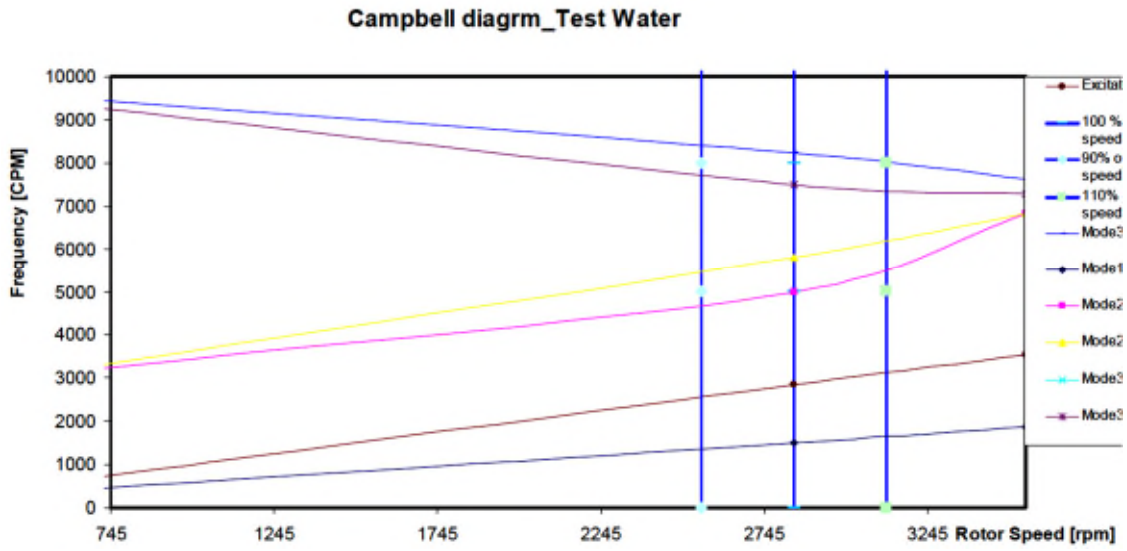

Figure 10 Campbell diagram example of analysis of a multistage pump (SPXFLOW Clydeunion pumps)

In lateral analysis, there is synchronous whirling encountered through an imbalance and there is another common trait in turbomachinery which is sub synchronous whirling of the rotor. This phenomenon is characterised as whipping of the rotor at high amplitude at a damped natural frequency below the running speed. Sub synchronous whipping is self-excited. It is the rotation of the shaft which provides energy for the instability.

The excitation force generated is opposed by a systems damping. Instability occurs if the tangential excitation force is greater than the tangential damping. Fluid film journal bearings can be a potential instability source. In order for the bearing to remain in equilibrium there must be radial and tangential forces, however the tangential force acts in the direction of rotation giving rise to instability as the cross coupling stiffness coefficient is destabilized.

2.5.2 Representation of Annular Seals

The modelling of annular seals is similar to that of fluid film bearings. The dynamic movements are small about a centred position. The seal effects have a significant effect on the vibration characteristic of a pump as they separate high pressure regions and low pressure regions, providing a load capacity. The purpose of annular seals is to minimise leakage flow. The permitted leakage across the seal has a bearing on the overall efficiency a pump can achieve. Large densities of the fluid pumped mean it is necessary to include mass coefficients. These are represented in the same linearized model shown in equation 3 with the incorporation of a mass matrix shown in equation 4.

$$\begin{pmatrix} F_x \\ F_y \end{pmatrix} = -\begin{pmatrix} K_{xx} & K_{xy} \\ K_{yx} & K_{yy} \end{pmatrix}\begin{pmatrix} x \\ y \end{pmatrix} - \begin{pmatrix} C_{xx} & C_{xy} \\ C_{yx} & C_{yy} \end{pmatrix}\begin{pmatrix} \dot{x} \\ \dot{y} \end{pmatrix} - \begin{pmatrix} M_{xx} & M_{xy} \\ M_{yx} & M_{yy} \end{pmatrix}\begin{pmatrix} \ddot{x} \\ \ddot{y} \end{pmatrix} \quad \textbf{Equation 5}$$

F_x = Force in x direction

F_y = Force in y direction

x = displacement in x direction

y = displacement in y direction

K = Stiffness coefficient

C = Damping coefficient

M = Mass coefficient

Subscript xx, yy correspond to the direct terms x, y and the subscript xy, yx correspond to the cross coupled terms

Equation 4 may be simplified by Equation 5 where the cross coupled terms are noted as k, c and m.

$$\begin{pmatrix} F_x \\ F_y \end{pmatrix} = \begin{pmatrix} K & k \\ -k & K \end{pmatrix} \begin{pmatrix} x \\ y \end{pmatrix} + \begin{pmatrix} C & c \\ -c & C \end{pmatrix} \begin{pmatrix} \dot{x} \\ \dot{y} \end{pmatrix} + \begin{pmatrix} M & m \\ -m & M \end{pmatrix} \begin{pmatrix} \ddot{x} \\ \ddot{y} \end{pmatrix} \quad \textbf{Equation 6}$$

Childs (1993) describes how the motion of the seal rotor in the x direction creates converging and diverging regions in the upper and lower halves of the seal, hence the cross coupled stiffness arises due to the fluid rotation, similar to that of a journal bearing.

The determination of seal coefficients accurately is fairly complex, computational fluid dynamics is an option but the most pragmatic approach used widely, is to apply bulk flow theory. This approach works on the assumption that flow in the clearance of the seal may be represented by excluding the radial variance of fluid properties and applying averaged velocities in the axial direction.

The bulk flow model utilises axial and circumferential Reynolds numbers (as shown here in equation 7.

$$\mathrm{Re}_z = 2 \cdot \rho \cdot v_z \cdot h / \mu$$
$$\mathrm{Re}_\theta = \rho \cdot R \cdot \omega \cdot h / \mu \quad \textbf{Equation 7}$$

Re_z = axial Reynolds number

Re_θ = circumferential Reynolds number

ρ = fluid density

v_z = fluid axial velocity

h = seal radial clearance

μ = fluid dynamic viscosity

R = shaft radius at seal

ω = shaft speed

Childs (1993) states that typically the axial Reynolds numbers exceed 20,000 therefore the seal axial flow is almost always turbulent.

The understanding of how the seal parameters influence the lateral equation coefficients is important. They can be generalised in the following list. Corbo et al (1998)

- The radial clearance ratio increases over time due to wear which results in the K and C coefficients decreasing. It is therefore recommended that worn conditions are analysed.
- Assume the seal pressure drop is proportional to speed squared. As speed increases stiffness coefficients increase with the square of the speed.
- Increasing seal pressure drop for a fixed speed increases the K, k and C coefficients.
- All coefficients are affected by the pumped fluid density. This can be challenging for light hydrocarbon pumping applications.

2.5.3 Representation of Hydraulic Forces

Hydraulic excitation forces occur and are represented in the same linearized model as annular seal considerations. The rotor can vibrate and cause the impeller to deviate around its centric position. This result this has is the pressure distribution changes at the impeller periphery. The interaction forces generated, similar to reaction forces in annular seals, act at the impeller outlet width and on the shroud. Conversely where seal contributions to increase stiffness and stability margin, hydraulic interaction effects decrease the systems stiffness and critical speed (Pace et al 1986).

The dynamic forces produced act as a radial load at the impeller periphery, general characteristics are presented (Corbo et al 1998)

- Direct stiffness K is negative and produces an “anti lomakin” effect on the shaft lowering the critical speed.
- The hydraulic design of the impeller and volute are in alignment only at one flow rate known as best efficiency point. At low flow rates the flow behaviour is fundamentally changed, large zones of flow separation and recirculation occur, this has great influence on the rotordynamic coefficients. For this particular condition the conventional method utilizing the linearized model is inadequate (Childs 1993).
- Increasing radial clearance provides a significant reduction in the magnitude of force generated.

To estimate the static radial force there are two empirical methods. One is given by Stepanoff (1957) and the second by the Hydraulic Institute (HI) standard. The load obtained is the minimum load which will occur at BEP operating condition and then an applied factor of that load is calculated as the operating point moves away from BEP. Both methods are for single volute pumps, working on the basis that for double volute casing construction the radial load is much reduced. The factor applied as the operating point moves away from BEP varies between methods; HI predictions show a higher rate of increase in radial load as operating

point is changed. The formulae for hydraulic force prediction is shown in equation 8.

$$F_{RH} = K_H \cdot \rho \cdot g \cdot H \cdot D_o b$$
$$F_{RS} = K_S \cdot \rho \cdot g \cdot H \cdot D_o b$$

Equation 8

F_{RH} = radial force HI method

F_{RS} = radial force Stepanoff method

K = Load factor

ρ = fluid density

g = gravitational acceleration

H = pump head

D_o = impeller outer diameter

b = impeller discharge width

The static radial load is dependent on rotor motion and can be categorised as reaction forces. A rotor can be subject to hydraulic forces which are independent of rotor motion known as excitation forces. The main source of excitation forces found in pumps is the hydraulic unbalance and the blade rate force, known as blade passing frequency.

It is the blade passing forces which are of interest in this work. The forces are present due to the non-uniform pressure and velocity distributions between the close running clearances of the impeller and volute lip.

The vane pass forces may be incorporated into a Campbell diagram to elude any potential resonance conditions. This is indicated by the intersection of the excitation line with the damped natural frequency line in the Campbell diagram plot.

The most common action to resolve vane passing frequency problems is to increase the cutwater clearance. Increasing this radial gap has a negative effect on pump efficiency which is not desirable; often it is a fine balance of reducing hydraulically induced vibration and optimising hydraulic pump performance. Presently there is no methodology for predicting the hydraulic forces arising from vane passing.

3 Literature Review

The literature survey focuses on four main areas, pump characteristics including low flow investigation, rotor-stator interactions and pressure pulsations, computation fluid dynamics applied to centrifugal pumps and finally pump rotordynamics.

The art in successful centrifugal pump engineering is in the hydraulic design and in the ability of a designer to build a good understanding of the flow behaviour within a given pump. Design strategies of centrifugal pumps have remained similar over the past 50 years, using a combination of classical fluid dynamic principles and other physical laws. Modern design methods incorporate Computational Fluid Dynamics (CFD) technology to predict and simulate the fluid flow through a pump. In the 1980's when CFD was first introduced to the turbo machinery industry there was some scepticism regarding the role of CFD within the design loop. However, there were many studies which show good agreement between numerical predictions and experimental data. It is now a widespread accepted design tool for many applications. The advent of numerical modelling has resulted in a decrease in experimental investigations; recent studies may include experimental results purely to validate numerical analysis.

Vast amounts of literature content have been explored which characterize the flow in a centrifugal pump. The majority of flow field studies were stimulated as part of the quest for greater pump efficiencies, which are on-design analysis studies. Fewer reported investigations in the area of "off design" analysis which is primarily the interest of this review as it is under these conditions that unsteady effects such as rotor-stator interaction are more pronounced. Many researchers have concentrated on the evaluation of the fluid flow through the impeller while significantly fewer publications are concerned with the interaction between rotating and stationary components. The pressure pulsations generated as a result of rotor-stator interaction are of great interest to pump manufacturers as high magnitude pulsations result in unwanted noise and vibration which lead to

reduced pump integrity. Although this phenomenon cannot be entirely eliminated the effects can be reduced giving improved reliability and performance, as is discussed in great detail in this review.

Literature defining the computation of the flow physics within a centrifugal pump has also been reviewed. However, few investigations exist which are representative of commercial pump design, especially at off design conditions. While there has been substantial improvement in computational power and greater accuracy of numerical methods, realistic simulation remains a challenge due to the complexity of the three-dimensional unsteady fluid flow within centrifugal pumps.

3.1 Characterisation of the Fluid Flow Through a Centrifugal Pump

An early investigation carried out by Fischer and Thorma (1932) compared two-dimensional predicted flow with actual flow behaviour using an early flow visualisation technique. Their experimental results showed that flow separation occurred at the suction side of the impeller and that it was predominantly at part load operation. Therefore, at decreasing flow rates the separation on the suction side of the passage increased. This phenomenon was not predicted in their theoretical work since it employed an ideal frictionless fluid.

By the 1970's two techniques for characterising flow velocities in an impeller were available, hot wire anemometry and photographic tracking techniques. Researchers such as Fowler (1968) and Lennemann and Howard (1970) conducted experiments at part load conditions using methods of photography to monitor tracers as well as hot wire anemometry. It was found that the reverse flow in the blade passage was due to the suction side separation and was a result of the secondary flow of the endwall boundary layer across the passage from the suction to the pressure side, giving a cross passage pressure gradient as discussed in some detail in a later publication by Abramian and Howard (1998).

Dean (1959) introduced the “jet wake” model where the relative flow was split into two parts, an invisicid potential core along the pressure side of the passage and a wake within the suction side of the passage.

In the mid-seventies a Laser Doppler Anemometry (LDA) technique was introduced allowing velocity measurements in turbo machinery impellers to be possible. Eckardt (1976), using the LDA technique, investigated the flow through a radial impeller and discovered that the “jet wake” behaviour introduced by Dean (1959) was caused by a combination of flow separation and secondary flows. Alder and Levy (1979) used Eckardt’s work as a comparison for a shrouded impeller with backward swept blades. One observation from their work was that a distorted inlet flow resulted in the “jet wake” structure to decay. They also reported that due to the backward swept blades at the design conditions the flow was in fact stable despite the distorted flow at the inlet. Zhang et al (1996) reported the “jet wake” structure formed is independent of flow rate and locations.

Krain (1981) investigated the effect of a vaneless or a vaned diffuser on the “jet wake” flow pattern. Krain’s research showed that the difference between vaned and vaneless diffusers on the “jet wake” pattern was little, only a weak effect on the impeller flow existed. Krain conjectures the findings were due to the low diffuser leading edge Mach number and the special vaned diffuser design, which is essentially a measure of the gap between impeller and diffuser blades.

Dong et al (1992a and 1992b) examined the flow in the area of the impeller and tongue and described it as being entirely “pulsating”. Also they concluded that the flow is dominated by the “jet/wake phenomenon” and is accompanied by turbulence between the “jet” and the “wake” and behind the blades. Gonzàlez et al (2002) explain how the tongue geometry modifies the jet- wake pattern and is one of the main causes of fluctuations at the blade passing frequency.

Chio et al (2000) experimented the unsteady flow field and noise generation of a centrifugal pump impeller. The conclusions drawn were that the unstable passage flow results in periodic pressure oscillation on the blade surface. It was

noted the unsteady effects were coherent from blade to blade and therefore form a rotating instability pattern containing rich harmonic content.

3.1.1 Low Flow Investigations

Peck (1950) carried out investigations on a single entry end suction pump, collecting experimental data through a visualisation window using a stroboscope. At very low flows he observed that a large re-circulation region, a “powerful forced vortex” was present. This extended far into the suction pipe. Pressure tapings in the casing indicated a circumferential pressure rise from cutwater to casing throat. Visualisation also confirmed a surging flow phenomenon at the cut-water.

Young (1956) observed that at 50% of design flow a complex flow pattern existed. Young noted that there were higher velocities on the leading blade face than on the trailing blade face. It was also noted that the flow from passage to passage is not the same. However, this phenomenon reported by Young, is indistinguishable to observations previously reported by Fischer and Thoma (1932). The phenomenon is explained as the stalling of alternate vane passages. No attempt in either paper is made to relate phase angle to the passage stall, resulting in limited conclusions being drawn regarding the rotor/stator interaction effects.

Binder and Knapp (1958) observed that at low flow rates a non-uniform pressure distribution within the volute was distributed. It was observed that as the area within the volute increased, from cut water to casing throat, the pressure increased. The minimum pressure recorded was local to the cutwater. Iversen (1960) and Kikuyama et at (1987) reported similar observations and determined the existence of the non-uniform circumferential pressure gradient around the volute. At “off design” flows, the pattern became unsteady with the greatest pressure oscillation noted at vane pass rate. This was dependent on the phase position of the impeller blade with respect to the cut-water, giving an indication of the circumferential pressure distribution caused by the rotor-stator interaction.

Using streak photographic techniques, Brownall et al (1985), demonstrated the existence of partial inflow to the impeller at the low-pressure in the region near the volute tongue. An earlier study by Alder and Levy (1979) had also noted this flow characteristic. Varying flow patterns were observed dependent on the blade relative position to the cut water lip. At the lowest flow (30% b.e.p) the tongue stagnation point moved into the volute. The separation zone, caused by the tongue, oscillated at vane pass rate demonstrating the impeller volute interaction. This observation is contrasting to Worster's (1953) earlier findings but in good agreement with Yedidah's (1985).

Goulas and Trouscott (1988) carried out experimental analysis of an end suction pump using Laser Doppler Anemometry (LDA) to explore the flow pattern at the impeller exit. At 27% of design flow the velocity vectors local to the cut-water were directed through the cut-water clearance, between the impeller and case, indicating localised low static pressure. This agrees with earlier observations made by Binder and Knapp (1958), Brownall et al (1985), Kikuyama et al (1987). Another observation by Goulas and Trouscott (1988) was a reverse flow region past the tongue on the impeller side similar to the one suggested by Yedidiah (1993).

3.2 Rotor- Stator Interaction Investigations

Rotor stator interaction and periodic unsteadiness have been a frequent research theme. Many of these investigations have reported on the interaction of the impeller and a diffuser. Although the interest in this thesis is primarily the blade and tongue interaction in an impeller/volute pump, it is necessary to assess other pumps as well.

Dring et al (1982) described rotor-stator interaction by dividing it into potential flow interaction (the circulation or blockage of a blade) and wake interaction. The

author's experimental work for an axial turbine found both potential flow and wake interaction for closely spaced blade rows (15 percent based on chord). Significant pressure fluctuations of up to 72 percent of the exit dynamic pressure were measured near the leading edge of the rotor.

Lino and Kasai (1985) provided analysis of unsteady flow induced by interaction between a centrifugal impeller and a vaned diffuser. Lino and Kasai measured pressure fluctuations and found that the fluctuations were dependent on flow rate blade/vane angles. This is agreeable with Arndt et al (1990). They investigated the interaction of the impeller blade and the diffuser vane. It was found by altering the radial gap that large pressure fluctuations occurred on the diffuser vanes on the suction side close to the leading edge. Increasing the radial gap by 3% resulted in decreased pressure fluctuations.

Hajem et al (2001) provides a detailed flow analysis of a diffuser machine using Laser Doppler Velocimetry (LDV) method incorporating two operating points. They conclude that the interaction of the impeller and diffuser does not have any upstream effects and is limited to the impeller outlet flow where a mixing of the impeller discharge is affected. Dupont et al (2005) present analysis of Particle Image Velocimetry (PIV) measurements of a vaned diffuser axial flow pump. Although the work is based on 2D measurements it is evident that the main unsteady effects caused by the interaction are at the impeller outlet region. They observed high values of turbulence in the diffuser passage and a stalled region at the pressure side of the diffuser vane. The stall region varies with impeller position in the diffuser frame. It can be said that the pressure recovery of the diffuser is therefore limited by the occurrence of this stall pattern and the impeller blade passing frequency.

A two-dimensional flow analysis of a volute type centrifugal pump was investigated by Miner et al (1992). They computationally modelled the interaction of the rotor and stator simultaneously. The work showed the flow is not uniform circumferentially as a consequence of the impeller and volute interaction. Their results also show that the stagnation point changes as a function of flow rate. Earlier studies by Brownell et al (1985) investigated the location of stagnation

points around the tongue tip and it was observed at low flow rates that a large recirculation occurred.

Dong et al (1992a and 1992b) introduced a method that is used for quantitative flow visualization. This allowed the authors to demonstrate how to obtain information regarding the velocity distribution within the volute of a pump. Many observations had been noted by Miner et al (1992). They added that the flow behaviour in the area of the impeller and tongue was entirely “pulsating”.

The concern of many researchers has mainly been with the velocity field within the volute and impeller passages rather than the impact the flow structure has on the pressure field. Chu et al (1992a and 1992b) presented two papers on the relationship between unsteady flow and pressure fluctuations. The velocity distributions obtained using a Particle Displacement Velocimetry (PDV) were used to compute the pressure field within the volute of a centrifugal pump. It was noted that a potential flow model does not alone adequately represent the fluid flow. The authors present results showing that the blade-tongue interactions are the principal contributor to pressure pulsations and are dependent on relative location of the impeller and volute tongue. Therefore minor changes to the gap between the volute tongue and impeller can cause considerable changes to pressure pulsations.

Wo and Bon (1994) investigated the flow within the volute of a centrifugal pump. The main objective for the research was to identify physical reasons for instability of the flow characteristic. If was found that adverse flow in the cutwater region was one of the main features contributing to instability in the pump’s characteristic.

Kaupert and Staubli (1999) present two papers involving experiments measuring the unsteady pressure distribution in a high specific speed centrifugal pump impeller. Part I, experiments with a sum of twenty-five piezoresistive pressure transducers was successfully situated within a single blade passage and within the volute a total of thirty-two pressure taps were located. Some of their observations have already been noted in previous research. For example they state that the pressure distribution is circumferential in the volute, the pressure

contour in the rotating system is unsteady and the blade passing frequency is the dominant pressure fluctuation, which is maximised at conditions further away from BEP. They show that as the flow moves away from the best efficiency point the pressure fluctuations from the impeller-volute interaction increase. Under this flow condition it is observed that the fluctuations reach 35% of the pump head. It is explained that the pressure fluctuation at the impeller outlet propagated upstream through the blade passage at acoustic velocity excluding those locations where blade curvature and rotation provided a phase lag. Part II, is concerned with the transient hysteresis as the impeller inlet and outlet recirculation commence and cease.

PIV and LDV methods were used by Pedersen et al (2003) to analyse flow through a centrifugal pump at design and off design conditions. Their conclusions show at quarter load a stall phenomenon was steady and non-rotating and therefore is not a periodic unsteady flow condition related to the rotor and stator interacting. This differs from earlier observations by Abramian and Howard (1998), who used LDV methods to obtain insight into pump flow by analysing an impeller with and without a volute. The flow was characterised to consist of periodic unsteadiness, fluctuations in the pressure fields and flow reversal into the impeller were all present at flows near to shutoff.

An extensive investigation was carried out by Parrondo-Gayo et al (2002) and provides excellent data concerning the impeller/cutwater interaction. They focused on the pressure fluctuations at blade passing frequency by varying the operating point. Pressure signals were located in 36 locations at the volute and the varying parameter, the pump operating point ranged from 0% to 160% of the BEP. They concluded that at off design conditions the impeller volute interaction had greater intensity and magnitude as seen in Figure 11. This was measured by analysing the amplitude and phase delay of the blade passing frequency. The authors were then able to identify that the pressure fluctuations at any point in the volute are caused by the passage of any impeller blade relative to that point, and the passage of each blade relative to the volute cutwater.

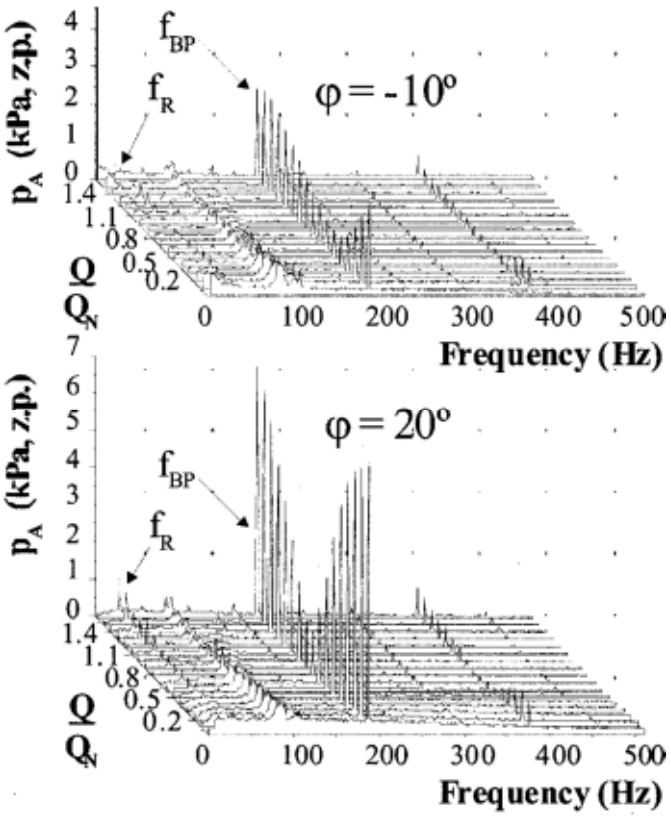

Figure 11 Pressure pulsations magnitude spectrum as a function of flow rate for positions -10° and 20° of cutwater. Parrondo-Gayo et al (2002)

3.3 Pressure Pulsation Investigations

An early theoretical study of pump noise by Simpson et al (1966) showed that there was a relationship to the static pressure fluctuations in the area of the volute exit. The investigation looked at the effects of pump load, cutwater and pump speed on noise levels within the pump. The paper concludes that the theory shows pump noise is due to the interaction of circulations around the impeller and volute and the vicious wake developed from the impeller. The paper is not just

concerned with the noise levels from the pump but comments that the fluid containing structures vibrate as a consequence of the pulsating behaviour of the fluid. This can lead to impeller fatigue. The work seeks to demonstrate the interaction of blade and shaft frequency however this was not successful based on theory alone.

An experimental study by Ivanyushin et al (1987) shows how the geometrical parameters affect pressure pulsations in a single stage high-speed pump. The concerns are when the rotational speed is increased the pressure pulsations increase. This then causes damage to fluid containing structures such as the impeller and volute as discussed by Simpson et al (1966). The radial gap used ranged from 4-6% of the impeller radius and the angle positioning of vanes at impeller outlet 22-25˚. The variants for the experiment were the change of distributor width. The investigation showed that the pressure pulsations were greatest when the distributor width was smallest.

Guelich and Bolleter (1992) investigate the design factors that are influential to the generation of pressure pulsations. The work consisted of 36 tests with different pump configurations. It is stated that the test results are valid for the pumps used in the tests and the results are dependent on the pump system and operation, therefore the statistical data is useful for similar studies as a comparison. The work gives a list of parameters influencing pressure pulsations, the characteristics of those pulsations and their effects. A thorough comparison of their results and recommendations are tabulated and referenced where appropriate, which gives an excellent summary of the current work that was evaluated experimentally. The work demonstrates the use of scaling for practical purposes. It is a square law between pressure pulsations and impeller velocity so scaling of any test data for a given size and speed pump. While there are limitations it appears useful for such an experiment as it shows good agreement with pressure spectra for given speeds and it has been adopted in other studies such as a work by Rzentkowski (1996).

It is stated that low-level pressure pulsations are unavoidable and are not detrimental to the pump, unlike high levels, which can be severe and damaging

to pump components. However, there is no given scale to what is a low level of pressure pulsations due to lack of standards regarding overall pressure pulsation limits. The measurements for the pressure pulsations were taken at the suction and discharge nozzles, which is limited as the area of significant pressure pulsations is in the region of the cutwater and therefore does not give an assertion for pulsations in regions away from the measured point.

A further study into influencing design factors was conducted numerically by Timouchev (1998). The study showed good validation between numerical and experimental results and shows agreement with Rzentkowski (1996); the dynamic loading on the cutwater depends much on the gap between the impeller and cutwater. A later study into a medium specific speed pump by Timouchev (2005) gives a precise prediction of the pressure pulsation in the volute casing using 3D numerical methods. Again, the demonstration of reducing the radial gap results in higher amplitude of vibration at the blade passing frequency. The influence of flow rate was also conclusive. At minimal flow (30% of BEP) rotor vibrations and their harmonics dominates the spectrum but as the flow is close to BEP then the blade passing frequency is the main frequency in the spectrum.

A detailed review following on from Chu et al (1992a and 1992b) for generation and control of pressure pulsations emitted from centrifugal pumps was published by Rzentkowski (1996). The paper explores the parameters within the pump in order to control pressure pulsations. These include volute lip clearance, geometry of the volute casing and volute tongue, impeller geometry, uniformity of the flow passage areas and eccentricity of pump impeller most of which were already recommended in earlier work by Guelich and Bolleter (1992). The main influence suggested to reduce pressure pulsations is the gap between impeller and the cutwater, however it is stated that too big a gap causes excessive flow recirculation.

One of most recent and relevant to this study is work carried out by Spence and Amaral-Teixeira (2006, 2007 and 2008). The work consists of a thesis and two papers which numerically investigate the pressure pulsation in a centrifugal pump. Discussed here, are the geometric variations which have been

investigated. These include cutwater gap, vane arrangement, snubber gap and sidewall clearance. A total of 27 transient analyses were evaluated incorporating 3 flow rates. A complete pump model of a double entry, double volute centrifugal pump was simulated, which incorporated leakage flow paths. The results showed that the most effective parameters were the cutwater gap and vane arrangement. Figure 12 shows the greatest pulsation occurring just before the pressure surface of the impeller blade passes the cutwater. The influence of the cutwater gap has been previously reported in earlier research. The findings show that the snubber gap and sidewall clearance have little effect on reducing the pressure pulsations. The author gives an “optimised” arrangement to reduce pressure pulsations they are as follows:

- The minimum cutwater gap should be 6% of the impeller diameter
- The vane arrangement should use a 30° stagger
- The diameter of the snubbber gap should be approximately 0.64% of the impeller diameter.
- The sidewall clearance should be 100% based upon a sidewall clearance of 12mm (Spence and Amaral-Teixeira 2008)

These recommendations are given to increase component life and to reduce vibration and noise emission from the pump.

Barrio et al (2008) presented a study evaluating the effectiveness of increasing the cutwater clearance in order to reduce pressure pulsations and loads exerted on the impeller. Varying the cutwater clearance has been reported by Dong et al (1997), Chu et al (1995), Spence and Amaral-Teixeira (2006), Gueilich (2002), Morgenroth and Weaver (1998), to name just a few. The focus of the paper is to extend the work done in an earlier paper by Gonzalez et al (2006) discussed in section 3.4.

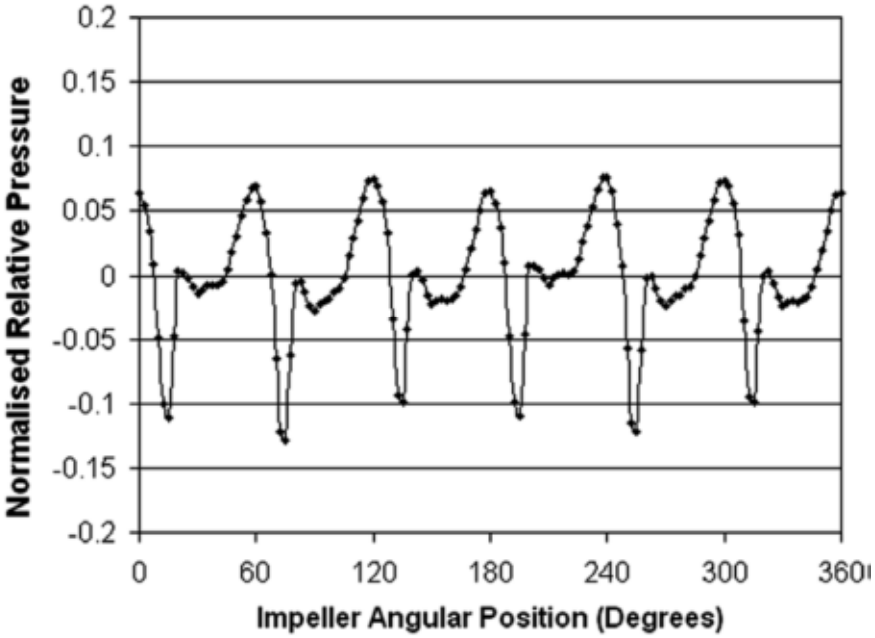

Figure 12 Output from CFD analysis providing time history of normalised relative pressure at cutwater. Spence (2009)

3.3.1 Pressure Pulsations and System Interaction

So far pressure pulsation generation and propagation and methods to reduce their effects have been discussed. This section is interested in how the piping system is affected by pressure pulsations.

Kuiken (1988) investigated the amplification of pressure fluctuations due to fluid structure interaction. It showed that if the excitation forces (interaction of guide vanes or impeller vanes in turbo machinery) generated coincide with the Eigen frequencies of the network system, this results in excessive and destructive vibration in the pipeline network.

Goto (1990) investigated the pressure pulsations in a centrifugal piping system and states that the pressure pulsation phenomenon is initially the generation of that pulsation and then the propagation of its oscillations. Goto (1990) concluded

that the pump is the primary source of the pressure pulsations and there is no evidence that the piping system is influential. The generation and propagation of the pressure pulsations is measured separately and it is the propagation of the waves which are of interest. The waves transmitted in the pipeline are related to the speed of the impeller tip. Although the pulsations are measured and can be obtained by calculation the author fails to suggest how it is actually affecting the piping system.

An experimental study into pressure pulsation excitation was performed by C.A.F De Jong et al (1995). The findings show that the system response characteristics are dependent on the source characteristics and therefore it is important to consider pressure pulsations when designing piping systems. While the method used successfully models pressure pulsations as a source the findings from the experiment are limited and it is evident that the method fails for some frequencies.

A similar study was conducted by Morgenroth and Weaver (1996). Their work like C.A.F De Jong et al (1995) focuses on the excitation of pressure pulsations in a centrifugal pump and how it affects the piping system. The study focused on the blade passing frequency and analysed the amplification of that frequency as an acoustic source at varying flow rate and pump speeds. Interesting modifications were made to the cutwater and it was concluded rounding the cutwater tip without any clearance changes successfully reduced the amplitude of acoustic pressure fluctuations. It is discussed that the pressure pulsations in a piping system can cause acoustic resonance and can lead to damaging effects of system mechanical components. However, this was not successfully concluded due to limited data obtained.

A later study by Rzentkowski and Zbroja (2000) reports on how pressure pulsations propagate away from the source in the form of standing waves, which induce excessive vibrations. These vibrations lead to stresses within the system. The method used was applied to a single stage double volute pump. The experiment shows that the pump variables lead to changes in acoustic pressure fields but appear to be free of acoustic resonance. Their method of assessing system behaviour appears favourable to previous methods.

Ismaier and Schlücker (2009) investigated the fluid interaction between water hammer and centrifugal pumps. Pressure surges influenced by centrifugal pumps has been disregarded, most attention has been with positive displacement pumps Vetter and Seidl (1989 and 1993). The experimental results show that the pressure pulsations sourced at the pump can interact with pressure waves caused by a valve. The result causes amplification and damping effects. They recommend that pressure pulsations should be considered for critical applications to avoid severe mechanical loadings on pipe systems.

3.4 Rotordynamic Effects due to Rotor Stator Interaction

Many experimental studies have been published regarding impeller vibrations, in particular excitation forces on the impeller. Hydrodynamic excitation forces acting on the impeller contribute to the destabilisation of the pump rotor, during specific running conditions, which has been established theoretically (Colding-J0rgensen, (1980,1989), Allaire et al (1982), Adkins and Brennen, (1988), Tsujimoto et al., 1988) and experimentally (Chamieh et al., (1982), Jery et al., (1984), Ohashi and Shoji, (1987), Adkins and Brennen, (1988)). Adkins and Brennen, (1988) isolated the impeller volute interaction effects from other influences, in order to measure the impeller forces accurately.

Bolleter et al (1987) show that the hydrodynamic forces generated by a vibrating impeller can be described in terms of standard rotor dynamic mass stiffness and damping matrices. However, the direct damping term was replaced by a value proportional to the displacement rather than velocity.

Guelich et al (1986) produced a detailed review of the parameters influencing hydraulic forces on centrifugal impellers. They state many publications have concentrated on single entry impellers and less information has been published regarding the influence of operational parameters and geometric considerations.

Various methods for measurement of the hydraulic thrust forces transmitted to the rotor were presented; these are the measurement of bearing forces, shaft deflection or shaft stresses. The advantages and disadvantages are also presented for each method.

Fongang et al (1998) investigate the hydrodynamic forces exerted on a rotating impeller. The model used for the experiment, was a distribution of unsteady vortices replacing the impeller periphery and volute contour, where the impeller centre is assumed to exhibit a whirling motion about the rotor centre. The results give good prediction when compared to Colding-Jorgensen (1980) , Chamieh et al (1985) and Adkins and Brennen (1988) experimental and theoretical results. The calculated results illustrate a stalled angular region in the impeller. This is due to volute asymmetry at off-design flow. Other observations include the destabilisation effect of the impeller on the pump rotor. Other analytical studies with similar conclusions are Domm and Hergt (1970), Lorett and Gepalakrishnan (1986) and de Ojeda et al (1995)

Baun et al (2000) investigated the hydraulic force characteristics of a circular volute centrifugal pump. They varied the impeller location within the volute to examine the effects of impeller volute relative position on hydraulic performance and hydraulic forces. Several flow rates were examined incorporating both design and part load flows, within circular and spiral volutes. They concluded that the impeller volute relative position largely affects hydraulic performance and radial hydraulic force characteristics. At optimum relative position a 5 to 3 percent increase in efficiency and reduced radial force were reported. Figure 13 shows radial force contour plots illustrating the change in force resulting from the change in relative position of the impeller to volute. A comparison of the two force contour plots indicates that as the flow coefficient changes the hydraulic centre shifts and that the force gradient has decreased. The authors state that the tests were only conducted for a single specific speed impeller and therefore further testing would be required to determine if the observed optimum location was consistent for various impeller shapes.

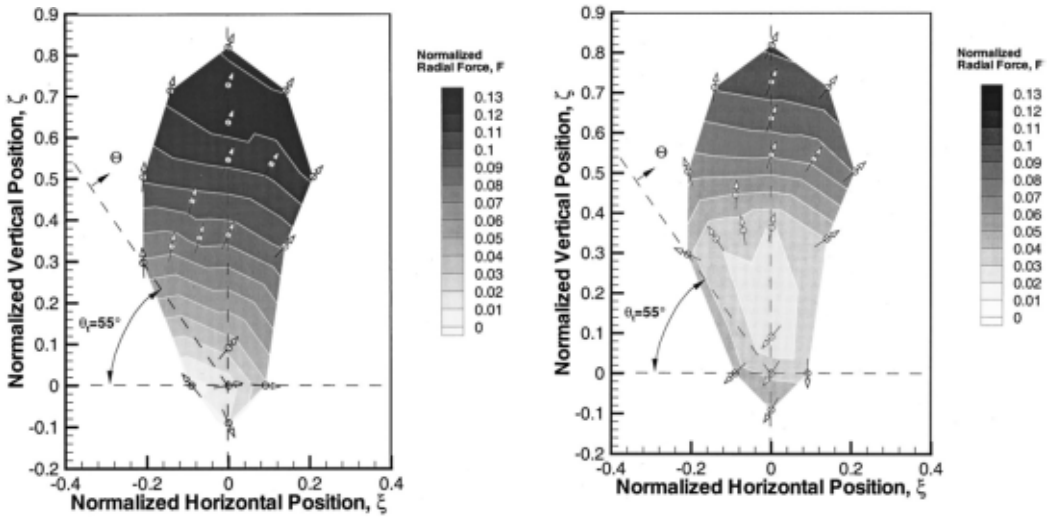

a) b)

Figure 13 Non-dimensional resultant radial force contours plots a) at flow coefficients 0.0 and b) at flow coefficients 0.75 Baun et al (2000)

Guo et al (2006) investigated the fluid forces induced by rotor stator interaction involving variants of guide vanes, flow rates and rotational speed. They conclude that fluid forces propagate in the direction of the pressure fluctuations and the fluid forces results in shaft vibration and fatigue of the impeller.

Benra et al (2006) investigated numerically the determination of pump impeller deflections as a result of hydrodynamic excitation forces. Benra et al incorporated a Fluid Structure Interaction (FSI) technique combining CFD with structural FEA. A one way coupled simulations and a full coupled simulation of the fluid dynamics and structural dynamics were carried out for a single blade pump. The conclusions drawn were that for the one way coupled method, a strong underestimation of the deflections, was given. A successful simulation for the full coupled simulation gave good agreement with experimental data.

Gonzalez et al (2006) and an extension of the work, Barrio et al (2008) experimentally and numerically investigated the effect of reducing the radial blade-tongue gap on the total fluid dynamic loading on the impeller. Four impellers were investigated, thus giving four radial gaps of 8.8%- 23% of the

impeller radius and at five flow rates. The findings show that at “off design” conditions and by reducing radial gap to form the maximum to minimum clearance, the unsteady radial forces are increased by a factor of 2.8 for low flow and 3.8 for high flow. Orbit plots were generated for the partial radial force on the impeller obtained from the integration of the pressure fluctuation data. This is shown in Figure 14. It can be seen from the orientation of the ellipses that there are some discrepancies. No attempt has been made to establish what effect the greater radial forces have or what loads are excessive.

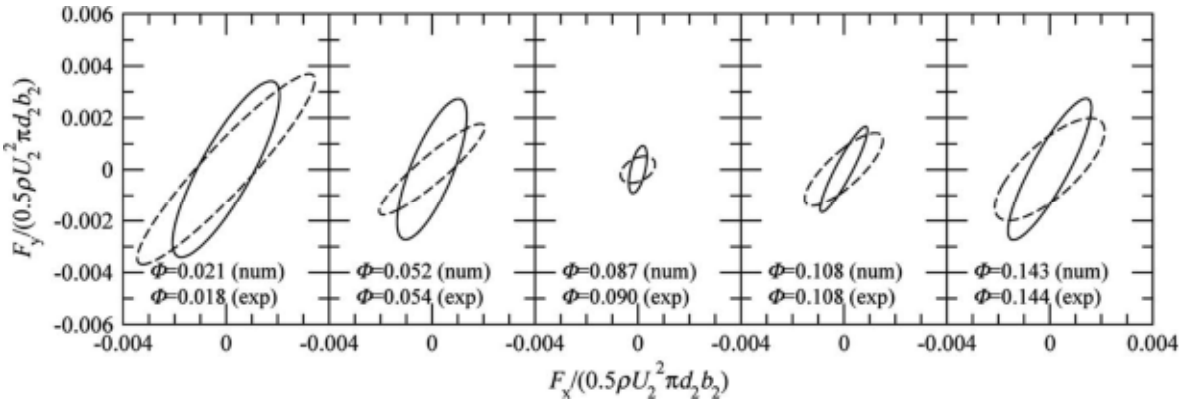

Figure 14 Orbit plot showing the predicted and experimental partial radial forces on the impeller, for the impeller with the greatest diameter, shown for each flow rate. Barrio et al (2008)

3.5 Computation of Flow Physics within Centrifugal Pumps

It wasn’t until the nineteen-eighties that CFD codes were incorporated in turbo machinery research. For industrial applications it is fairly complex to computationally model turbulent fluid flows found within centrifugal pumps. With advancing computational power and greater accuracy of CFD codes a reliable source of numerical investigations is presented in this section.

One of the earliest respected CFD work using CFX-TASCflow was carried out by Graf et al (1993). Graf et al performed a 3-D computational analysis of a blade channel. For “on design” analysis they show good agreement with experimental data however for “off design” conditions validation was limited.

Cooper et Graf (1994) published work, using CFX-TASCflow, to analyse the flow in a single blade impeller passage and stationary crossover separately. They captured suction and discharge recirculation at flow rates 5%-21% of the BEP. The paper also gave typical solution times related to grid size and the relevance of including all regions that may affect flow in the model. The authors’ illustrated CFD’s capability have been integrated into the design process.

Miner (2000) investigated the use of coarse grids to assess and predict an impellers performance. The meshes consisted of 22000-40000 nodes. In comparison to finer grid densities the results of the study show a close correlation of the velocity and pressure profiles. The greatest differences were reported in the prediction of the tangential velocity and it is noted that this is due to the downstream boundary conditions. The study shows the effectiveness of incorporating CFD in a design optimisation stage in industry. The work is agreeable with a paper produced by Cheah et al (2007) which also states for performance characteristics there is no significant difference between using fine and coarse grids.

CFD studies focusing on interaction affects of volute type machines or diffuser type machines are far more complex, with considerable computation times. Chen and Liaw (1997) presented an “on design” CFD study concerning the interaction affects between the rotor and stator. They performed a full transient computation simulation of a four bladed impeller within a volute, employing the frozen rotor interface between each component. In order to reduce computation time flow results were taken each 18 degrees of revolution. Observations are agreeable with LDA and PIV measurement studies showing at design flow there is no flow separation at the cutwater and that the flow rate in the impeller passages are independent of the position within the volute. Chen and Liaw also provided

predicted radial force data which is valuable when considering rotor dynamic and vibration effects.

Shi and Tsukamoto (2001) conducted a numerical study for the prediction of pressure fluctuations caused by impeller–diffuser interaction. They concluded that impeller–diffuser interaction is caused largely by potential interaction and wake impingement with the diffuser vanes. Other observations from the simulations include that the ‘jet-wake’ flow structure at impeller discharge affects the wake–diffuser interaction, but it is stated that it accounts for a relatively small amount compared with stronger viscous wake interactions in the pump.

Timouchev (2005) presents a comparison study of a 2D and 3D numerical assessment of the pressure pulsations generated in a medium specific speed pump. To capture the pressure pulsations, the rotor/stator interface option was used. It is demonstrated by the author that the 3D predictions show good agreement with experimental data where as the 2D predictions show underestimated results for the blade passing frequency amplitude.

Asuaje et al (2006) investigated the velocity field, pressure and radial thrust distribution within a single stage centrifugal pump. The three dimensional quasi unsteady flow simulations comprised of a range of turbulence models and presented a grid sensitivity study. While the authors show their results are in agreement with Gonzales et al (2002) it appears they have merely repeated work already noted by Gonzalez et al (2002) and Dong et al (1997).

Spence and Amaral-Teixeira (2008,2009), previously discussed in section 3.3, performed extensive 3D CFD analysis using CFX-TASCflow of an entire double entry, double volute centrifugal pump. The total analysis time is stated to equate to a total of 45,000 hours computation analysis time. The authors also ensured leakage flow paths were included into the model. The entire pump model consisted of a total of 870,500 hexahedral elements. The correlation of the results with experimental data shows good agreement at duty conditions and slight deviation at lower flow rates, which appears to be common to all CFD literature cited.

Cheah et al (2007) presented work simulating unsteady flow of a centrifugal pump at “on design” and “off design” conditions, however the analysis was under steady state conditions and does not give any indication of validation of the unsteady flow characteristics reported.

A group of researchers at the University of Oviedo in Spain have published several papers both experimental and numerical. The CFD investigations are discussed here. Further to initial experimental and 2D validation work by Parrondo-Gayo et al (2000,2002), detailing investigations concerning pressure fluctuations within a centrifugal pump, Blanco-Marigorta et al (2000) investigated the pressure fluctuations at the blade passing frequency utilizing a 3D numerical model. The authors state that in order to achieve greater accuracy, it is advised to specify and control the total pressure inlet condition. However, they also note at low flow conditions it results in poor convergence, less stability and increased analysis time. A reasonable conclusion for this is the impeller volute interaction and generation of pulsations.

Gonzalez et al (2000,2002) produced two papers of a three-dimensional transient simulation capturing the dynamic effects due to impeller volute interaction, using a sliding mesh technique. They successfully validated results for prediction of the amplitude of the blade passing frequency for various flow rates, although only at 60% of design flow and higher. It is not stated whether this is to do with convergence issues reported in a previous paper by Blanco-Marigorta. The study however does provide a model for dynamic interaction predictions. The numerical model consisted of 330,000 cells for the entire pump model. This is relatively course when compared with recent studies although larger than that detailed by previous authors at that time. As discussed in section 3.3, Barrio et al (2008) investigated the fluid dynamic pulsations and dynamic radial loads exerted at the blade passing frequency. The authors employed a Fluent code and the sliding mesh technique to obtain numerical pressure fluctuating data, which allowed the authors to estimate the radial forces and torque as a function of flow rate and varying cutwater clearance. Like previous research difficulties were discussed

with low flow predictions when compared with experimental data. The CFD study at duty conditions, successfully capture the blade-volute interaction effects.

3.6 Pump Rotordynamics Investigations

The pump rotating element is the origin of energy transfer and the source of vibration excited by the pump Gulich (2008). The reliable prediction of shaft vibration and limitation of hydraulic excitation forces are therefore important for the safe operating of high energy pumps.

The speed range of pumps has increased to provide greater flexibility on pump operating point and to achieve higher efficiencies in an overall lighter package. Rotordynamics has therefore become an important aspect of the pump design process. Pump rotordynamic problems, frequently manifest as wear and failures of bearings, seals and impellers Corbo et al (1998).

Pumps in the field suffer fewer failures due to rotordynamic problems in comparison to other turbomachinery Nelson (1987). It is noted that wet critical speeds are not normally observed due to the significant damping providing by the annular seals and from the pumped liquid. Pace et al (1986) state that even at worn conditions there is enough damping to prevent operating near a critical speed.

Corbo et al (1998) and San Andres (2006) provide a comprehensive introduction to pump rotordynamics. Both publications provide a detailed methodology for assessment of lateral vibrations that can occur in pumps. Recommendations for modelling of annular seals and impeller interaction forces are also discussed.

San Andres (2006), provide an example of a rotordynamic investigation of a multistage pump. Assumptions were made regarding the impeller interaction forces and the author recommends verifying the predictions with test data. Childs (1993) suggests the linearized model, (equation 2.3), for representing impeller volute interaction is inadequate for part load conditions.

A critical speed analysis was carried out on an eight multistage centrifugal pump by Atkins et al (1985). Four prediction methods were evaluated against experimental data. Particular attention was paid to the fluid seal effects. It was concluded that there was a significant variance between methods for estimation of seal properties. The most comparable results with experiments was utilising the finite-length method developed by Childs-Kim (1985). It is noted further research is required to understand fluid seal effects and the modelling techniques which should be applied.

Agrati and Piva (1999) investigate the rotordynamic and structural advantages of a two types of impeller configurations for a horizontal boiler feed pump. The two designs analysed are the back to back impeller arrangement and the inline impeller design. A complete calculation of the rotordyanmic behaviour is presented. The method employed for the investigation is finite elements. The conclusion to the investigation was the back to back impeller arrangement design was less sensitive to increase in clearances as it was found the damping factor remained high and would therefore be a more reliable pump design.

An extensive numerical investigation was carried out by Simon and Frene (1989) concerning the static and dynamic characteristics of annular seals. The research provides advancement in the capability of “Reynolds- equation” models for analysing turbulent seals, carried out using computational fluid dynamics (CFD). The authors note there are limitations with the technique as the analysis approach does not allow for added mass coefficients. They show for a taper geometry an increase in direct stiffness is observed, this is in agreement with Childs (1993). The CFD approach, limits the assumptions made in other methods, for smooth seals the results are comparable with bulk flow predictions, similar finding was published by Nordmann et al (1988). However, the time required for CFD modelling is considered to be extensive.

Ghoneam et al (2011) investigate the dynamic performance of a centrifugal pump operating at range of speeds and controlled through a Variable Speed Drive (VSD). The experiment consisted of experimental modal analysis and operation modal analysis to establish the dynamic behaviour. It is concluded that vibration

increased slightly with speed and no resonance condition was observed. There was inconsistency between techniques although these values were not noted in the paper. Due to the discrepancies it is unlikely this method could not be employed at design phase for variable speed pump application.

There have been many publications evaluating rotordynamic analysis methods such as transfer matrix and finite elements method (FEM). Computer algorithms are employed for calculating a systems undamped and damped critical speeds, unbalance response and stability Nelson (1987), Ozguven and Levent Ozkan (1984), Genta (1988), Jei and Lee (1992). Mohiuddin and Khuief (1994) provide a comparison of FEM model and experimental results and illustrates the computational trade off which can arise for complex geometry, for simple geometry there is good agreement between results.

3.7 Chapter Summary

From the literature cited it can be determined there is scope for further work concerning hydraulically induced vibration and to what extend it transmits into destabilization of the pump rotor, leading to reduced pump integrity.

There have been some extensive pressure pulsation investigations (Spence and Amaral Teixiera, Guliech and work done by the University of Oviedo of Spain) illustrating the need to consider pressure pulsations when opting geometrical parameters of hydraulic components as well as the effect of operating point on pressure pulsations. Less focus has been in relating the pulsation effects to the vibrations found the bearing housing and other mechanical components.

Attempts have been made to assess the radial loadings on the impeller discussed in section 3.4, although more work is needed in order to establish a design method. Benra using FSI modelling was able to couple the fluid and structure interaction, while this technique captures the hydraulic vibration and structural

response there were some underestimations reported indicating further work is required before the method can be adopted in industrial pump applications.

There are a limited number of publications concerning pump rotordynamics. This is most likely due to the fact the “wet” critical remains above the operating range for the majority of pump designs. However, it is well documented in literature as pumps move away from the BEP, the vibration, typically measured at bearing housing increases significantly and can be outside acceptable limits. Multistage pumps are at greater risk of reduced integrity if duty conditions are changed. There is greater attention to performing lateral analysis during design phase; an observation is the current methodology does not incorporate the hydraulic forces generated by impeller-volute interaction. The accuracy of radial load estimations is dramatically reduced for part load operation, and inclusion within a rotordynamic analysis, further research is required within this field.

CFD can provide a wealth of information as pressure is calculated for each grid element within the model whilst experimental investigations are limited to specific locations. This provides an opportunity to capture pressure pulsation data and hydraulic force data acting on components at multiple locations. There are numerous difficulties in obtaining good experimental data for pressure pulsation studies and there are limitations as results can only be obtained for specific locations. Parrondo- Gayo et al (2002) state that pressure pulsations vary significantly depending on location.

The survey on numerical investigations cited of similar centrifugal pumps provide good insight into the modelling techniques for simulating the fluid flow and capturing pressure pulsation data which has been considered when developing the strategy for the present study. Particularly for low flow investigations the literature review has reported upon the common findings of the flow fields at this operating condition. Literature cited of experimental investigations such as Kaupert and Staubli (1999) and Parrondo- Gayo et al (2002) provide background to experimental technique to capture unsteady pressure fluctuations where good agreement with numerical studies have been reported upon. Details of test

apparatus, measuring uncertainty and test programmes are all fields which ensure a suitable method is developed for the present research.

In summary the four key areas, low flow investigation, rotor-stator interactions and pressure pulsations, computation fluid dynamics applied to centrifugal pumps and finally pump rotordynamics have been reviewed providing knowledge and guidance on direction for the present research. CFD is reported to be a useful tool for capturing pressure pulsation data although it is essential whilst new methodologies are being developed validation with experimental data is required. Research efforts related to pressure pulsations have led to sophisticated guidelines, despite this work a methodology for predicting amplitudes of pressure pulsations are absent, along with quantification of the resultant vibration transmitted to seals and bearing locations within a pump

4 Modelling Aspects for a Simulation of a Single Stage Overhung Pump

In this chapter a brief introduction to the commercial CFD package used for the numerical work and the appropriate theory to CFD is provided. Thereafter a numerical model of the single stage overhung pump at nominal flow is presented. Details of the assembled model such as properties and boundaries are outlined and the solution parameters chosen for the analyses are specified.

4.1 Introduction

The aim of the simulation of the single stage overhung pump is to obtain the radial hydraulic force data numerically with the objective to feed the data into a rotordynamic model as outlined in section 1.1. The chosen pump for the numerical work is a commercial pump within the SPXFLOW clydeunion pump OH2 Overhung type 2 product range. A test pump is available for experimental testing for validation purposes of the CFD code which is provided by the sponsor.

To capture the unsteady interaction effects a complete pump model incorporating all of the major flow paths is mandatory and a fully transient simulation using a CFD code is required. However, this is a fairly broad process and requires extensive computation time. For the purpose of the present study and to suitably meet the aims of the present research a simplified model consisting of three domains, an inlet pipe, impeller and volute (neglecting leakage paths) is investigated.

The CFD code employed in the present study is ANSYS CFX in its version 14. CFD involves a number of stages and are outlined as follows: -

- Creation of geometry- BladeGen / CAD
- Grid generation- CFX Turbogrid / ICEM

- Pre-processing-CFX Pre
- Investigation and solution- CFD Solver.
- Result report and visualisation- CFX Post

4.2 CFD Theory

The mathematical basis of fluid dynamics is constructed from three physical laws, conservation of mass, momentum and energy. CFD software provides a 'Navier-Stokes' solution which is essentially a viscous flow problem applying the full governing equations. This numerical solution is an acceptable algebraic approximation to these equations describing the fluid flow.

The following section provides the briefest of introduction to CFD theory. It is recommended for background information and for a full derivation of the governing equations, published work should be referred to such as Andersons (1991) and Versteeg and Malalasekera (1995).

4.2.1 Basic Equations

The physical laws governing the movement of fluids are shown in this section in the final derived state.

4.2.1.1 Conservation of Mass

The governing equation for conservation of mass defines the transfer of mass flow into and out of a control volume. The final derived state is shown here for incompressible flow:

$$\frac{\partial u}{\partial x}+\frac{\partial v}{\partial y}+\frac{\partial w}{\partial z}=0$$ **Equation 9**

4.2.1.2 Conservation of Momentum in Three Dimensions

Newton's second law describes that the rate of change of momentum of a particle is equal to the sum of the forces acting on the particle.

The two types of forces exist on fluid particles

- Surface forces
  - Pressure
  - Viscous
- Body forces
  - Centrifugal
  - Coriolis

The derivation of the momentum equation can be found again in Versteeg and Malalasekera (1995) but the final equation is shown in equation 9.

$$\rho\frac{Du}{Dt}=\frac{\partial\left(-p+\tau_{xx}\right)}{\partial x}+\frac{\partial\tau_{yx}}{\partial y}+\frac{\partial\tau_{zx}}{\partial z}+S_{mx}$$ **Equation 10**

-p :- Compressive pressure

τ :- viscous stresses in j direction

Smx :- Source term including the body forces

$\frac{D}{Dt}$:- derivative following the fluid, including local unsteady and convectional accelerations which can also be written for y and z directions.

The inclusion of the viscous stress, require a methodology for the solution of these unknowns.

This methodology, for a Newtonian fluid, supposes that the individual viscous stresses are proportional to the rate of change of deformation of a fluid element. The viscous stresses can be written as:

$$\tau_{xx} = 2\mu \frac{\partial u}{\partial x}$$ **Equation 11**

Given for the x direction. This represents the result of linear elongation, deformation

$$\tau_{xy} = \mu\left(\frac{\partial u}{\partial y} + \frac{\partial v}{\partial x}\right)$$ **Equation 12**

$$\tau_{yz} = \mu\left(\frac{\partial u}{\partial z} + \frac{\partial w}{\partial x}\right)$$ **Equation 13**

These shown above represent the effects of linear shearing deformation where:

μ :- dynamic viscosity

The equations 10,11 and 12 shown above can be substituted into the momentum equation to provide:

$$\rho \frac{Du}{Dt} = -\frac{\partial p}{\partial x} + \frac{\partial}{\partial x}\left(2\mu \frac{\partial u}{\partial x}\right) + \frac{\partial}{\partial y}\left[\mu\left(\frac{\partial u}{\partial y} + \frac{\partial v}{\partial x}\right)\right] + \frac{\partial}{\partial z}\left[\mu\left(\frac{\partial u}{\partial z} + \frac{\partial w}{\partial x}\right)\right] + S_{mx}$$ **Equation 14**

This is generally re-written as

$$\frac{\partial u}{\partial t} + div(uu) = -\frac{1}{\rho}\frac{\partial p}{\partial x} + \upsilon divgradu + Smx$$ **Equation 15**

υ :- kinematic viscosity

The substantive derivatives $\frac{Du}{Dt}$ and $\frac{\mu}{\rho}$ have been split into a local unsteady acceleration $\frac{\partial u}{\partial t}$ and a convective acceleration div(uu), where uu represents the divergence of a second order tensor field which is acting on separate components of the velocity field

The y and z components of the Navier-Stokes equations can also be derived in this way.

Four equations are generated for the mass conservation and the three Navier-Stokes equations. These can be solved for four unknowns.

4.2.2 Turbulence Modelling

The numerical solution is described as an approximation to fluid flow equations as the turbulent flows in centrifugal pumps provide a level of complexity which surpasses present computer capability. A turbulence model is therefore utilised. The concept of applying a turbulence model describes the replacement of unsteady velocity with a time averaged velocity with turbulence fluctuation. Several turbulence models are available and are listed as follows.

1. $k-\varepsilon$
2. $k-\varepsilon\, ASM$
3. $k-\varepsilon\, RNG$
4. $k-\varepsilon$ With a scalable wall function
5. $k-\varepsilon\, ASM$ With a scalable wall function
6. $k-\varepsilon\, RNG$ With a scalable wall function
7. $k-\omega$
8. $k-\omega SST$

For this reason, it is good practice to investigate the influence of different turbulence model on the quality of the solution. Dyson (2007) carried out an investigation to compare the effect of the different turbulence models listed above had on a centrifugal impeller passageway. The data obtained suggested that the turbulence models have no significant effect on the accuracy of simulating the flow through an impeller. The recommendation was to utilise k-epsilon ($k-\varepsilon$**)** as it is distinguished for being robust. This is agreeable with another similar application Newton (1998).

4.2.2.1 Near Wall Treatment of Turbulent Flows

In the region close to the wall the turbulence is damped and a thin boundary layer exists known as the laminar sub layer. It is important to control this region within the computational solution as the numerical treatment can determine the development of the boundary layer and can influence the onset of separation. Viscous effects with rapid changes in flow across the boundary layer are expected near the wall region, along with strong velocity gradients at the outer part of the near wall zone, all of which must be accounted for. To capture this data a finer grid close to the wall regions is ideal however this vastly increases the solution time. A standard approach is to employ a semi-empirical function which allows a coarser grid to be evaluated. Standard wall functions are available within CFX software these standard functions can be problematic as the tangential velocity approaches zero at the separation point part of the equation becomes singular. An alternative to the standard function is a scalable wall function as employed by Launder and Spalding (1974) which provides a better prediction.

The y^+ is a non-dimensional distance from the wall to the first grid point. When applying a scalable wall function, the y^+ values must be within a certain range to ensure that this point falls within the region of the boundary layer to represent the wall and the full turbulent flow.

The principle of the scalable wall function is to assume that the surface coincides with the edge of the viscous sub-layer. For this condition it is given $y^+ = 11$ and is in the region between the logarithmic and linear region wall profile. The computed y+ is not allowed to fall below this limit.

4.2.3 Grid Generation

The domain in which the Navier-Stokes equations are solved is divided into a vast array of small cells namely elements. This task is not to be underestimated. Poor quality of distribution of cells equates to a less than acceptable approximation of the fluid flow calculations.

The complex shapes of hydraulic passage ways in pump components provide challenges at the grid generation stage in the CFD process. A grid may be generated as structured (rectangular elements) or unstructured (tetrahedrons elements) the latter does impair the desired angle of gridlines at walls. This is an important control as an improvement in accuracy is seen by having as near as achievable perpendicular gridlines to walls. A structured mesh predominantly constructed of layers of parallel elements to walls, the alignment is therefore streamlined and reduces numerical diffusion, Figure 15 shows a structured mesh generated for an impeller passageway. A strategy to reduce the use of unstructured mesh and improve accuracy is to combine the two types of grid generation and limit the unstructured grid to small areas where angles are great, such as a volute lip.

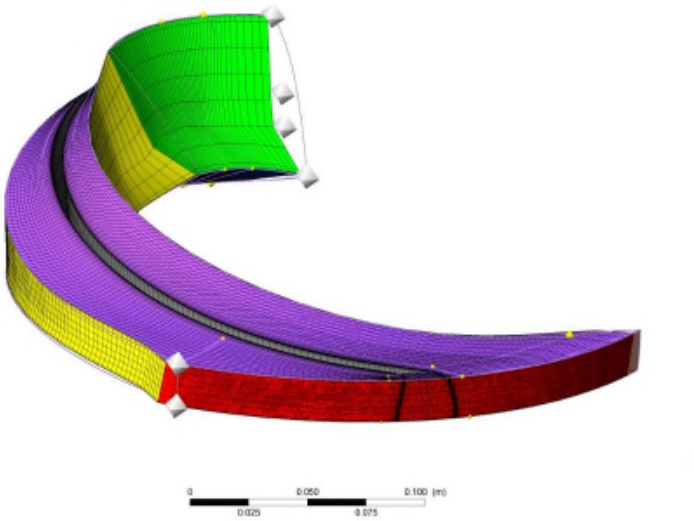

Figure 15 Structured grid of an impeller passage

A fine grid provides greater success in reliable results this does come at a cost as considerable computer processing is required. A strategy must therefore be applied when assessing accuracy vs. time for each application. It is good practice to carry out a grid sensitivity study to determine a reasonable level of accuracy. A grid sensitivity study was carried out on a pump impeller to investigate the effect the grid density has on the impeller flow distribution. A course medium and fine mesh was used consisting of 19341, 111943 and 257312 respectively nodes. The impeller meridional plan is non uniform whilst turning the flow from axial to radial. The velocity distribution is largely effected by the blade design. The inlet, outlet span-wise meridional velocity distribution is important when controlling the inlet and outlet blade angles and to do so the boundary layer effects must be captured. Traditionally the meridional profiles are refined based on empirical analysis and estimations of the averaged flow velocities. The investigation is shown in appendix A, in summary the findings show that the coarse grid did not capture the true meridional velocity profile. The medium and fine mesh showed little difference on the velocity distributions. Therefore, for the present study a medium mesh is deemed sufficient.

4.2.4 Rotor- Stator Simulations

To solve the unsteady interactions between rotating and stationary components numerically three schemes are available.

1. Stage interface
2. Frozen rotor
3. Fully transient

Stage interface applies a circumferential averaging to unsteady interactions. The principle of this technique assumes a substantial relative gap between rotating and stationary parts so that the velocity profile decays before entering the

collector. The gap in centrifugal pumps is relatively small therefore it is not an appropriate technique for centrifugal pump simulation

Frozen rotor scheme is a steady state analysis that provides a snapshot of the flow regime by fixing the relative position of the rotor and stator in time. The calculated performance is consequently dependent on relative position. It does provide a good initial estimation to the solution.

Transient scheme is the ultimate numerical solution. The solution accounts for all interaction effects between components of varying relative motion. Although this type of solution scheme requires large computational resources in terms of processing and disc space computers are advancing at rate whereby this type of analysis could start to emerge in the routine design environment.

4.2.5 Iterative Convergence

For any CFD study convergence is paramount. It is essential it is controlled. Two common ways to ensure adequate control is to insert a maximum number of iterations or set a normalised residual target point. The latter is the most accurate measure of convergence. The residual is the error calculated in a linear system of the discrete equations. Solution convergence can be judged and deemed good practice to monitor the RMS residual. For this study and commonly for transient unsteady cases additional monitors can be viewed to assess periodicity of the time history. For the present simulation the forces acting on the rotor during the CFX solve process are monitored. The forces on the blades will appear fully periodic and it this can be judged as simulation convergence; any further iteration will not change the force data.

4.3 Single Stage Overhung Pump Model

The single stage overhung pump is classified as an OH2 within the SPX product range. The pump is 6x6x14 OH2, describing a six-inch suction inlet duct, six-inch discharge outlet and a fourteen-inch impeller. It has a double volute as shown in section 2.2 in Figure 3. For this simulation the best efficiency flow of 400m^3/ hr was chosen.

The impeller has the following features

Exit diameter	D_2 = 355.6 mm
Exit width	b_2 = 19.05 mm
Entry diameter	D_a = 165.1 mm
Number of blades	Z_r = 5
Blading exit angle	β_2 = 23 deg
Nominal rotation speed	N = 3560 rpm (ω = 372.8 rad/s)
Reference volume flow	Q_n = 0.110 m^3/s
Total head	H_n = 215 m

4.3.1 Geometry Modelling

Three domains are required for this analysis, an inlet pipe, impeller and a collector. Computer Aided Design (CAD) models exist for the impeller and pump casing, these models were provided by the sponsor. The impeller geometry was inputted into CFX bladegen to obtain three data files outlining the hub, shroud

and blade profile curves, each in the polar (r, θ, z) coordinate system. The information is delivered into the meshing profile CFX Turbogrid. To construct the inlet pipe, impeller geometry from Turbogrid has been exported into ICEM CFD. ICEM CFD has a Cad facility it is therefore advantageous to construct the geometry and mesh within one CFD programme. Attention is made to the pipe outlet geometry matching the impeller inlet geometry to avoid numerical error in the interface. The two surfaces must match as closely as achievable, shown in Figure 16 is the profile curves from the impeller used for the design of the inlet pipe. A nose is designed which represents an impeller lock nut, used to secure the impeller to the shaft. It is optimised to have a smooth surface to avoid adding complexity.

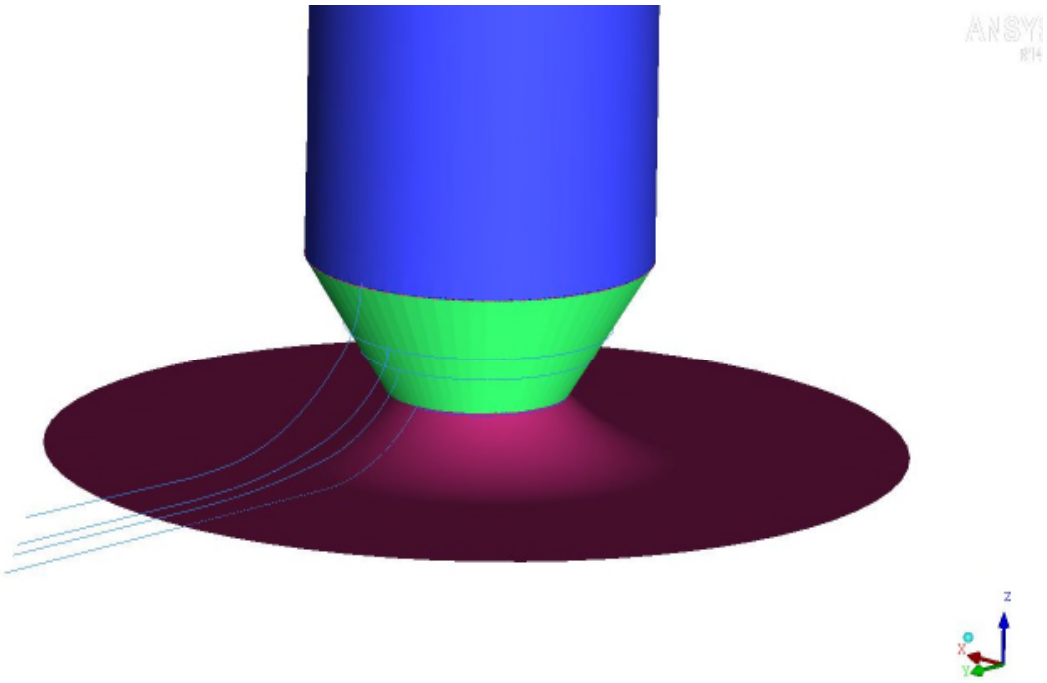

Figure 16 Inlet pipe (blue) with pipe outlet (green) and impeller hub (purple) in ICEM CFD

The author utilised the casing CAD model to obtain the wetted surface area of the collector this was carried out in Solidworks CAD package and imported into ICEM CFD, as shown in Figure 17. To simplify the model, the leakage flow areas are modified into walls and an extension of the outlet pipe is constructed, Figure 18.

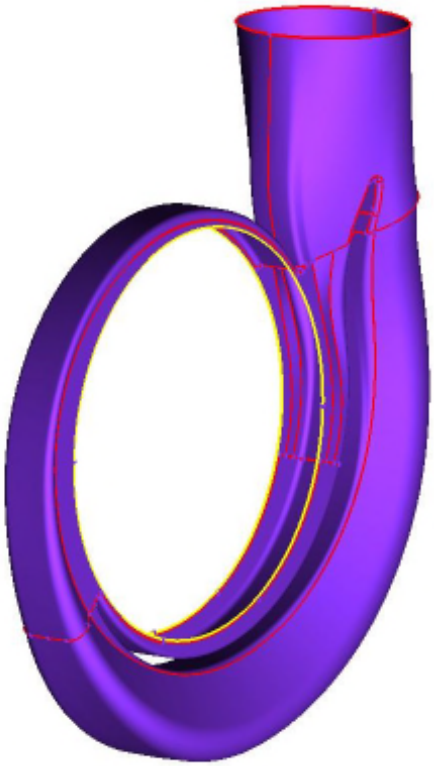

Figure 17 Wetted surface of the OH2 volute

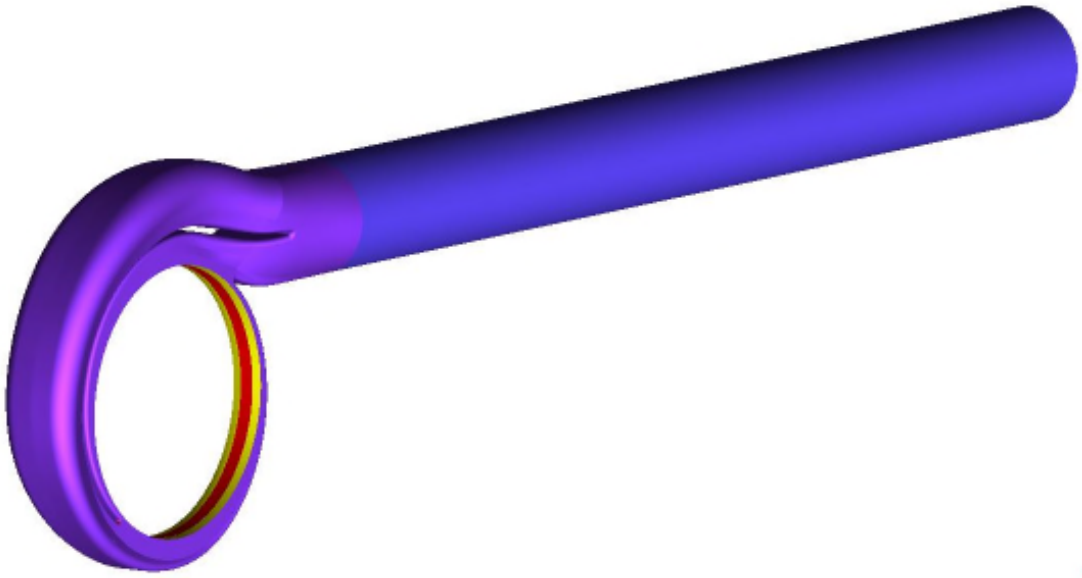

Figure 18 Collector model with inlet (red), wall (yellow) volute (purple) and pipe (blue)

4.3.2 Mesh Generation

Impeller geometry is loaded into CFX-TurboGrid, which is specifically designed to mesh periodic turbo machinery components; a 3D computational grid was assembled as shown in figure 15. CFX-TurboGrid models and generates the mesh of the impeller geometry as a single blade passage. As similar flow characteristics are dominant in every other blade passage of the impeller this method is appropriate. A high quality grid was produced utilizing a single block grid template where a mapping function consisting of H/J/C/L grid was applied. Based upon the grid dependency study outlined in section 4.2.3, a medium mesh density was chosen for the investigation.

The volute and inlet pipe domains were meshed in ICEM CFD. Due to the complexity of the volute design, with sharp angles particularly at the volute lip regions, an unstructured mesh is appropriate. The mesh method exploited is named Octree. It is a robust method where the user may specify minimum and maximum element size within the entire model. Allowing a refinement in certain areas where curve radius is extreme. Firstly, a volume mesh is computed using a tetrahedral element; secondly a prism layer is incorporated at walls. The prism layer improves the solution as the near wall elements are parallel and gridlines perpendicular, to walls. The objective is to have refinement near the volute lip and at the inlet. To reduce computing time a courser mesh is computed in other regions. Figure 19 illustrates the volume elements of the volute on a longitudinal plane.

For the inlet pipe a structured mesh is desired as this can be achieved with minimal effort. However for the initial CFD investigation the same technique applied to the volute has been used for the inlet pipe. This is deemed satisfactory for the simulations for the present study however for greater accuracy a structured mesh would be employed.

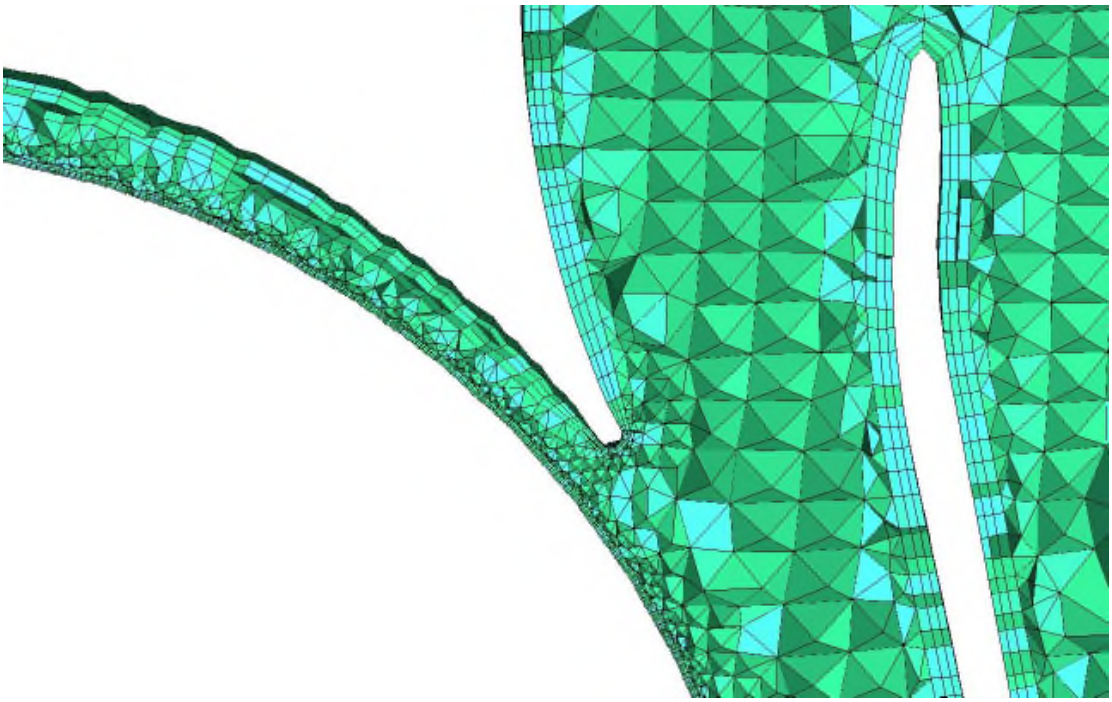

Figure 19 Volute mesh refinement using prism layers

A summary of mesh statistics is shown in Table 1

Table 1 Mesh statistics

	Inlet	**Impeller**	**Volute +Outlet**
Number of elements	258,191	449,560	931,075

4.3.3 Simulation Set-up in CFX Pre

CFX- Pre has a variety of modes for many applications. Turbo mode is specifically designed to handle all turbo machinery simulations. Once the three domains are assembled, the next stage in the set-up is interface definition. The connection of two surfaces in CFX Pre is named General Connection Interface GCI. It accounts for discrepancies in grid matching of two surfaces. A frame change may be applied between a rotating and stationary domain. Two GCI are applied in the model, at the pipe outlet to impeller inlet and impeller periphery to volute inlet.

Boundary conditions additional to interfaces are applied to all parts in each domain. At inlet and outlet boundaries CFX pre has a few options. The most robust is mass flow at the inlet and static pressure at the outlet. Spence (2008) reported on this selection and conducted analysis using this arranged and in the reverse. The findings were that for the arrangement of mass flow at the inlet and static pressure at the outlet was signicantly more stable and converged faster than the reverse. Gonzalez et al (2002) reported similar findings.

In the rotating domain, the impeller, all surfaces are rotating walls.

The inlet pipe is a stationary domain and has three boundaries.

- Inlet to the pipe
    - Mass flow rate 110 kg/m^3
- Outer cylinder is a wall in the reference frame
- Nose is a rotating wall
    - Rotational speed 3560 rpm

The volute domain has an outlet boundary of static pressure at the discharge pipe outlet, all other surfaces are walls.

A pragmatic approach to reduce simulation effort is to run a frozen rotor steady state analysis prior to embarking upon a transient state analysis. The purpose being is to use the frozen rotor result as initial results for the fully transient simulation, hence saving computational time.

A frozen rotor steady state analysis was therefore carried out initially; those results were used as the starting point to run a fully transient simulation. For the transient analysis a study by Koumoutsos (1999) of a five blade, centrifugal impeller/volute interaction using both 500 and 250 time steps per revolution. The conclusion of the study was that the solution was not affected by the time step. The two examples consulted, Guilloteau (2011) and Brodard (2012) both simulate a single stage pump of similar physical size, using 125 time steps per revolution it was therefore decided for the present study a total number of 125 time steps per revolution of the impeller were specified. The studies simulated three complete cycles of impeller rotation with CFX Solver and therefore it was in the present study three revolutions were performed to observe periodic unsteady convergence related to the hydraulic force acting on the impeller.

4.4 Summary of Numerical Results at Nominal Flow

The performance characteristics of the pump are compared to test data and shown in table 2.

Table 2 Pump Performance Comparison at Nominal Flow

Performance Results	Head (m)	Power Absorbed (Kw)	Efficiency %
Test	214.3	293.4	78.3
CFD	214.9	277	83.2

The results show the head calculated in CFD is slightly higher than the measured data taken during testing of the pump. The numerical result shows the absorbed power is underestimated and therefore the machine efficiency is higher. The

efficiency has been obtained numerically from the power ratio, rate of work output to the rate of power in i.e. the hydraulic head divided by the hydraulic power shown in equation 16.

$$\eta = \frac{\dot{m}\mathrm{Pt2} - \mathrm{Pt}}{\rho\, M\omega} \qquad \text{Equation 16}$$

Where

η= is the efficiency from power

$\dot{m}$ is the mass flow through the pump

P_{t2} is the mass averaged total pressure at the pump outlet

P_{t1} is the mass averaged total pressure at the pump inlet

ρ is the density

M is the torques

ω is the rotational velocity

Efficiency for the experimental results is obtained using the same method only the power ratio, rate of work output to the rate of power in from the measured power input from the meter readings of the motor and the gearbox output powers utilising efficiency curves are obtained to provide the pump input power, followed by pump input power calculated by equation 17.

$$P_h = \frac{Q\rho gh}{3600} \qquad \text{Equation 17}$$

The likely underestimation of absorbed power is due to the CFD model being simplified to neglect leakage flow passageways. In addition, the mechanical losses and actual surface roughness is not represented in the CFD simulation. Suggestions to improve the performance deviations by incorporating major leakage paths over a flow range is described in the further work chapter 8.0 of this thesis.

4.5 Discussion on Flow Features

Analysing the fluid flow behaviour inside the pump can offer a measure of verification of the results. The structure of the flow, the location of the stagnation point and the position and extension of the wake are all indications that offer a way of checking the soundness of the simulation. The simulation will also provide visualisation of particular flow features. The most obvious feature to verify first is that of pressure progression as it leaves the impeller periphery and diffuses along the volute passageway. This observation is particularly interesting when several flow rates are analysed as at low flow the classic jet-wake structure will be captured, therefore this will be discussed in more detail later in the study. For now, Figure 20 shows a pressure contour plot in a longitudinal cut. The volute has a split configuration which receives fluid at 180 degrees of the impeller, resulting in a pressure rise around both passageways. This can be seen as fairly equal in both regions of the volute in Figure 20. as the pressure regions are essentially balanced the radial forces acting on the shaft are minimised. Another important observation is that for best efficiency point the velocities at the entire impeller periphery are the approximately the same as shown in Figure 21, this is aim of the hydraulic design of an impeller for BEP. What is also noted is as the volute passage ways, two in this case for the double volute show the high region of velocity is at both cutwaters, which quickly reduces. This is what you would expect as the flow leaving the impeller is decelerated through the volute; hence the pressure increase reaching maximum as the fluid flow exits the volute into the discharge passageways, conforming to the characteristic of kinetic energy conversion to potential energy.

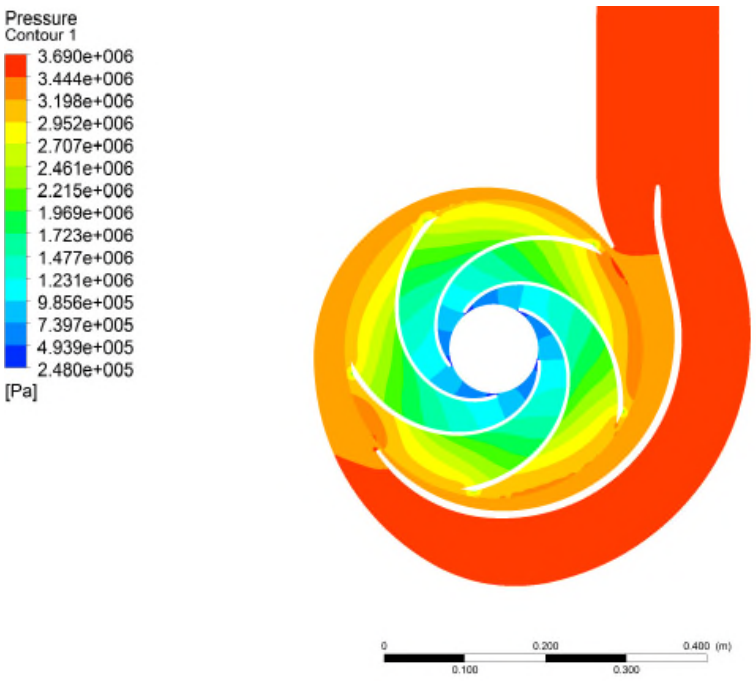

Figure 20 Pressure contour plot on a longitudinal cut for Q_n equal to 1

At BEP flow condition, the flow path follows that of the volute, tangential to the impeller. The only distorted flow ought to be seen at the cutwater. Plotting vectors on the same longitudinal cut confirms this flow behaviour, as seen in Figure 21. At low flow conditions the flow is deflected at the cutwater region, creating energy losses but remains tangential. Contrastingly at high flow rates you would expect to see the opposite occurring, the flow is exerted by a strong radial component leading to recirculation present at the volute exit.

a)

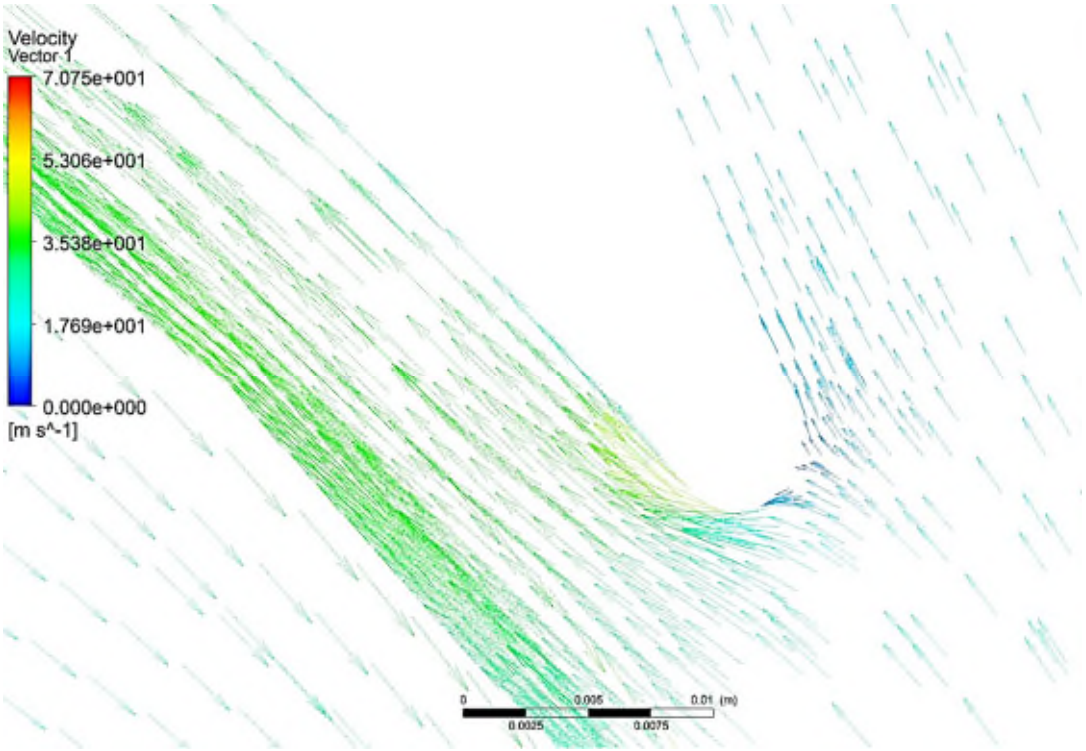

b)

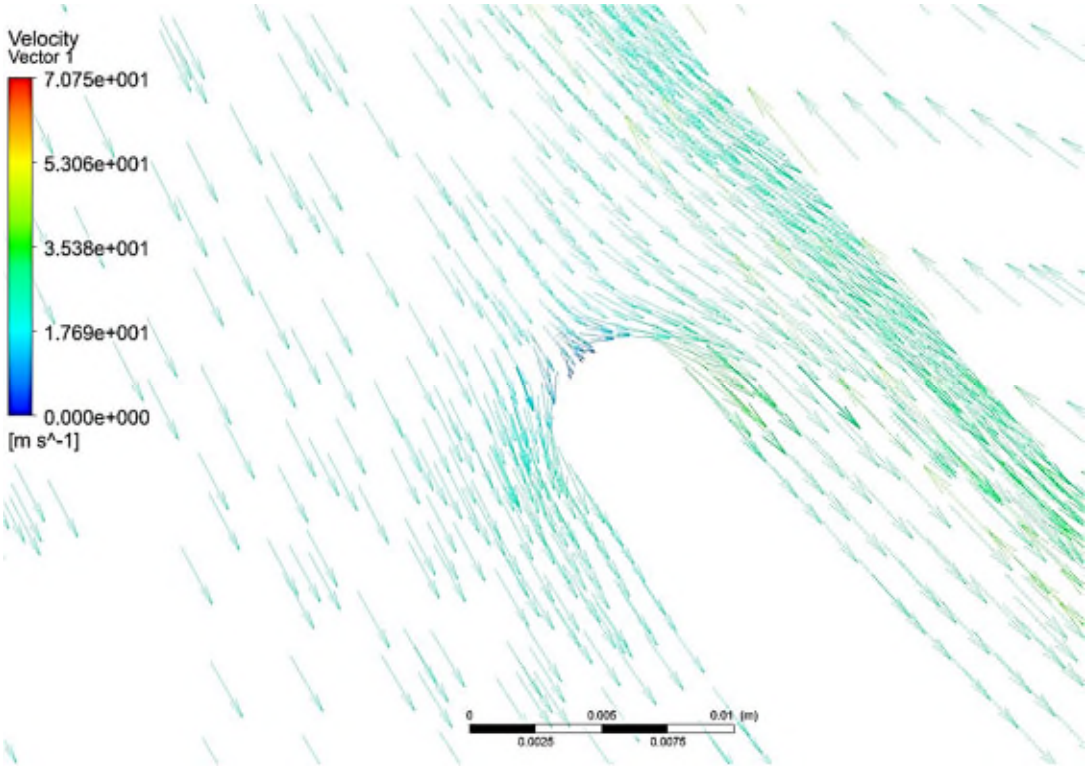

Figure 21 Velocity vectors around cutwater a) at top volute lip b) at bottom volute lip

Impeller volute interaction phenomenon is observed in the form of a velocity profile. As the impeller rotates and the blade relative position to cutwater changes, the velocity profile is modified. As a blade passes a cutwater a high velocity region is observed which extends with rotation to the outer wall of the volute passage, this can be seen in Figure 22.

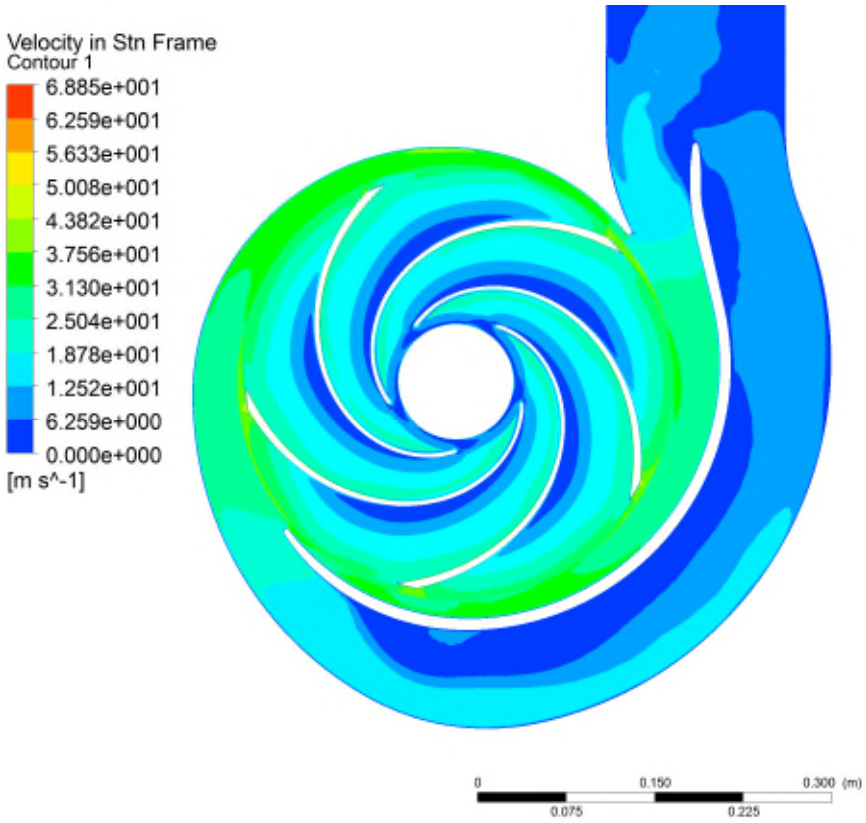

Figure 22 Velocity contour in the longitudinal cut

4.6 Hydraulic Force Acting on the Impeller

The pressure integration over the hub, shroud, blades and nose surfaces are calculated in order to extract hydraulic forces acting on the impeller. The expression is monitored during the CFX solver run. The plotted curves are in the rotating reference frame and can be seen in Figure 23 for the simulation of the single stage pump.

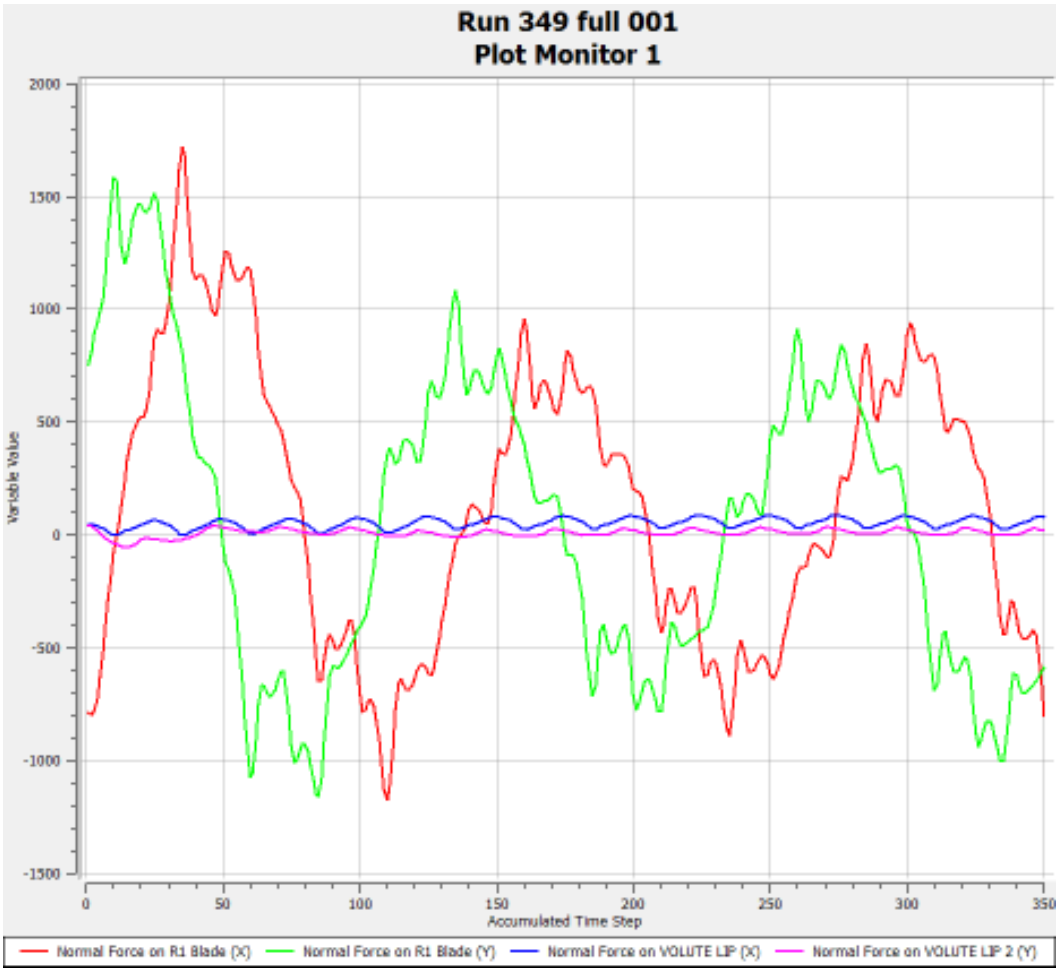

Figure 23 Monitor of forces acting on the impeller

The conversion from the rotating reference frame to the absolute frame is performed in Microsoft EXCEL and is expressed in the formula:

$$Fx = Fx' * \cos(\omega t) - Fy' * \sin(\omega t) \qquad \text{Equation 17}$$

$$Fy = Fx' * \sin(\omega t) + Fy' * \cos(\omega t)$$

The plot of force in direction x and y are shown in Figure 24. Importantly what is observed in Figure 24 is the periodicity of the forces and is therefore confirmation of the convergence. The force data was averaged between impeller revolution two and three. It then converted in to a load formula for incorporation within a rotordynamic model and is discussed in section 6.2.3

a)

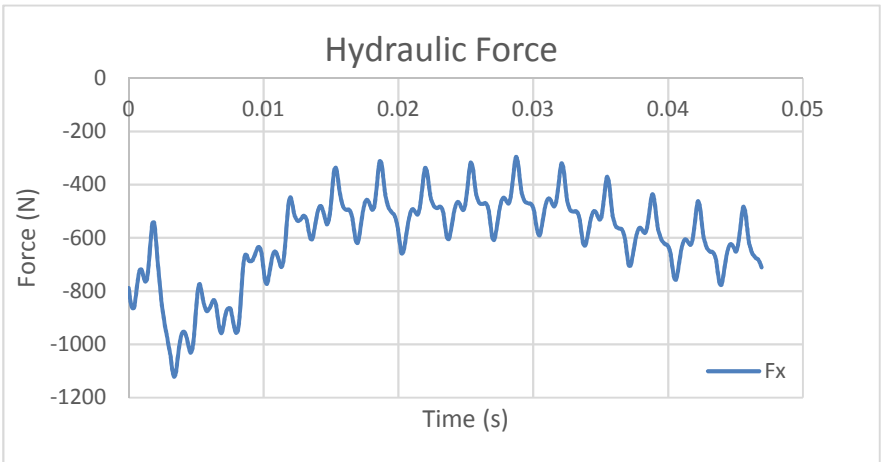

b)

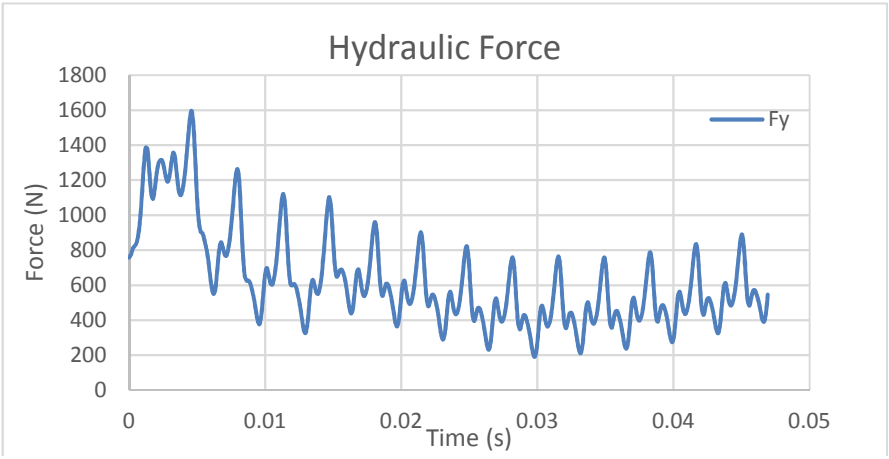

Figure 24 Hydraulic force acting on impeller blades in a) x direction and b) y direction

5 Experimental Investigation on a Single Stage Overhung Pump

It is recognised that when undertaking CFD analysis work, the results obtained are appropriately validated by means of experimental data. A systematic approach has therefore been constructed for the validation of the CFD analysis of a commercial end suction single stage overhung pump, provided by the sponsor. The radial flow pump consists of a vane-less volute and single impeller with backward swept blades, the pump performance characteristics are shown in Figure 25. The series of tests are to focus on investigating the magnitude of the unsteady pressure fluctuations related to the blade passing frequency, over a range of operating points. In addition to this aim, the fluid forces which are transmitted via the shaft are to be measured in order to validate the rotordynamic model. This task is fairly complex due to a number of restrictions in the test pump preventing access points on the shaft for measurements to be taken.

5.1 Test Pump

The test pump was manufactured in the SPXFLOW clydeunion pump at the Burlington facility for the purpose of research and development. The pump was made available to the author for the investigation of transient interaction effects in centrifugal pumps. The pump is categorised by frame size and is a 6x6x14 OH2, describing a six-inch suction inlet duct, six-inch discharge outlet and a fourteen-inch impeller for the overhung pump type 2 product range. The performance characteristics of the tested pump is shown in Figure 25.

a)

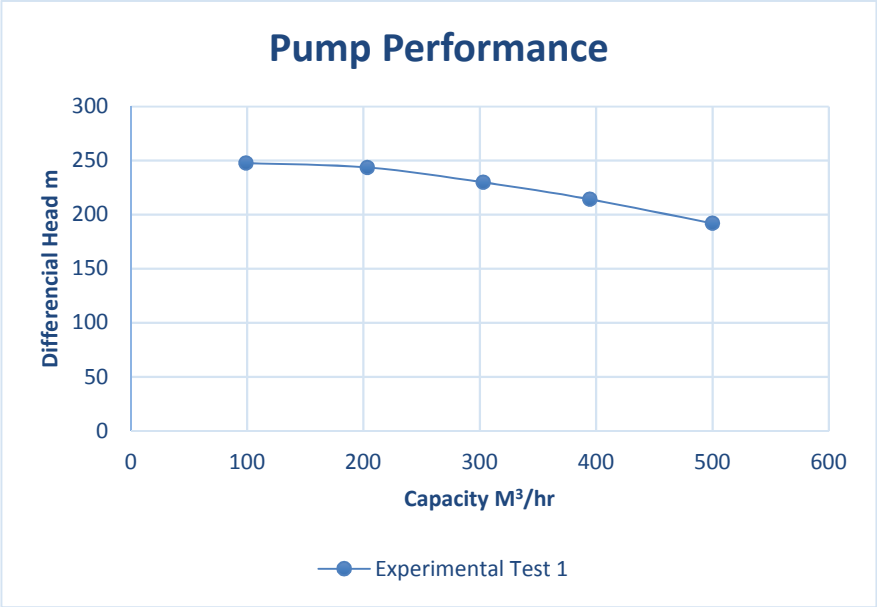

b)

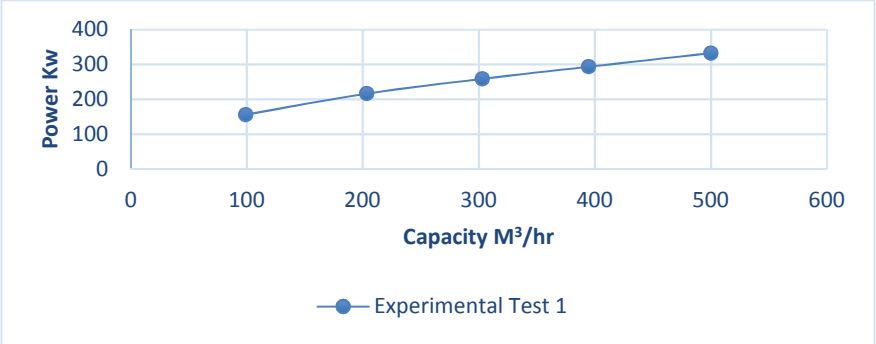

c)

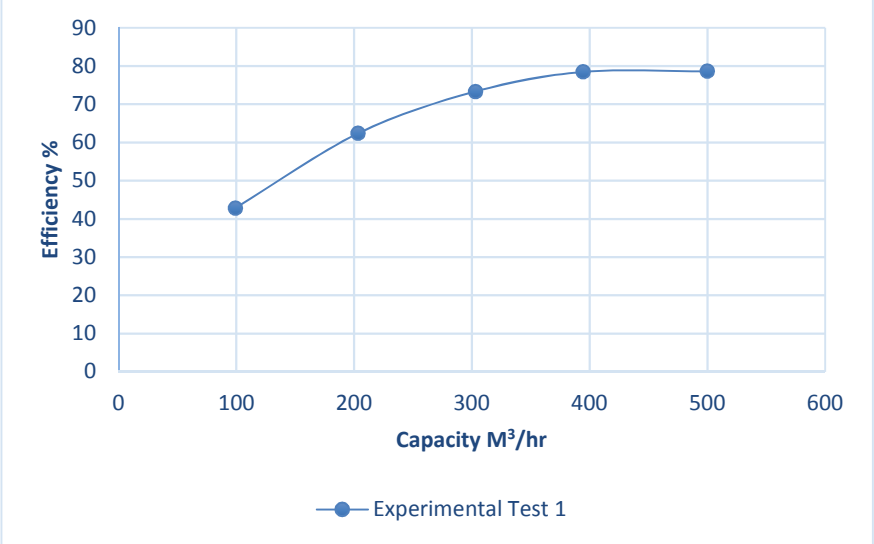

Figure 25 Performance curves of the test pump showing, a) head b) power c) efficiency

5.1.1 Test Impeller

The test impeller was produced for the experiment from an available pattern. The original pump impeller was trimmed as part of a previous experiment and it was important to test the pump at the maximum impeller diameter in order to capture the greatest level of hydraulically induced vibration generated from the close proximity of the volute lip and the impeller. The impeller design features are the same as the modelled impeller described in chapter 4.3.

5.1.2 Test Casing

The pump has a double volute casing of a trapezoidal shape at the cutwater regions forming into the conventional circular section towards the pump outlet. The volute cutwater is located forty degrees from the pump centreline on a 381mm diameter, giving a cutwater clearance of 3% calculated using equation 2.1 shown in chapter 2. The cutwater positions are offset by an angle of 180º.

5.2 General Arrangement of the Test Rig

The experimental campaign was performed in the Clydeunion Pump test facility. A schematic diagram of the test set up is shown is Figure 26, illustrating the closed loop system. The pump was set up and tested in accordance with BS EN ISO 9906:2012 and API 610 11th Edition shown in Figure 27 with inclusion of a gearbox. Whilst an existing commercial test facility was utilised for the series of experimental tests the author contributed to the installation and configuration of the current vibration monitoring system whilst fulfilling the role of Test Manager within the sponsoring company. The fluid medium tested was water drawn from a suppression tank with a capacity of $50m^3$. Flow rate was finely controlled by means of a discharge control valve located downstream of the pump discharge nozzle. The flow rate was measured by a Danfoss

magnetic flow meter on a 150mm diameter which allows flow measurement accuracy over a flow range of 5.3m^3/hr up to 2680m^3/hr. Measurement uncertainty is estimated at +/-2.5%. The pump was tested at constant speed of 3560 rpm be means of an DC motor and gearbox governed by a digital tachometer showing a continual display of rotational speed to a precision of +/-1rpm. Suction and discharge pressure was measured by Rosemount pressure transmitters Type 3051C ranging from 0.1-7bar a, for the suction pressure and 1.4-110 bar a, for the discharge pressure to an accuracy of 0.35% and 0.55% respectively. All of the instrumentation is within calibration.

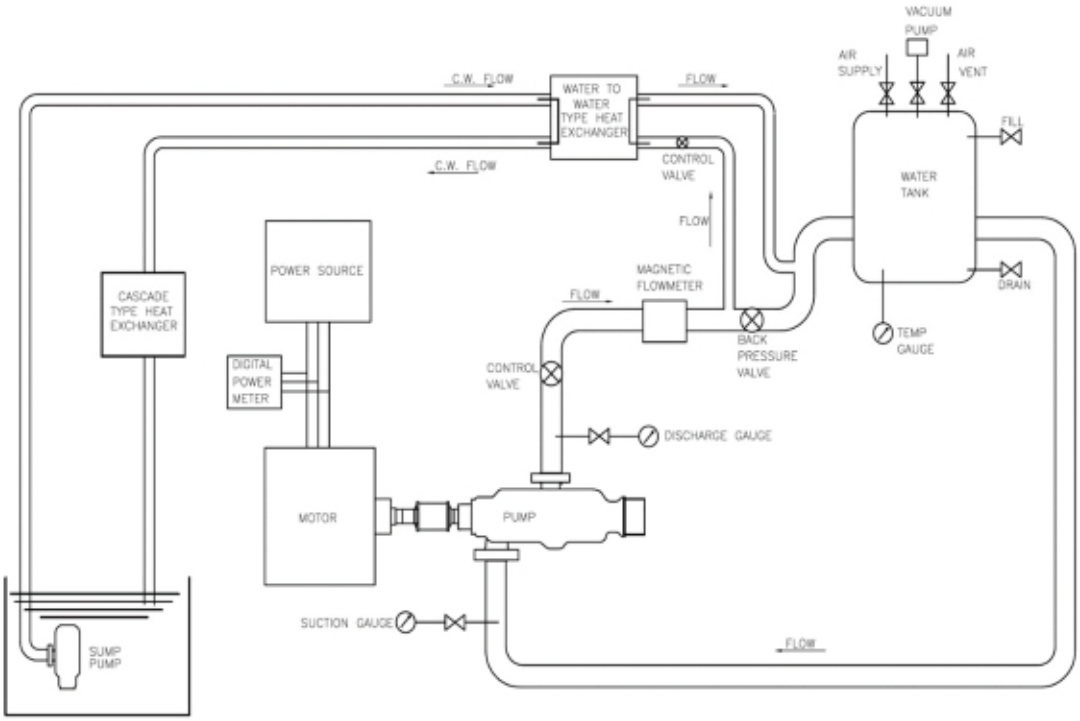

Figure 26 Schematic of the closed loop test set up

Figure 27 Photograph of the test pump set up on the test bed

5.3 Technique

To capture the unsteady pressure fluctuation, dynamic pressure transducer readings were taken utilising four Kistler 701A, shown in Figure 28 and mounted within the pump in Figure 29b. The transducers are fast response piezo-resistive, with a natural frequency >70kHz and an uncertainly of less +/-1.5%. The pressure transducers were provided by the sponsoring company. The signals were amplified, digitised and FFT processed in order to obtain the spectral distribution of pressure. A sampling rate of 1024hz were recorded this provided a reasonable check that the readings were consistent and repeatable.

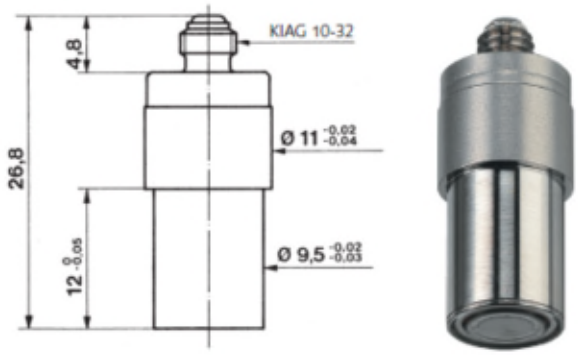

Figure 28 Kistler 701A Dynamic pressure transducer

A list of the positions for the pressure transducer is given below and a diagrammatical representation of the positions is shown in Figure 29a and shown mounted in the volute casing in Figure 29. The positions are shown as channel number e.g channel 1 is noted as C1, the same monitoring point are observed for the CFD analyses and are presented in chapter 6. The pressure transducers are mounted flush with the volute inner wall of the pump casing this is preferred mounting arrangement as it avoids air entrapment when utilising an adapter and tapping. Due to the tested pump being a commercial cast casing the monitoring points were selected based upon areas around the sidewall in the volute where an adequate surface area could be found using a nut adapter connection. The pump case casting construction was designed with ribs on the outer wall and with pump feet located on the centre line which is a common pump design however this has led to unfortunate limitations with regard to location and quantity of monitoring points. For the present study a total number of eight monitoring points were recorded. The cutwater diameter is 381mm and the impeller peripheral diameter is 355.6mm, the transducers were located on the sidewall on a diameter of 368.3mm equidistance between the outlet of the impeller and the volute lip diameter and for angular position around the impeller, φ (degrees)

Sidewall position where φ = 0 º is at the pump centreline in the x direction

C1 – 10mm ahead of the leading edge cutwater, φ = 35º

C2 – 10mm past the leading edge cutwater, φ = 42º

C3 – 30mm past the leading edge cutwater, φ, 48º

C4 – 50mm past the leading edge cutwater, φ = 54º

C5 – φ = 88º

C6 – φ = 122º

C7 – φ = 156º

C8 – φ = 190º

a)

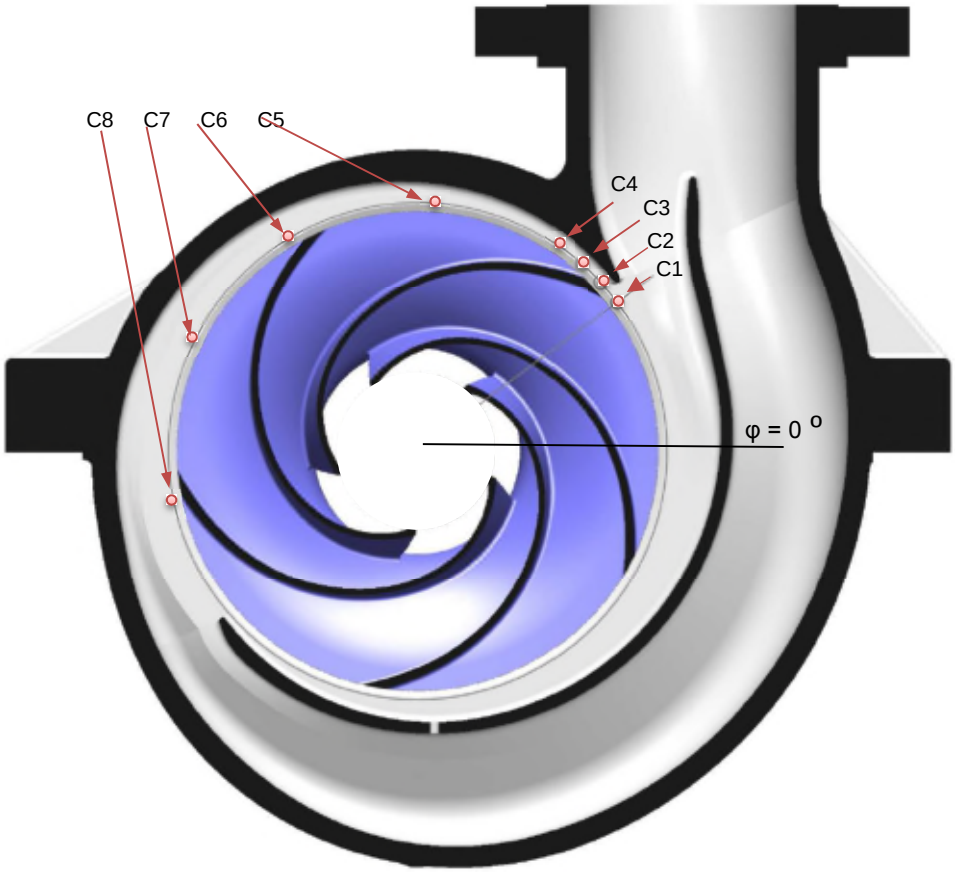

b)

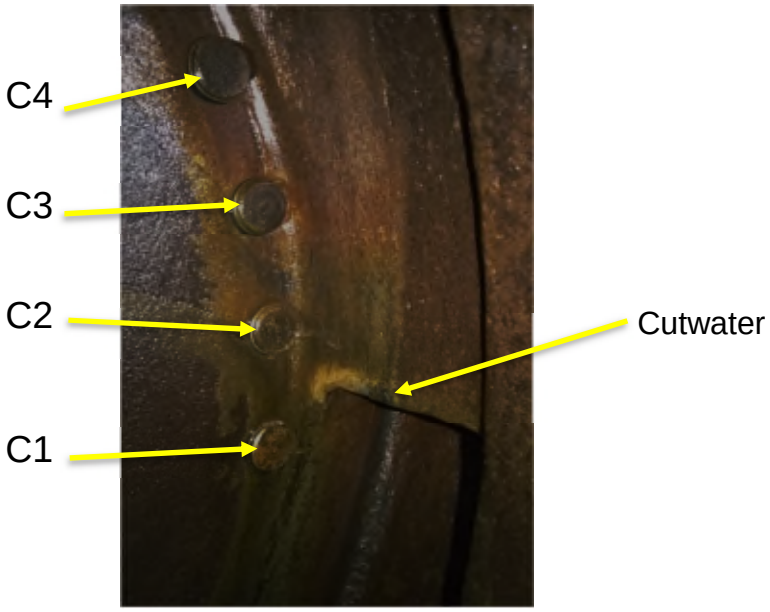

Figure 29 a) Pump section illustrating the circumferential position of the sidewall pressure transducer locations C1- C8 b) C1-C4 mounted flush within the pump casing

In order to validate the translation of the dynamic forces from the blade tongue interaction Bently Nevada proximity transducers were used for direct measurement of shaft vibration in accordance with API 670. A rotor-dyanmic imbalance response analysis has been carried out of the pump rotor to provide insight to the expected deflection in order to strategically place a sensor. As expected for an overhung type pump the greatest deflection is at the impeller location. This would have been the obvious choice to validate the rotordynamic model however a proximity probe cannot be mounted in this region due to restriction of the pump stuffing box. Figure 30 identifies location on the shaft that is accessible for measurements to be taken. A review of the mode shape which corresponds to the first bending mode at a speed of 3560rpm identifies there will be a lower level of deflection when compared to the impeller region, however it will be high enough to measure lower levels of the transposed forces corresponding the blade volute interaction behaviour. The proximity probe will be supported by means of a clamp arrangement mounted direct to the test stand bed plate. This will ensure the probe is reading absolute shaft movement as oppose to relative movement of adjacent pump components.

a)

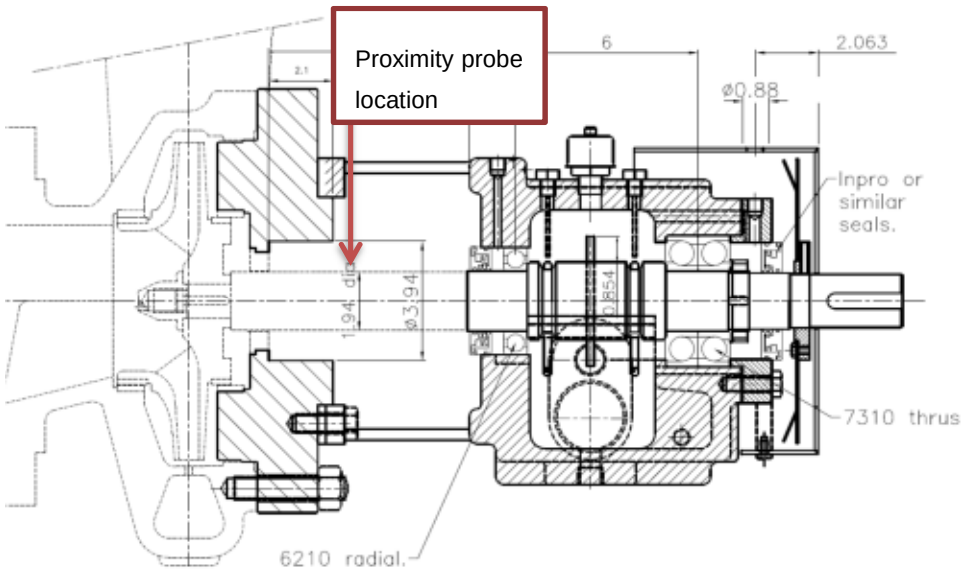

b)

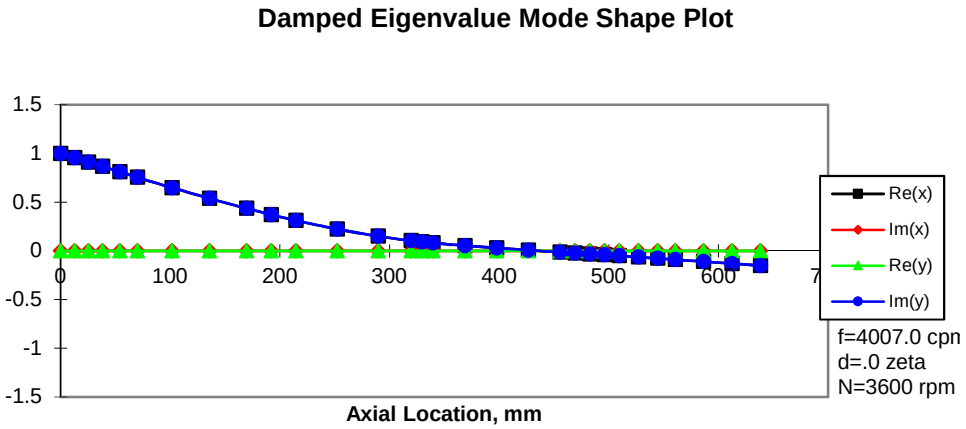

Figure 30 a) Pump cross section and b) Rotordynamic analysis

5.4 Test Method

The test rig was initially run at a constant speed of 3560+/-1rpm over a flow range where Q_n (best efficiency flowrate) is equal to 0.25 0.5, 0.75, 1 and 1.25. The adjustment in flow rate was achieved by a discharge control valve as indicated in section 5.1. A total of five flow rates was investigated. Readings of suction and discharge pressure, flow rate, power and speed were taken to generate the performance data for the pump. Bearing housing vibration data was taken throughout the test regime with accelerometers type Bruel and Kjaer Type 4391(frequency range 0.1 - 12000 Hz) mounted in the vertical, horizontal and axial position. Due to limited number of dynamic pressure sensors the unsteady pressure measurements were taken in the two regions C1-C4 and C5-C8 over two separate tests as shown in Figure 31. This will be repeated for each flow point to ensure consistency of readings. An optic device pointing to the shaft shall be utilised as a trigger signal in order to ensure all readings are taken at the same impeller location. The shaft vibration will be measured at each flow condition. All vibration will be FFT processed utilising an OROS OR38 16 input Real Time FFT Analyser.

Figure 31 Photograph of the pump set up with pressure transduces in positions C5- C8

5.5 Test Programme

For the present research the test programme is constrained to one speed and for a single configuration of the pump impeller. The author carried out additional test variations for the further research opportunities as an extension to the present study. In total four variations of test were carried out. The test impeller was trimmed to provide two geometric variations which is shown in table 3. For each of the impeller configurations and corresponding cutwater clearance, data was extracted over five operating conditions. For each impeller configuration the pump was operated at two speeds and readings taken across the same flow points. As referenced above test 01 is relevant for the present research, test 02-04 were carried out for further research opportunities and therefore only test 01 has been written within the results chapter.

Table 3 Experimental Test Programme

Test	Speed Rpm	Impeller configuration	Cutwater/Impeller Clearance %
01	3560	A	3
02	3000	A	3
03	3000	B	4
04	3560	B	4

5.6 Experimental Test Results

Within this section the results obtained for test 01 conducted by the author is presented. Firstly, the raw data collated throughout the testing regime will be discussed and the method for interpretation shown. As described in chapter 2.3, in order to evaluate the vibration signature, the data in the time waveform is transposed into a frequency spectrum, which is amplitude of vibration vs. frequency. The time waveform consists of many simple periodic waves and when arithmetic added they produce a complex wave. Each vibration gives a vibration signature at different frequencies. Therefore, the vibration results obtained are displayed in a frequency spectrum and once separated and the discrete frequency can be associated with a physical excitation mechanism in the machine and is discussed here. Secondly the unsteady pressure fluctuations and displacement measurements associated with the blade passing frequency are presented as a function of flowrate and general observations are discussed.

5.6.1 Presentation of Results

Upon conducting the experimental testing the results were analysed and processed, using fast Fourier transform with a hanning window and digitising

frequency of 1024Hz sample. The unsteady pressure measurements results are presented in an averaged power spectrum. The power spectrum provides a direct measure of the amplitude of the fluctuating pressure. Pressure pulsation measurements are to be processed in RMS value in units of kPa over a frequency range of 5Hz- 1KHz. The displacement reading shall be in an average spectrum display in unit's micron pk-pk.

To utilise the experimental data for comparison with numerical data the results are required in a common format.

A common approach when investigating pressure pulsations is to present in a normalised form which was introduced by Guelich and Bolleter (1992). They recommend for general spectrum analysis of pressure pulsations for a given pump a square law relationship be applied, shown in Equation 18.

$$\Delta p^* = \frac{\Delta p}{\rho \frac{u_2^2}{2}} \qquad \textbf{Equation 18}$$

Δp^* :- normalised pressure pulsation

Δp :- pressure pulsation

ρ :- density of the fluid

u_2 :- circumferential speed at the impeller outlet

Based on the above widely used method this format has been adopted for reporting the findings for the experimental work and for the numerical results that are presented in Chapter 6.

5.6.2 Spectral Vibration Analysis

For each of the measured vibration locations a raw time waveform is available, the raw data was FFT processed and analysed to review the dominant frequencies. Examples are included in Appendix B. As expected the dominant frequencies correspond to the rotational components within the pump. The pressure spectra showed the frequency related to the running speed of the pump at 60Hz and the blade passing frequency at 300Hz. Both these discrete frequencies are found in each of the measured vibration readings for the bearing velocity measurements, shaft displacement and dynamic pressure pulsation readings. Within the pressure pulsation measurement spectrum another frequency is present, that of electrical interference. The likelihood of source of the electrical interference is from the electrical motor at a frequency of 50Hz, it has therefore been ignored.

5.6.3 Blade Pass Vibration

There a several general observations related to the blade pass vibration behaviour that can be noted from the series of tests carried out. Firstly, discussed is the unsteady pressure measurements C1-C8.

Figure 32 a and b shows the normalised pressure pulsation measurements for each of the monitoring positions. The key observation relates to the pulsation magnitude is highly dependent on flowrate the pump is being operated at and also is dependent upon the location of the transducer. It can be observed that the pressure amplitude is at a minimum at the range of flowrates around the best efficiency point. The amplitude increases at the low flow and high flow regions. Figure 32 shows for C1 and C2 the pulsation amplitude is at its greatest level at off design conditions in the low flow region. C1 and C2 are located ahead and past the cutwater respectively, due to the interaction effects of the impeller and the cutwater is not surprising the greatest levels were observed in these

monitoring positions. It can be seen that there is little difference in readings between Q_n of 0.8 and 1. As the monitoring positions move further downstream of the cutwater the magnitude of pulsations reduces as can be seen by comparing Figure 32a and 32b. Interestingly a Q_n of 0.25 the separation margin between the readings increases. At off design conditions there are strong interaction effects that occur this is particularly seen at low flow points where recirculation and flow separation manifest. The same pressure transducer was used for C4 and C8 and are fairly inconsistent with the other channel readings. Although the appropriate calibration was carried out on all of the instruments used for the testing it is likely the transducer was not reading correctly.

a)

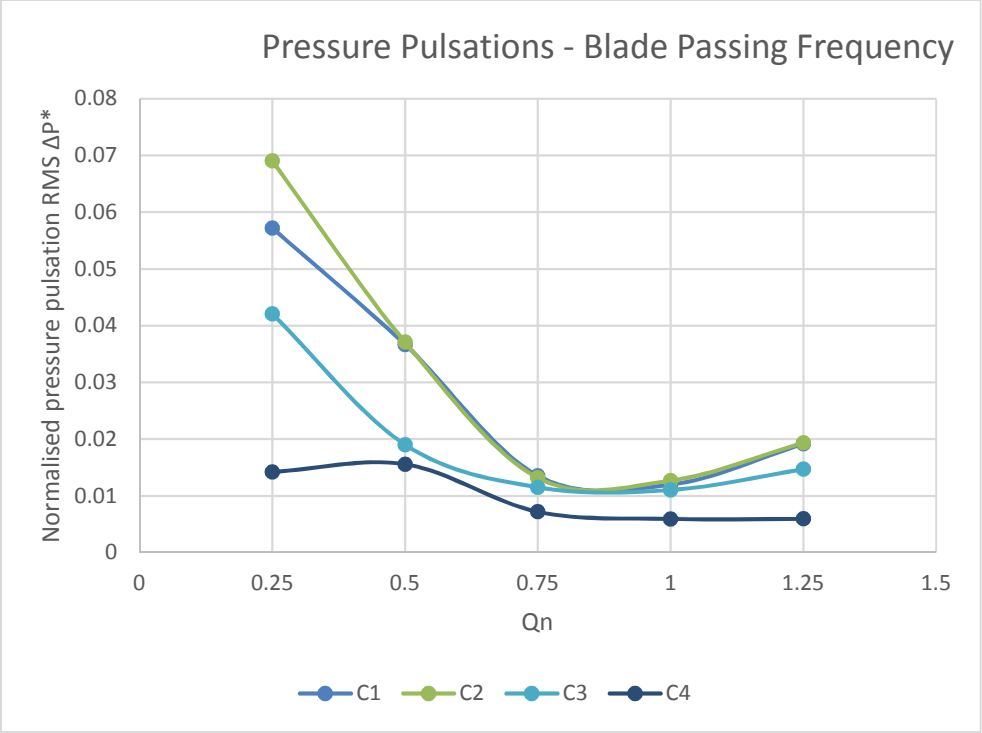

b)

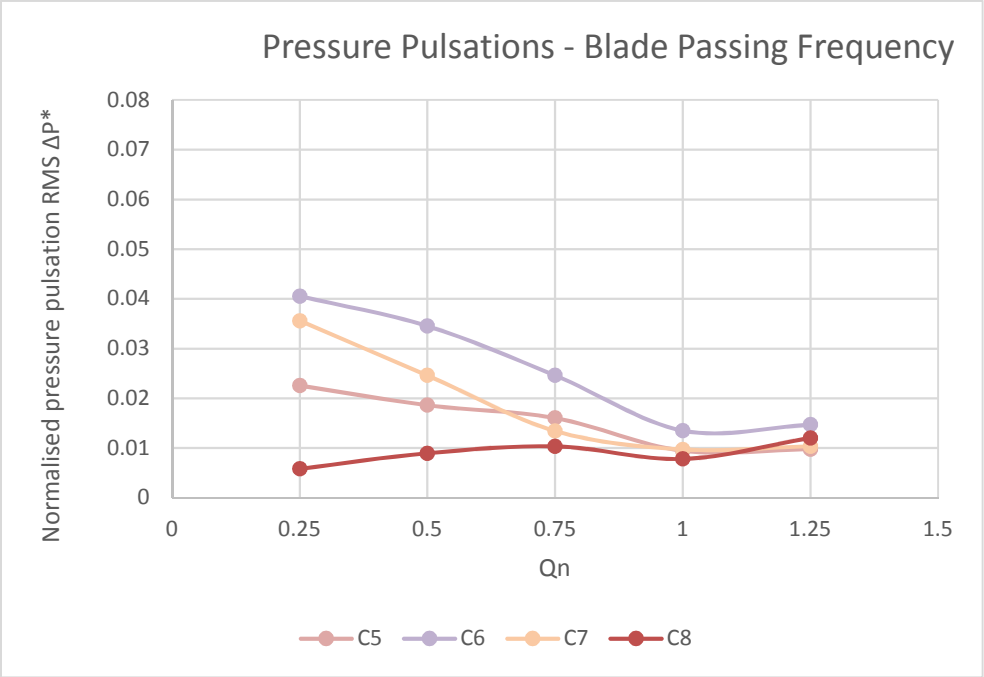

Figure 32 Pressure pulsation measurements at locations a) C1 – C4 and b) C5 – C8 as function of best efficiency flowrate Q_n

Figure 33 presents the measured shaft displacement in the y direction, at the seal location as indicated in Figure 30, and is plotted as a function of Q_n. Within the frequency spectrum the largest peak corresponds to the rotational speed of the pump shaft and a peak relating to the blade passing frequency was also observed which is of interest for this study. The shaft displacement readings corresponding to the blade passing frequency followed a similar trend as the unsteady pressure measurements, maximum values found at the low flow region. This is turn verifies the transmission path of hydraulically induced vibration to seal location and one can assume this continues to the bearings via the rotating pump shaft. What can be observed is for Qn=0.75 the displacement is higher than expected when compared to the results from the pressure pulsation measurements which is likely caused by physical restrictions within the pump radial bearing limiting movement at low flow operating conditions.

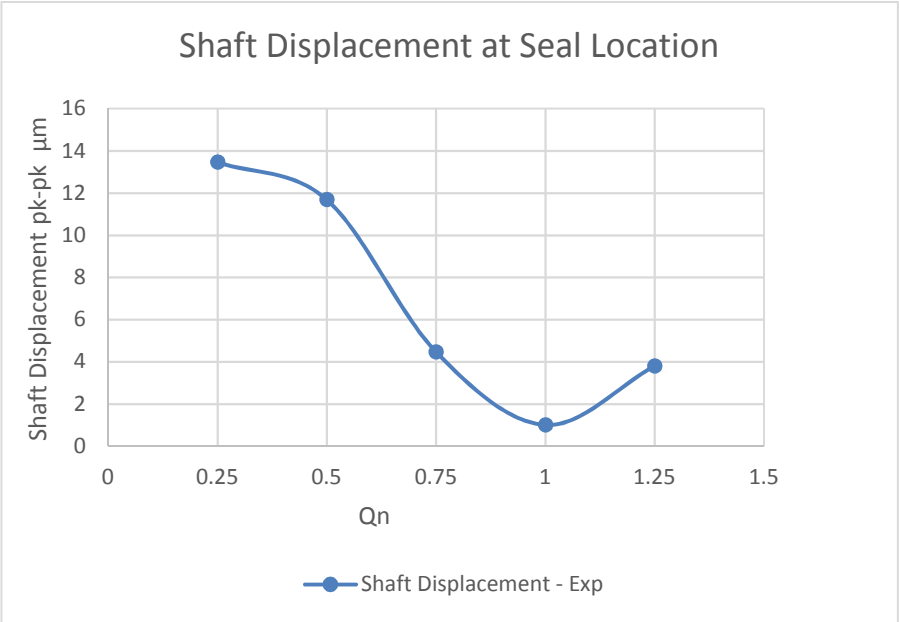

Figure 33 Shaft displacement related to the blade passing frequency in the y direction, as a function of Q_n

5.7 Chapter Summary

A systematic approach has been applied to the testing of a single stage volute pump. The tests conducted have obtained a reasonable set of data to compare with numerical results. The test regime focused on capturing the unsteady pressure fluctuations at a number of position around the impeller periphery at the sidewall location. The results of the investigation are summarised as follows:

- The greatest amplitude of pressure fluctuation occurred at 0.25 Q_n
- The highest fluctuations were measured at the volute cutwater position
- Spectral analysis showed the blade pass vibration was present in the dynamic pressure measurements, the displacement measurements and bearing housing velocity measurements.
- Shaft displacement corresponding to the blade passing frequency followed a similar trend to the unsteady pressure measurements.

6 Numerical Investigation of the Transient Effects in a Single Stage Overhung Pump

This chapter presents the CFD analysis of a single stage overhung pump of which the numerical method and nominal flow investigation was presented in section 4.4. The CFD investigation focuses on simulating the fluid flow across four additional operating conditions in order to obtain a complete characterisation of the pump performance and to quantify the hydraulic forces acting on the impeller. Thereafter the rotordynamic investigation is presented where the forces generated by the rotor-stator interaction from the CFD analysis are incorporated. The rotordynamic model seeks to quantify the extent of which these excitation forces are transmitted to the bearing and seal locations in order to form an assessment of potential vibration problems of a given pump. The final section of this chapter summarises the vibration prediction methodology explored in this chapter.

6.1 CFD Investigation

The CFD approach presented in chapter 4 for the nominal flow study, Q_n equal to 1, was employed across four additional operating conditions Q_n of 0.25 0.5, 0.75, and 1.25. To control the operating point in CFD the boundary condition for the mass flow inlet was changed for each of the respective flow points. All domain definitions and other boundary conditions were kept the same as the nominal flow investigation presented in section 4.3.

The first step in processing of the results is to demonstrate that the pump performance is within an acceptable approximation to the experimental performance test results. The numerically predicted head for each given operating condition is shown in figure 34 plotted with the experimental test results for the head performance. The numerical head calculation is performed by the

turbo performance macro within CFX post process and is calculated from the mass averaged differential of the absolute total pressure across the pump. It can be seen in figure 34 that the head performance correlates well with the experimental test data and is of the same order. There is slightly greater deviation in results at the lower flow regions which is a common issue when simulating part load conditions and is further discussed in 6.1.2. As discussed in section 4.4 the simplified model provides an overestimation of efficiency based upon the leakage passageways being neglected from the present study, it is therefore not reported upon in this section, however opportunities to optimise the CFD model are discussed in section 7. Once the general performance is verified in the present case the head verification is sufficient, a description of the flow features can be reported upon. Unlike experimental studies CFD provides insight to the complex three dimensional flow involving turbulence and unsteadiness. These features can be visualised by the means of static pressure and velocity variations in the form of contour plots across the flow domains. The flow analysis is followed by reporting of the complex interaction effects at specific locations over a period of time as opposed to static pressure variation at a specific moment.

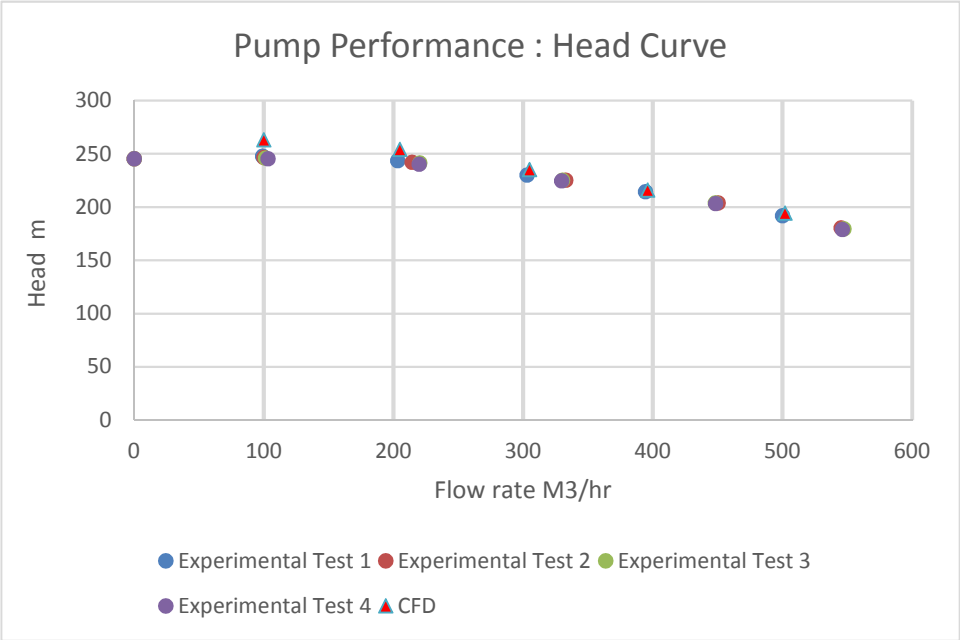

Figure 34 Pump performance (non-dimensional head) for experimental and numerical investigation

6.1.1 Visualisation of the Fluid Flow

In this section the static pressure and velocity variations are discussed.

6.1.1.1 Pressure Distribution

The pressure distribution is presented in Figure 35 for each of the five operating conditions. It is observed that as at Q_n equal to 1, the pressure around the impeller periphery is fairly uniform. As the flow is decreased it is visible that the pressure distribution is uneven and fairly distorted particularly for operating at the low flow region where Q_n equals 0.25 and 0.5 and at the maximum flow point $Q_{n\ of}$ 1.25.

Another fluid flow feature dependant on flow rate is that of shock loss or local pressure loss at the cutwater region. It is expected that as the impeller blade passes the cutwater at zero degrees and 180 degrees positions respectively, it causes a pressure loss local to the cutwater position. This phenomenon is unavoidable due to the close proximity of the rotating and stationary components. It is caused by a local increase in velocity as the impeller blade passes the cutwater region in the volute. The cross sectional area of the volute then increases and as the blade rotates, the high velocity fluid decelerates into the slow velocity fluid of the volute which leads to some pressure being regained. It can be seen that for $1.00Q_n$ and $0.25Q_n$ flows the pressure loss increases as the flow rate decreases.

The maximum static pressure increases as it transitions towards the cutwater regions with the peak becoming higher as the flow rate decreases

Another observation is the static pressure distribution in the impeller is higher on the hub side than the shroud. This is due to the direction of the flow turning from axial to radial. A surface contour plot is shown in figure 36 of the blades and shroud.

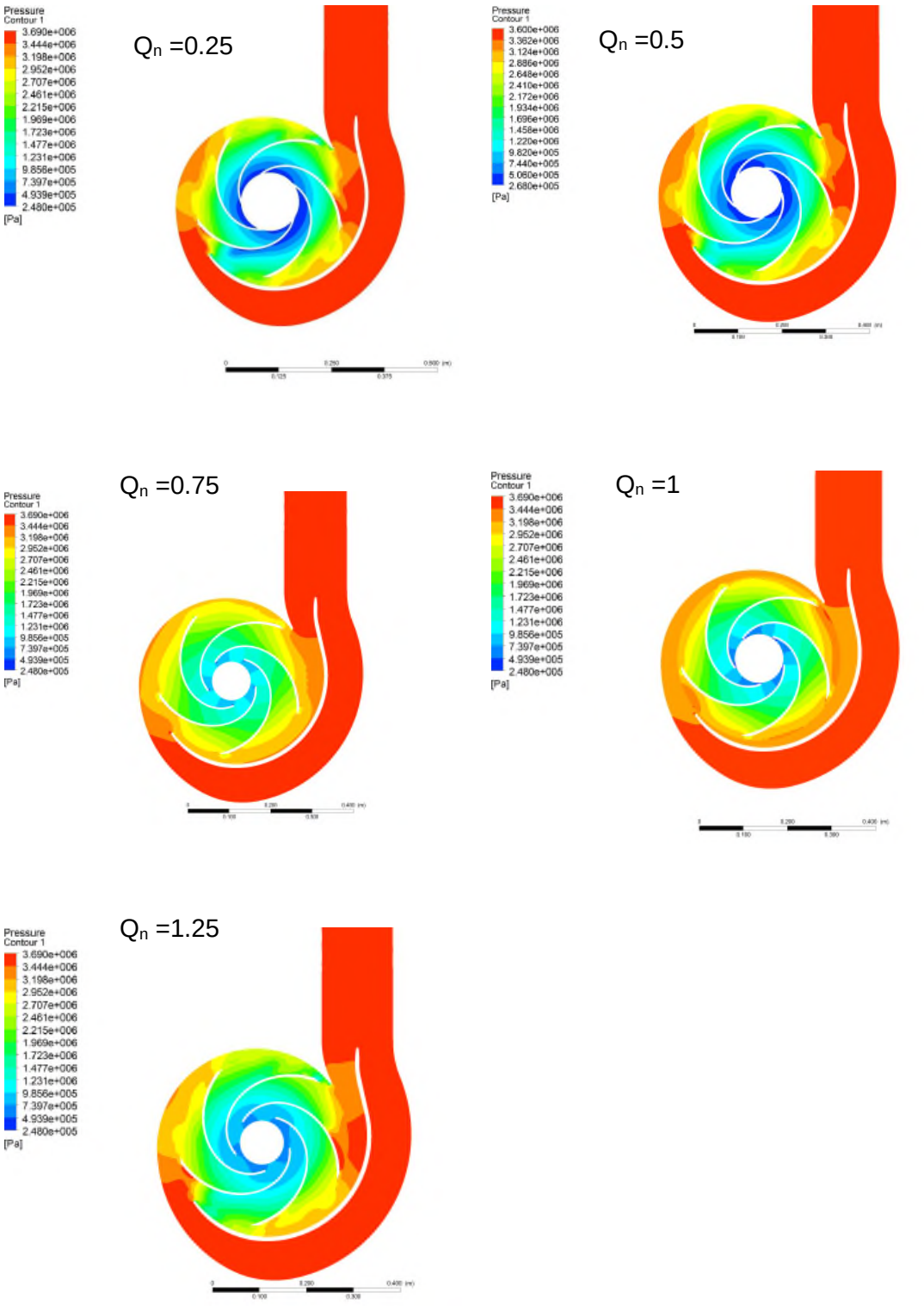

Figure 35 Static pressure contour on a longitudinal cut

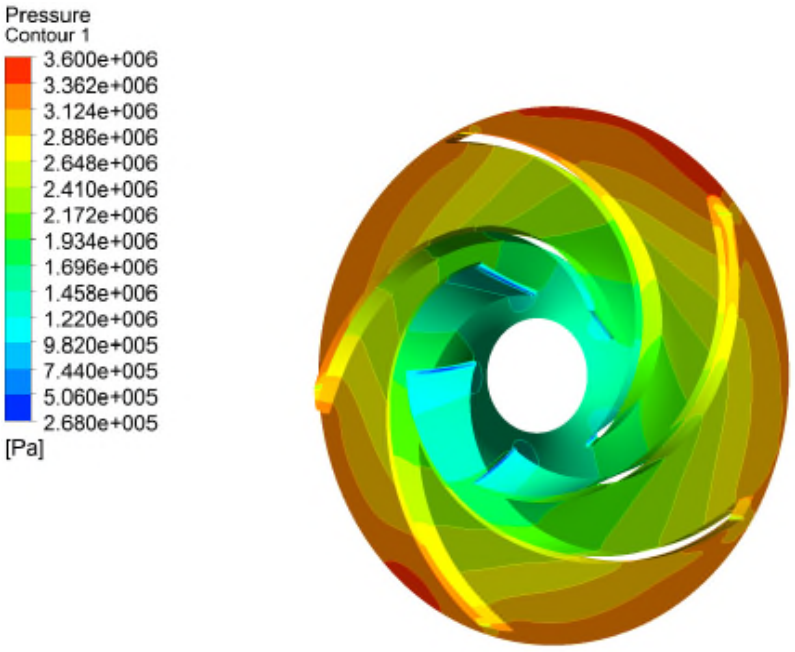

Figure 36 Static pressure contour at nominal flow in the impeller

6.1.1.2 Velocity Profile

As discussed in section 4.5 for the nominal flow investigation, impeller volute interaction phenomenon is observed in the form of a velocity profile. As the impeller rotates and the blade relative position to cutwater changes, the velocity profile is modified. As a blade passes a cutwater a high velocity region is observed which extends with rotation to the outer wall of the volute passage. This is evident to a greater extent at low flow and high flow regions.

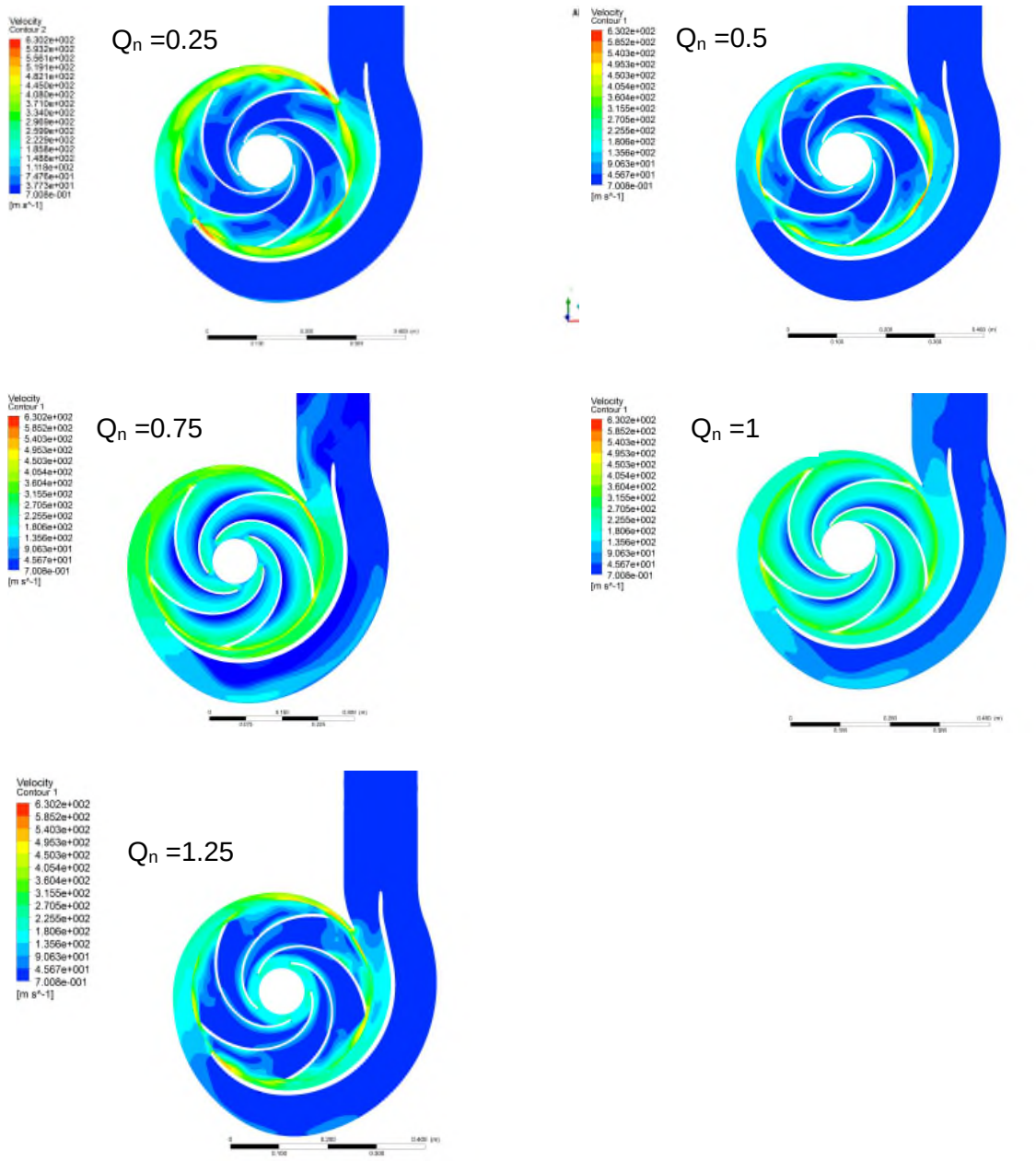

Figure 37 Absolute velocity in the volute and relative velocity in the impeller contour on longitudinal cut

Analysing the velocity vectors around the cutwater position at four progressive blade positions shows the volute interaction effect, Figure 38. As the blade transitions towards the cutwater the velocity field exiting the impeller passage meets the outer flow in the volute and is impinged by the volute lip at the cutwater. The jet-wake phenomenon can be observed and it can be seen that the flow is

distorted significantly as the blade is ahead and in close proximity to the cutwater position. As the blade moves past the cutwater the flow structure recovers slightly. Within the impeller passageways turbulence can be seen to dominate and are increasingly turbulent at low flows as shown in Figure 39 which provides a visualisation of the high turbulent regions utilising the CFX post parameter turbulent kinetic energy contour plot.

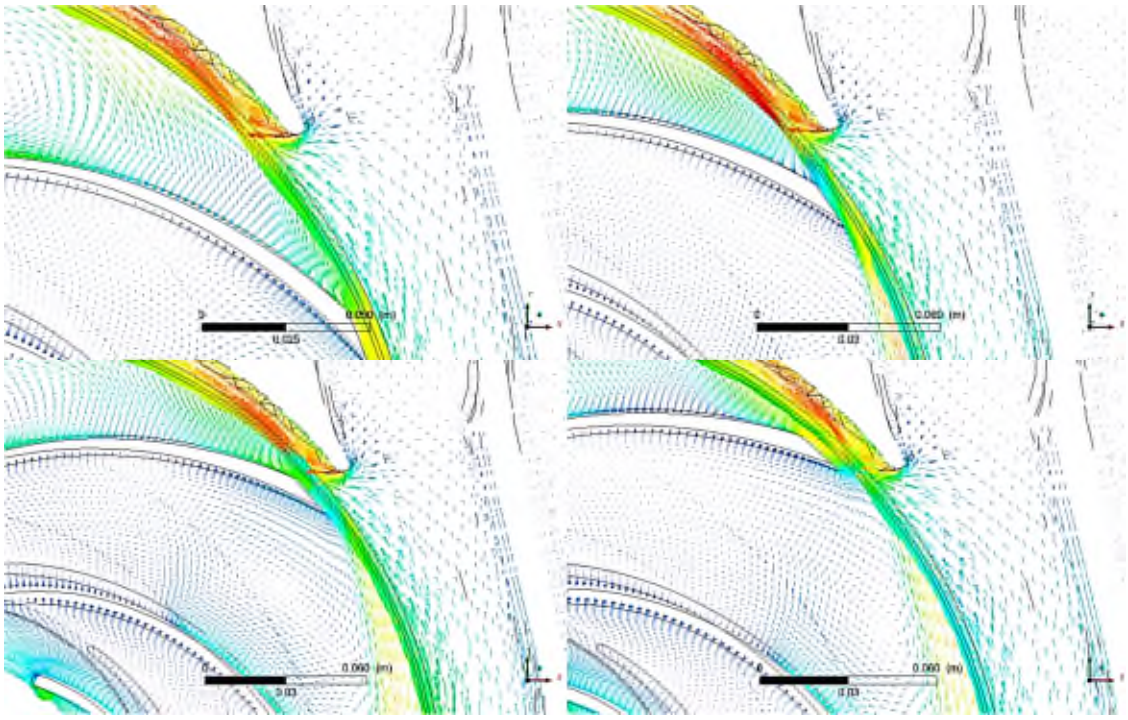

Figure 38 Impeller volute interaction at the cutwater position Qn=0.25

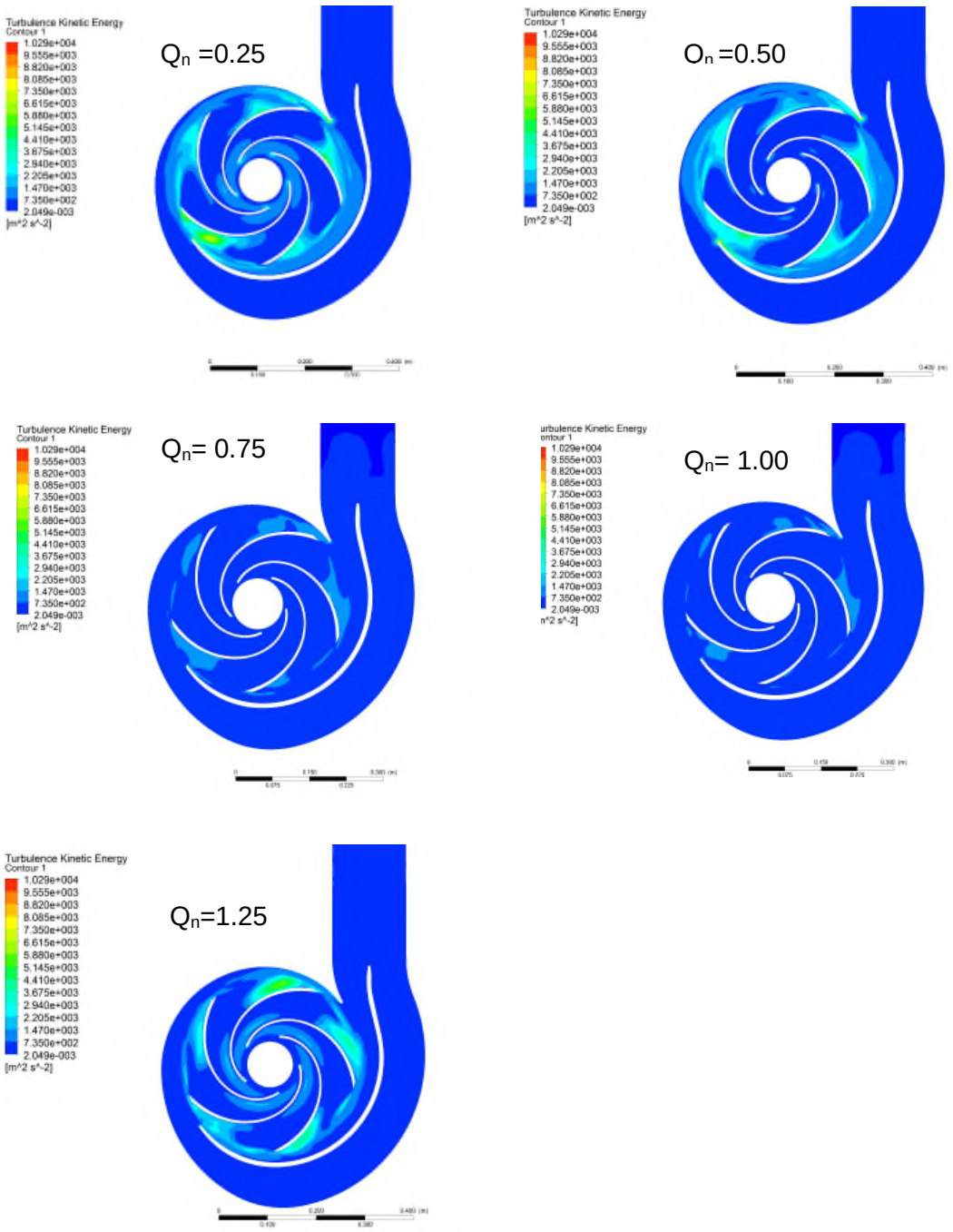

Figure 39 Turbulence kinetic energy contour plot on a longitudinal cut

The turbulent kinetic energy noted; k, is the energy per unit mass and is proportional to the velocity magnitude square U^2 and to the turbulence intensity square I^2. For low flow operation the turbulent zones can be seen at the impeller

outlet with some concentrations around the cutwater. As the flowrate is increased the turbulence zones decrease only small amounts can be identified near the blade tip and cutwater. At higher flow regions turbulence can be observed.

6.1.2 Part Load Operating Point

A pump is said to be operating at part load, at flowrates significantly below the best efficiency flowrate. Operating a pump at part load leads to large variations of flow pattern. CFD allows visualisation of the flow pattern changes and can support design optimisation investigations. As discussed in the literature survey in section 3.1.1 it is understood that the flow at part load is highly inefficient due to flow separation and recirculation at the impeller inlet and outlet. The blade angles and channel cross section are designed for nominal flow conditions which are too large for the low flow conditions.

In this section the variation in fluid flow behaviour captured, for simulations $1.00Q_n$ and $0.25Q_n$ specifically, are discussed. The first comparison is to check the CFD simulation for $0.25Q_n$ follow typical part load flow behaviour. It can be observed on a meridional plot in Figure 40, flow recirculation in the impeller inlet and outlet is apparent, whereas the flow through the impeller for $1.00Q_n$ is fairly uniform.

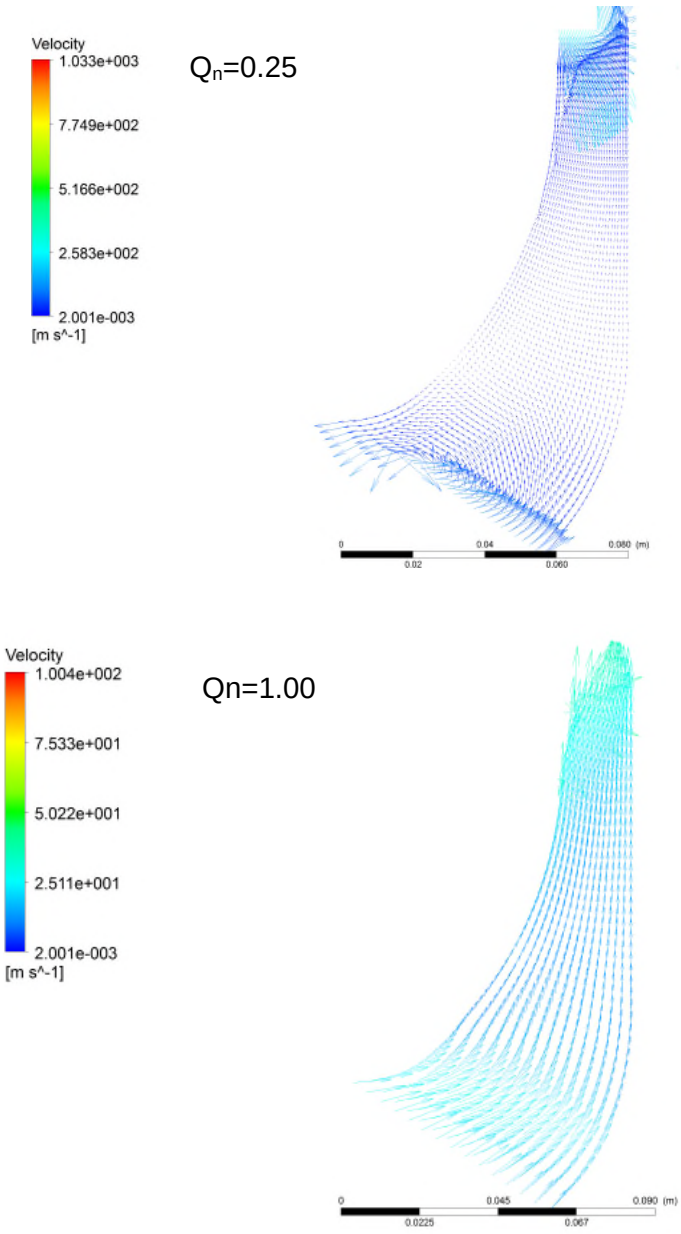

Figure 40 Meridional plot for $0.25Q_n$ and $1.00Q_n$

When comparing the velocity vectors around the cutwater in Figure 41, for $0.25Q_n$ and $1.00Q_n$ it can be seen that the flow is deflected at the cutwater to a greater extent for the minimum operating condition. For the nominal flow operating condition the flow path follows the curvature of the volute with some minor deflection at the cutwater. It is seen that the flow at part load largely effects the

flow at the volute exit. For 1.00Q_n the flow is passing equally into the volute and to the pump outlet, however at part load the outer flow is circulating back towards the cutwater and is then deflected into the volute region.

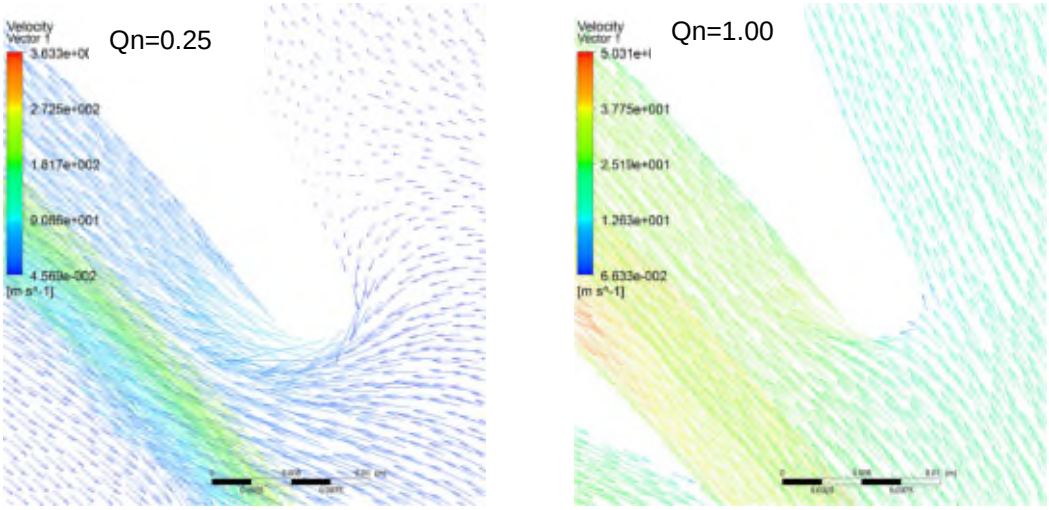

Figure 41 Flow around the cutwater velocity vectors shown in the relative reference frame

The interaction effects from the rotating and stationary components at the inlet and outlet regions largely determine the flow behaviour at part load and have an effect on hydraulic excitation forces and the pump performance characteristics. Designing of these features is still heavily dependent on experience of design hydraulic engineers and experimental data. CFD can provide greater visualisation of flow behaviour which can lead to the interaction effects being investigated numerically. The hydraulic forces and pressure pulsations can be estimated at part load which is an interest to the present study.

6.1.3 Hydraulic Excitation Forces

To form a comparison between the CFD numerically predicted pressure pulsations and the experimental results, the same monitoring positions have been used for the CFD model. To capture the time dependant pressure pulsations, the data at each of the monitor locations is required for every time

step. This is performed in CFX post and is a lengthy task as it involves loading each of transient time steps and exporting the data into an excel spreadsheet. A sample is shown in Figure 42. The volume of data equates to 125 items of time history data for one revolution of the impeller. In total this would be 625 for each flowrate. Therefore, in the interest in time, it was decided by the author to focus on three flow rates. The three flow rates considered here are Q_n equal to 0.25, 1.00 and 1.25.

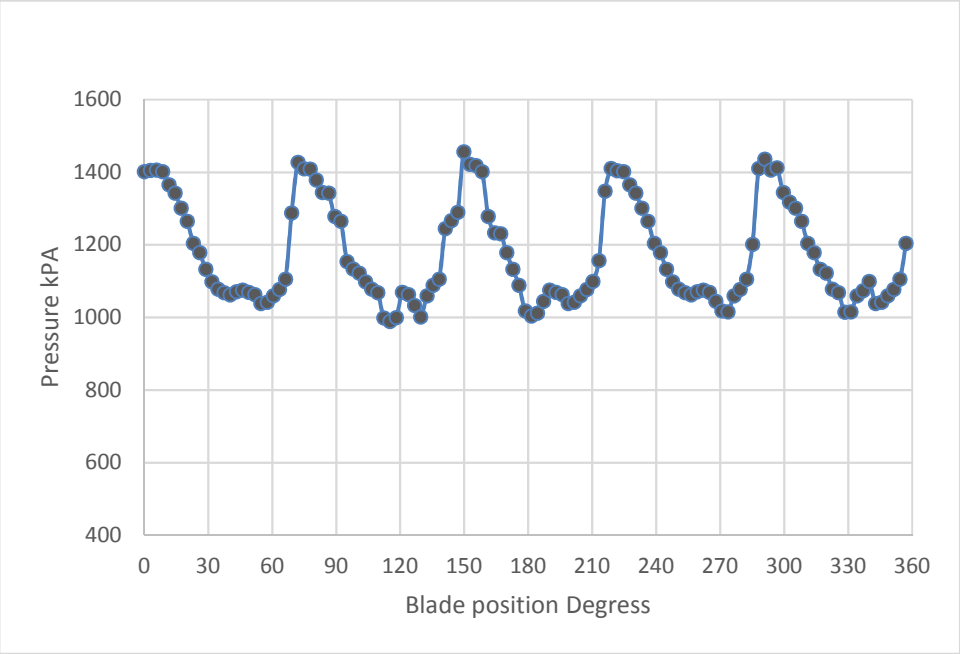

Figure 42 Sample pressure fluctuation at monitoring point C1 at 0.25Q_n

Performing an FFT process in excel provides insight to the frequency of the pulsations however this is fairly course based on the sampling and simulation time carried out which has affected the frequency resolution. It is visible from the time history data collected for one revolution the frequency of the pressure pulses relates to that of blade rate. It can be observed that the pressure fluctuations show periodicity. The pressure pulsation relating to the blade pass frequency was then converted to normalised form for the three operating conditions, the results are shown in Figure 43. For the purpose of commonality, the normalised pressure

pulsations are in the form RMS. This was achieved numerically by taking the peak-peak value for each of the monitored points and applied (Equation 3). It can be observed that the normalised pressure pulsation predictions follow a similar trend to the data obtained experimentally. It is noted as indicated by Gulich 2008, the values obtained and shown in the RMS format are for estimations purposes due to the equation being suited to a true sinusoidal signal. However this is the most common description of pressure pulsations and is used in many of the literature cited in section 3.3

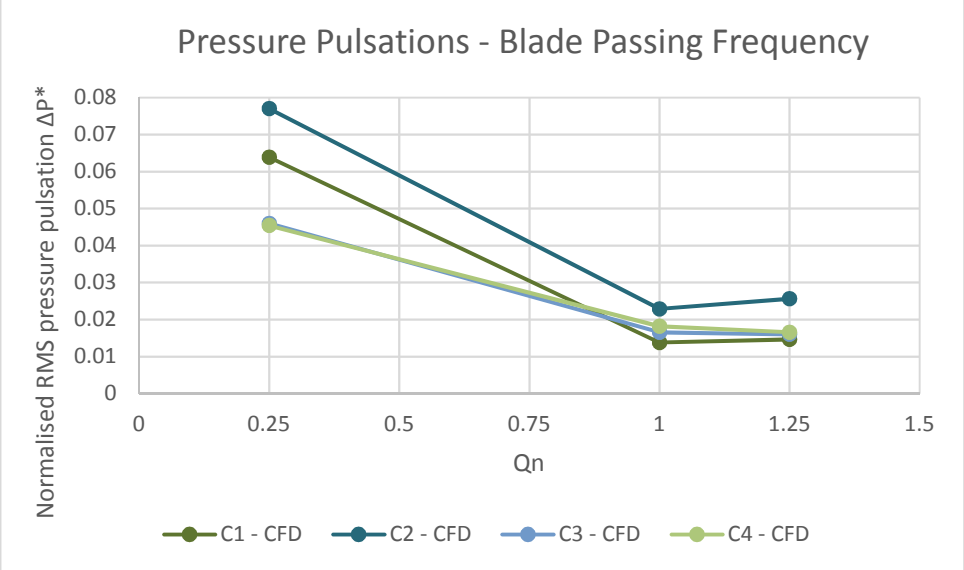

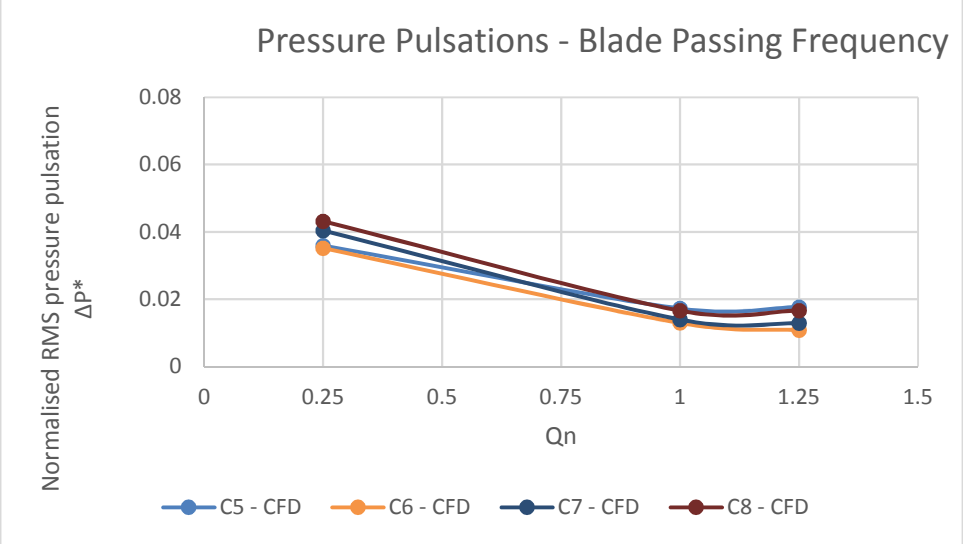

Figure 43 **Normalised pressure pulsation for CFD analysis for monitoring positions C1 to C8 at three flow rates**

As the interest for the study was the hydraulic excitation forces acting on the rotating element the forces on the impeller monitored during the CFX solve process have been extracted for each operating condition and converted in excel from the rotating reference frame to the absolute frame using equation 18. The forces for the nominal flow point shown in section 4.6 corresponded to the blade passing frequency, for one revolution of the impeller, five pulses can clearly be seen, Figure 44.

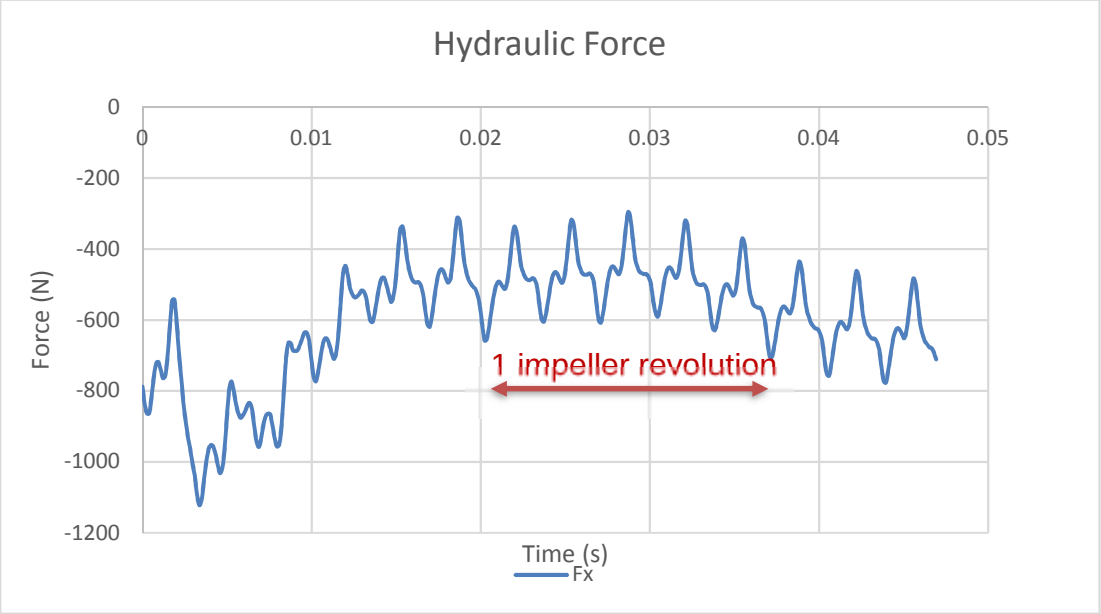

Figure 44 Hydraulic force acting on the impeller at nominal flow

The forces captured for the minimum and maximum operating points were less uniform than the forces shown in Figure 44, however the forces remain periodic. As the operating point is decreased the estimated forces acting on the impeller increase in amplitude as expected. Figure 45 provides a visual illustration of the variation in signal for the minimum operating condition in comparison with the force plot for the nominal operating condition for one revolution of the impeller;

125 time steps. What can be seen from the illustration is for Qn=0.25 evidence of recirculation and turbulence is present.

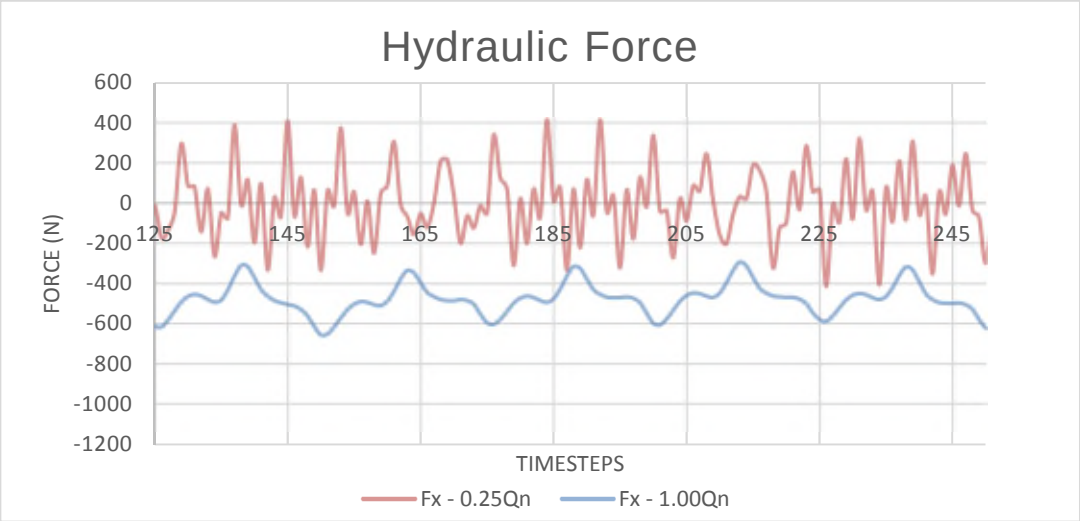

Figure 45 Illustration of the variation of force imposed on the impeller at $0.25Q_n$ and $100Q_n$

The principal periodic pressure pulsation at the blade passing frequency is shown in table 4 in peak to peak form for each of the operating conditions and plotted in Figure 46 as a function of flow rate.

Table 4 Peak-Peak values for the hydraulic force acting on the impeller

Q_n	0.25	0.5	0.75	1	1.25
Fx	605	489	293	157	459
Fy	666	545	345	223	537

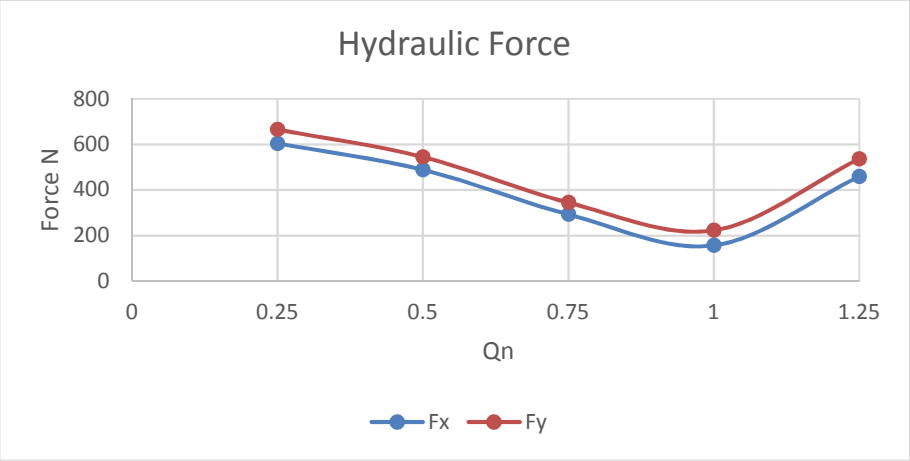

Figure 46 Hydraulic force in the x and y direction (pk-pk)

Figure 46 demonstrates the numerically calculated forces follow a similar trend to vibration measurements obtained during the experimental testing of the pump shown in section 5.6.3. It is not surprising the forces captured for the x and y direction are of similar magnitude based on the hydraulic design for the case being a double volute, with cutwater positions opposed by 180 degrees. Therefore, the forces are fairly balanced in the x and y directions. Axial force relating to the blade passing frequency for this type of pumping machine is relatively low and therefore not considered for this study. This can be seen in the velocity vibration measurements measured at the bearing location shown in Appendix B.

6.2 Rotordynamic Investigation

Accurately assessing the dynamic behaviour of pumps can be challenging. For high energy multistage pumps and pumps with multiple operating points over a speed range, rotordynamic analysis is essential. The focus of a typical analysis carried out is for critical speed. It is also important to not only evaluate critical speeds for a pump but to assess the damped rotordynamic response and also have a level of understanding of potential rotor displacements when not running in a region where there is a natural frequency.

A pump rotor is subject to certain forces. As discussed in section 2.4 mechanical forces acting on a pump rotor can be calculated fairly easily however the hydraulic excitation forces caused by rotor stator interaction are dependent on hydraulic design and operating conditions. A limitation to predicting rotordynamic characteristics of a pump can arise due to the uncertainty in the hydraulic forces acting on the rotor. The objective of this investigation is to establish a design method for predicting the response of a pump rotor to the hydraulic forces captured in the CFD transient simulations.

There are many sophisticated mathematical tools available to carry out a rotordynamic investigation; the chosen programme for this work is XL rotor. XL rotor is a comprehensive software programme which delivers fast results via a user friendly interface. The numerical method the programme utilises is Polynomial Transfer Matrix and for complex cases the facility for finite element method can be applied.

In this section mechanical construction of the single stage pump is introduced and a basic lateral analysis is carried out. The hydraulic forces extracted from the numerical study are inputted as a transient load to the XL rotor model and the results are discussed.

6.2.1 Single stage overhung pump mechanical features

As previously mentioned in section 1.1, the single stage pump chosen for the preliminary work was selected based upon a test pump being available to carry out experimental testing to validate the numerical results. A schematic of the cross section of the pump is shown in Figure 47.

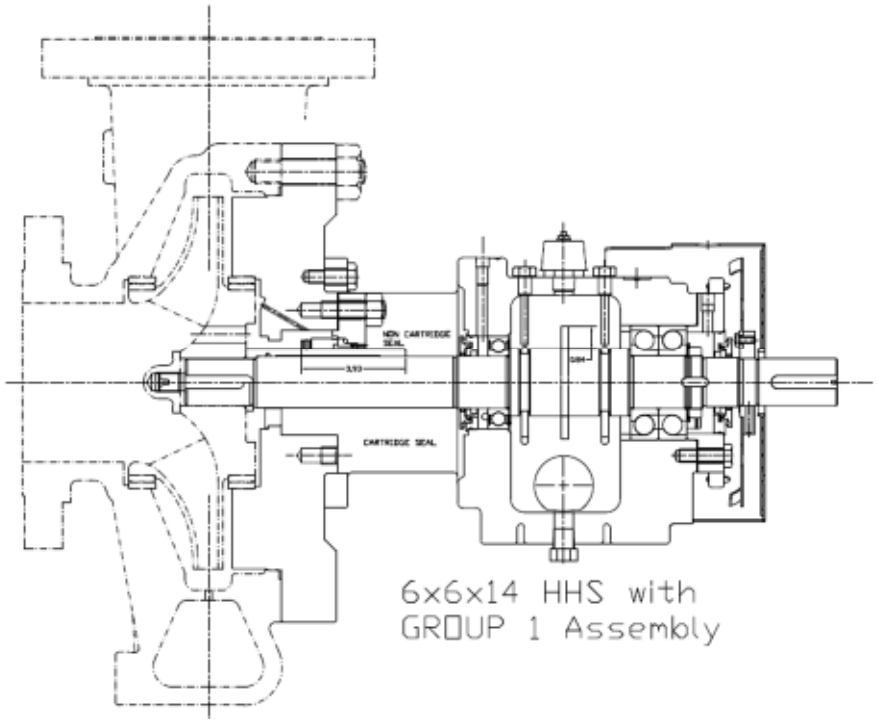

Figure 47 Cross sectional schematic of the single stage overhung pump (SPXFLOW Clydeunion Pumps)

The shaft is a “stiff shaft” design in accordance to API 610 standard for all single stage pumps to have their first critical speed in air above running speed. The shaft is supported by a single radial ball bearing and two single row angular contact ball bearings, which also provide thrust capability. A coupling hub is fitted to the end of the shaft and is to be considered in the rotordynamic study.

The impeller is shrink-fitted to the shaft and housed into the pump volute casing with a mechanical seal and stuffing box. The materials of the components are steel.

6.2.1.1 Mathematical Model of the Single Stage Pump Rotor

The first stage of the investigation is to create the model comprising of disk and shaft elements. The dimensions of the rotor are taken directly from the engineering drawings provided by the sponsor. Details of the bearing locations are also taken from engineering drawings, table 5 shows the shaft dimensions and mass and inertias of the impeller (station 4), mechanical seal (station 9) and coupling half (station 27). When modelling a shaft, it is recommended to follow the guidelines outlined in the book, Machinery vibration and rotordynamics Vance (2010). The ratio of length and diameter is important to control accuracy as a general rule L/D equal to 1 is sufficient. Once the beam elements and associated mechanical properties is complete a geometry model is then generated, Figure 48.

Table 5 XL rotor beam and station definitions

Station	Length	OD	ID	Density	Elastic Modulus	Shear Modulus	Added Weight	Added Ip	Added It	Speed Factor
#	mm	mm	mm	kg/m^3	N/m^2	N/m^2	kg	kg-m^2	kg-m^2	
1	12.7	12.7	0	7833.545	2.068E+11	8.273E+10	0	0	0	1.0
2	12.7	12.7	0	7833.545	2.068E+11	8.273E+10				1.0
3	12.7	44.45	0	7833.545	2.068E+11	8.273E+10	0	0	0	1.0
4	15.875	44.45	0	7833.545	2.068E+11	8.273E+10	16.684	0	0.102	1.0
5	15.875	44.45	0	7833.545	2.068E+11	8.273E+10				1.0
6	31.75	44.45	0	7833.545	2.068E+11	8.273E+10				1.0
7	34	49.2125	0	7833.545	2.068E+11	8.273E+10	0	0	0	1.0
8	34	49.2125	0	7833.545	2.068E+11	8.273E+10				1.0
9	22.5	49.2125		7833.545	2.068E+11	8.273E+10	2	0.002	0	1.0
10	22.5	49.2125	0	7833.545	2.068E+11	8.273E+10				1.0
11	37.5	49.2125	0	7833.545	2.068E+11	8.273E+10	0	0	0	1.0
12	37.5	49.2125	0	7833.545	2.068E+11	8.273E+10				1.0
13	30	50.02022	0	7833.545	2.068E+11	8.273E+10	0	0	0	1.0
14	10	50.02022	0	7833.545	2.068E+11	8.273E+10	0	0	0	1.0
15	10	50.02022	0	7833.545	2.068E+11	8.273E+10	0	0	0	1.0
16	28.9751	65.0748	0	7833.545	2.068E+11	8.273E+10	0	0	0	1.0
17	28.9751	65.0748	0	7833.545	2.068E+11	8.273E+10				1.0

18	28.9751	65.0748	0	7833.545	2.068E+11	8.273E+10				1.0
19	28.9751	65.0748	0	7833.545	2.068E+11	8.273E+10				1.0
20	13.5	50.0126	0	7833.545	2.068E+11	8.273E+10	0	0	0	1.0
21	13.5	50.0126	0	7833.545	2.068E+11	8.273E+10	0	0	0	1.0
22	13.5	50.0126	0	7833.545	2.068E+11	8.273E+10	0	0	0	1.0
23	13.5	50.0126	0	7833.545	2.068E+11	8.273E+10	0	0	0	1.0
24	17.4371	46.83252	0	7833.545	2.068E+11	8.273E+10	0	0	0	1.0
25	17.4371	46.83252	0	7833.545	2.068E+11	8.273E+10				1.0
26	16	45.212	0	7833.545	2.068E+11	8.273E+10	0	0	0	1.0
27	25.908	44.45	0	7833.545	2.068E+11	8.273E+10	13.15	0	0.33	1.0
28	25.908	44.45	0	7833.545	2.068E+11	8.273E+10				1.0
29	25.908	44.45	0	7833.545	2.068E+11	8.273E+10				1.0
30	0	0	0	0	0	0	0	0	0	1

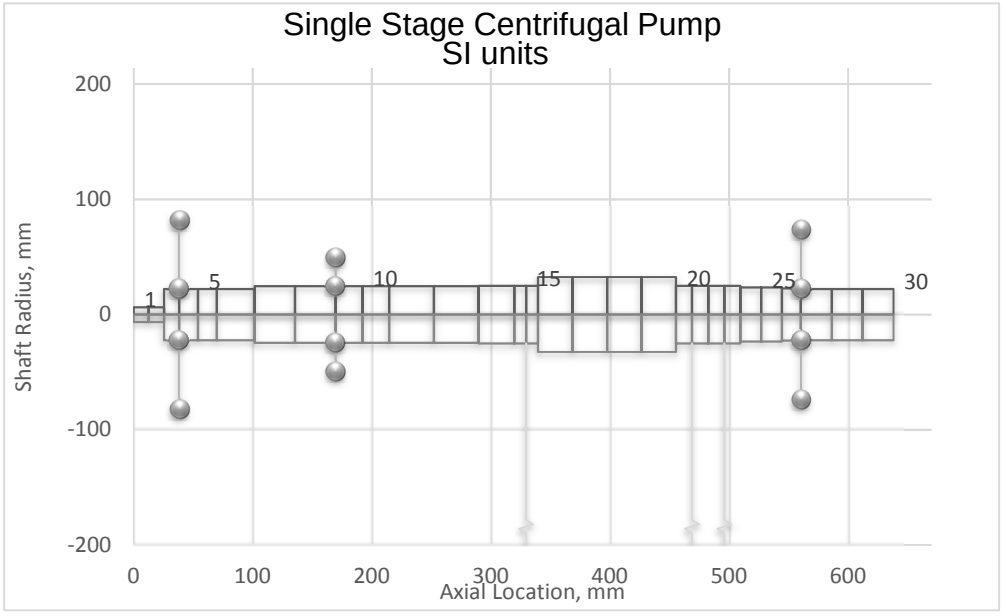

Figure 48 Geometry plot XL model of the single stage pump rotor

6.2.2 Rotordynamic Study Expectations

Due to the characteristics of a single stage pump and the shaft being of a “stiff shaft” design it is not expected to uncover concerns with the mechanical construction. Although it is known the natural frequencies are much higher than

the operating speed for the pump being analysed, a lateral analysis is carried out and is included in Appendix C.

The pump has a double volute, therefore the radial force acting on the impeller is minimised. If the pump was a single volute it be expected the impeller-volute interaction forces to be of greater significance.

The preliminary numerical study at BEP operating point provides visualisation of the flow features when hydraulic components are in design alignment. At this condition the expectation is the vibration related to the blade passing the volute tongue would be benign. The single stage pump analysed for a range of flow rates (presented early in this chapter) show that at low flow conditions and at high flow conditions the flow would become distorted around the cutwater region and the forces acting on the impeller increase.

6.2.3 Transient response to hydraulic load

The CFD transient simulations captured the fluid forces acting on the impeller for three revolutions of the shaft in the x and y direction. These forces extracted from the CFD simulation are discrete forces for the x and y direction, in the rotating reference frame. Figure 49 shows the volute orientation. Firstly, the forces are converted to the absolute reference frame using equation 18. The transient function in XL rotor requires a continuous function. The plotted forces, for one revolution of the shaft are inputted in to MATLAB where a curve fitting tool, allows a load formula to be derived to represent the hydraulic force.

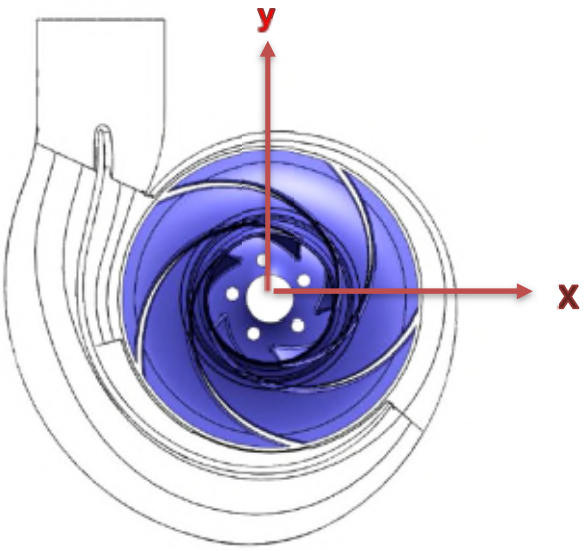

Figure 49 Volute orientation

.

The derived function is incorporated into the rotordynamic model as a time dependant load formula for the x and y direction. XLrotor program calculates the corresponding displacements and velocities at a specified location. This can be calculated at the mechanical seal and bearing locations as a function of time.

The function representing hydraulic excitation forces is loaded at station 4 which corresponds to the impeller location. The output stations are at the mechanical seal (for comparison with experimental data) and the radial bearing at locations 9, and 15 respectively.

The results of the rotordynamic investigation are presented in Table 6 showing displacement fluctuations in the peak to peak form.

Table 6 Estimated displacement vibration at output stations corresponding to the mechanical seal and radial bearing

Displacement Transient response units µm							
Station	Location	Direction	Qn				
			0.25	0.5	0.75	1	1.25
9	Mechanical Seal	x - XLrotor	17	5.3	1.7	0.13	2
		y - XLrotor	23	11	3.1	2	5
15	Radial Brg	x - XLrotor	2.1	1.1	0.46	0.4	0.5
		y- XLrotor	4.9	2.4	1.4	0.9	1.3

6.2.3.1 Resultant Vibration at the Seal Location

The seal location vibration was investigated to compare with the displacement measurements obtained experimentally in chapter 5.6. Therefore, the displacement estimated at station 9 within the rotordynamic model has been assessed. Figure 50, shows a sample displacement response from the hydraulic force, at station 9. As the load formula function in XLrotor is truly for a time dependant function it can be observed that the response to the hydraulic force decays. This is because the formula inputted relates to one revolution of the impeller. As the impeller rotates continuously at a speed of 3560rpm it can be assumed that the transient response would also continue for the period of pump operation. A further point to consider is that for a transient force input the possible effects of dynamic amplification effects may not be captured.

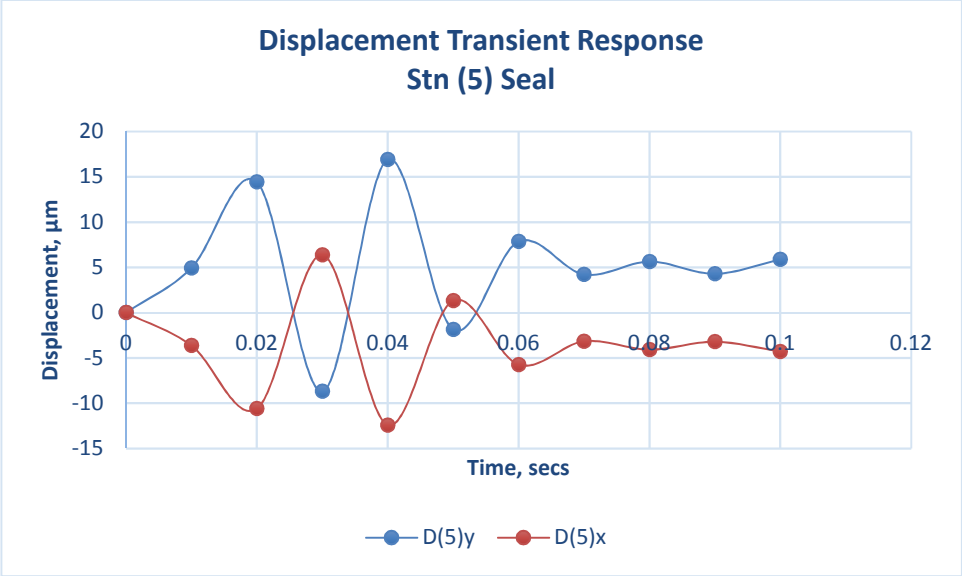

Figure 50 Sample displacement response to hydraulic force at the mechanical seal location with units µm

The response to the hydraulic forces has been calculated for each of the pump operating conditions and is shown in Figure 51.

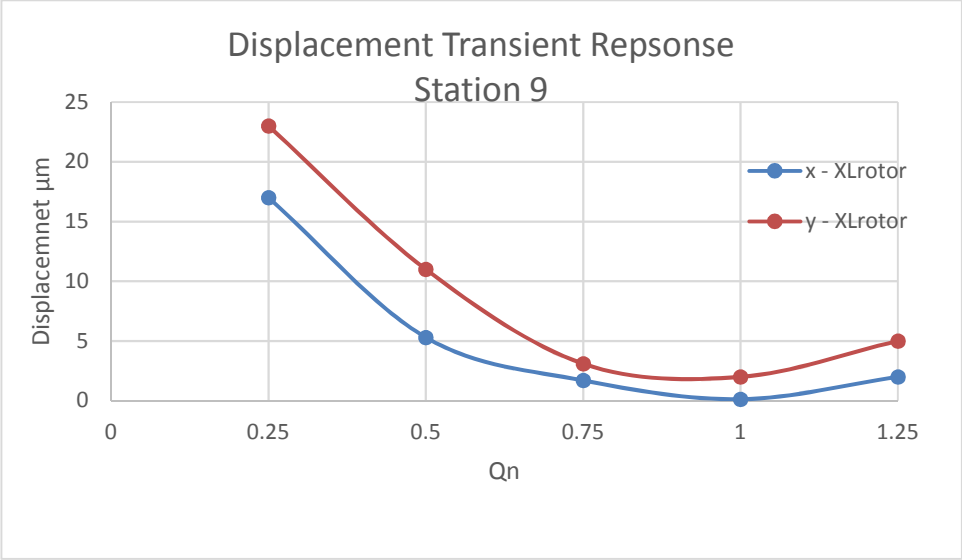

Figure 51 Displacement Transient response plotted as a function of Q_n

It is observed that the displacement response follows a similar trend to the experimental results in that at the low flow operating region the displacement is at a maximum and the lowest displacement is located at the nominal flow

condition. The displacement vibration is lower in the x direction than in the y direction which corresponds to the hydraulic force data.

6.2.3.2 Resultant Forces at the Bearing Location

The resultant estimated displacement vibration at the bearing location, from the hydraulic force, is shown in Figure 52 as a function of Q_n. Unsurprisingly the trend is similar to that found at the seal location however the values are much less as predicted by the unbalance response shown in figure 30 in section 5.2. There is also greater deviation between the displacement in the x and y direction particularly at the low operating region. The actual values are not of great significance the radial bearing can withstand the level of vibration estimated and this was an expected outcome of the results for this particular pump design.

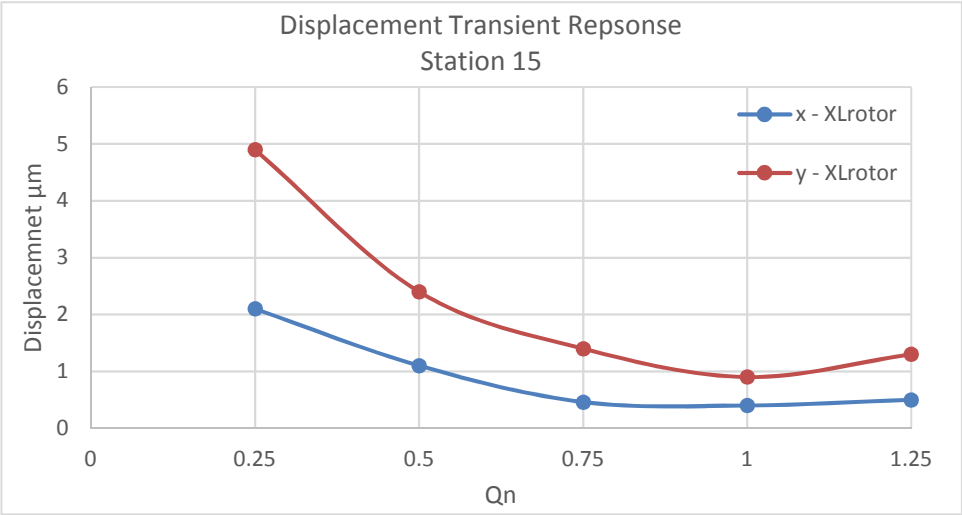

Figure 52 Displacement Transient response plotted as a function of Q_n at the radial bearing

6.3 Summary of Numerical Investigation

This chapter has presented the numerical investigation of a single stage pump across five operating conditions. The numerical results obtained for pressure pulsations, hydraulic force data and rotordynamic response have been obtained. The following is a summary of the findings:

- CFD can be utilised to visualise the fluid flow behaviour of a pump, in particular part load conditions can allow a pump design to be evaluated where the fluid flow patterns are highly disturbed and three dimensional
- Pressure distributions around the volute have been reported upon and compared for varying operating conditions
- Velocity vectors generated numerically clearly identify fluid flow features that concur with published literature
- Time dependant pressure pulsation data estimated numerically follows a similar trend to experimental data in that the highest fluctuations were shown to be at the minimum flow condition and at the cutwater region
- Hydraulic forces acting on the impeller were obtained for each operating condition
- Hydraulic forces were incorporated into a rotordynamic model for a series of operating conditions
- Transient response to the hydraulic forces were reported upon at the mechanical seal and radial bearing locations
- The displacement vibration estimated for the single stage pump proved to be within acceptable levels

7 Discussion of Results

In this chapter a review of the comprehensiveness of the numerical model exploring hydraulic interaction in a centrifugal pump, is presented. Firstly, a comparison study between the experimental work presented in chapter 5 and the numerical investigation shown in chapter 6 is discussed. Secondly recommendations of how the model can be optimised are presented.

7.1 Comparison of numerical and experimental results

To compare the numerically calculated unsteady pressure fluctuations with the experimental results presented in chapters 5 and 6 respectively, eight monitoring points were employed to capture the data. The channels named C1 to C8 measured the time dependant pressure and are presented in the normalised form.

7.1.1 Discussion of pressure pulsation results

Figure 51 shows the unsteady pressure fluctuations for each location as a function of flowrate. The experimental results are plotted for five operating conditions whereas the numerical results obtained were for three flowrates where Q_n equals 0.25, 1.00 and 1.25.

C1-C4 monitoring points are located in close proximity to the cutwater and C5-C8 are at monitoring location around the volute at circumferential positions as outlined in Figure 29 in section 5.3.

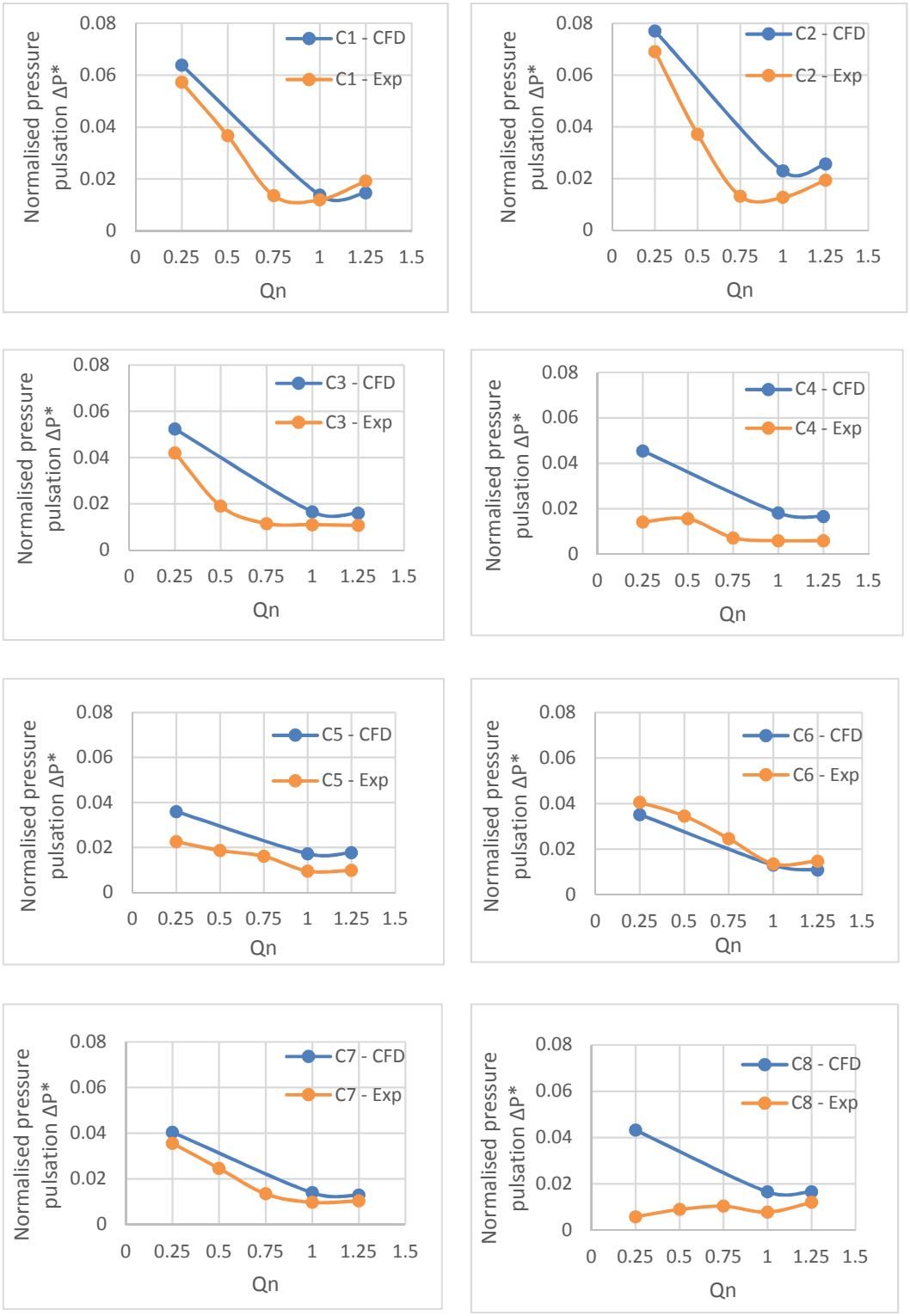

Figure 53 Comparison of normalised pressure pulsations at locations C1-C8 estimated numerically and experimentally

7.1.1.1 Pressure Pulsations Obtained at C1-C4

In all four locations the numerical results are higher than the experimental results with one exception at location C1, upstream of the cutwater, at the high flow operating condition the CFD prediction is lower than the experiment result. The highest pressure pulsations are observed at location C2 which is just past the cutwater position. This is an expected result as this is the area where the rotor stator interaction effects are greatest based upon the relatively small clearance between the impeller and volute lip. The pressure pulsations follow a similar trend with the exception of the experimentally estimated pressure pulsation at monitoring position C4. The plotted curve is fairly flat and inconsistent with the general results. This can also be seen in the experimental result for channel 8. It is likely that the experimental result for channel 4 and 8 is not valid and that the pressure transducer was not measuring correctly as the same transducer was used for both these positions.

It can be observed that the CFD results at nominal flow are closely approximated to the experimental data. However, when comparing the results at part load the CFD results appear to be slightly overestimated. As the flowrate is decreased there is likely to be a greater degree of error in the numerical estimations. Part load numerical modelling is renowned for being a complex process. In addition the pump model investigated is a simplified model where the leakage flow passageways were neglected, considering the leakage passageways would lead to greater damping and therefore the approximations would likely be decreased and therefore improving the accuracy of the simulation.

7.1.1.2 Pressure Pulsations obtained at C5-C8

The CFD results obtained for locations C5-C8 generally are fairly consistent and are closely approximated to experimental data, with the exception of C8 for the experimental result as discussed above.

Surprisingly C6 reports an inverse trend, the CFD estimations are below those obtained experimentally. In addition, the maximum flow condition reports a lower level of pressure pulsation than at nominal flow point. However, the results remain of similar order.

7.1.2 Discussion of Results for Displacement Vibration

The displacement vibration estimations follow a similar trend. Figure 54 shows the experimental result and numerical result plotted as a function of flowrate. It is noted that the displacement measured during the experiments was measured in a single plane corresponding to the y direction. This was due to limited areas for direct measurement of the shaft displacement in the area of the mechanical seal. Therefore, the results have been compared for the y direction only.

It can be seen that the displacement at Q_n equal to 0.25, the numerically estimated displacements are higher than measured experimentally, but are closer in value at flows greater than 0.75 Q_n and are fairly well at 0.50 Q_n.

The displacement result captured experimentally might be lower due to the physical clearance of the radial bearing.

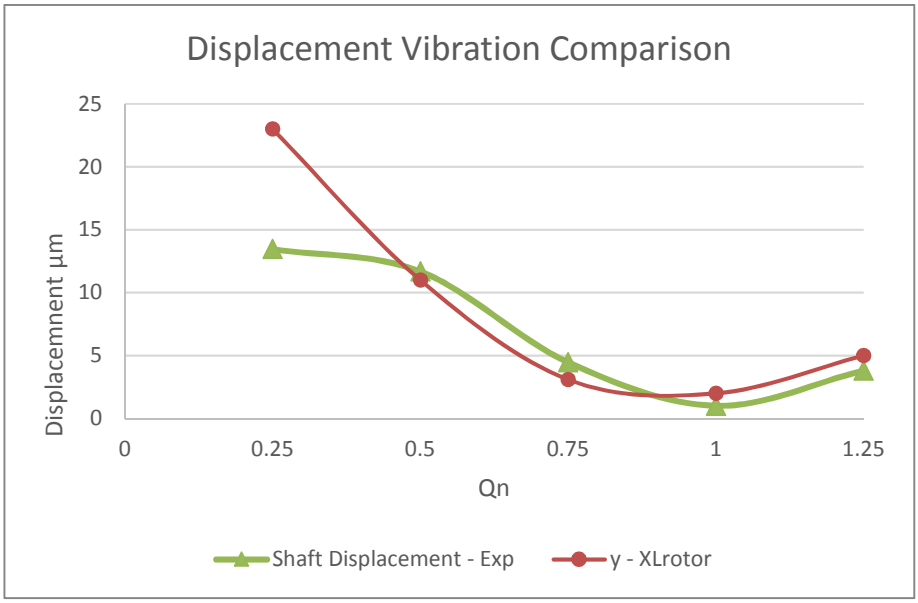

Figure 54 Comparison of numerical and experimental estimations for the displacement at the mechanical seal location

7.1.3 Summary of Results

The compared results are generally in good agreement, where similar trends have been identified.

The pressure fluctuation results are in close approximation at flowrates close to the nominal flowrate of within 15% when comparing the numerical estimates with the experimental data. It was observed that there were greater deviations of up to 23% between the results at “off design” conditions and this was for locations close to the cutwater region.

Some discrepancies in the experimental data for channel 4 and channel 8 have been identified relating to the unsteady pressure fluctuations however the other channels or monitoring locations show good agreement.

The results show that the unsteady pressure is within an acceptance tolerance of +/- 5% which provides validation that CFD can be a useful tool in estimating the hydraulically induced vibration with the requirement for optimisation of the numerical model for part load operation.

Displacement measurements proved to be less accurate showing some large discrepancies at low flow regions of up to 70%. The method for measuring the displacement experimentally was fairly crude by means of a clamp arrangement and restrictions within the pump prevented measurements being taken at the desired location at the impeller. The results were within a closer margin at midway flow points for 0.5Qn and 0.75Qn. Interestingly at BEP the experimental estimate was half that of the numerical estimate however the levels of displacement are relatively low at 1 and 2 microns respectively.

The process for incorporating hydraulic force data into a rotordynamic model has been demonstrated. There is further work to carry out for refinement of the load formula to represent the hydraulic forces to account for the hydraulic force data being fully periodic. As the transient response decayed this effected the peak-peak measurements obtained, therefore it is likely that the presented data is overestimated.

7.2 Numerical Method Optimisation

The numerical model utilised in the present research was simplified and neglected leakage flow passageways. This has led to some variation in results for the estimated unsteady fluid flow behaviour particularly at low flow operating conditions. To accurately assess the hydraulic excitation forces an entire pump model is recommended consisting of a suction inlet, impeller, leakage flow passageways and volute.

Around the cutwater the flow is largely effected by the rotor stator interaction effects. It is likely that to obtain greater accuracy in this region greater refinement of the grid is required. A further grid optimisation requirement is that in the inlet pipe, for the present study an unstructured mesh was used however a structured mesh would be beneficial in order to ensure the flow is accurately predicting the flow entering the impeller. This is particularly important when investigating low flow operating regions.

As previously discussed in section 7.1.3 the load formula representing the hydraulic forces requires further investigation to represent a continuous fluctuating force.

CFD convergence factors which can affect the accuracy of the hydraulic forces captured in CFD could be further optimised. For the present study unsteady periodic convergence was utilised, where three complete cycles were deemed sufficient to meet the aims of the present research. However, increasing time step from 125 to 200 and allowing the solution to run for four to five revolutions may be of interest to improve the accuracy further.

7.3 Summary of Chapter

This chapter has evaluated the numerical method for quantifying the hydraulic interaction behaviour found within a centrifugal pump. A summary of the key findings is as follows:

- CFD captured the unsteady flow features at part load and shows good agreement with cited literature
- An analysis of the results obtained both numerically and experimentally for unsteady pressure fluctuations in a centrifugal pump has been compared and found to be of a similar trend. A comparison of the results for nominal flow operating condition, the estimations are within 15% shown in figure 53, at the cutwater (position C1). For off design conditions the estimations are within 23%.
- The estimated forces have been included in a rotordynamic model and compared with experimental data. It was found that the numerical method overestimated the transient displacement vibration at low flow regions by up to 70% but was within greater agreement at flows close to nominal flow conditions. Although the separation margin between the results is too high to be considered as validated, the trend was consistent with the overall results, in that the highest level of vibration was at the low flow region. The experimental technique employed to

measure the displacement vibration was not ideal due to restrictions preventing the probe access points to the shaft, this could have possibly contributed to errors.

- Importantly the rotordyanmic model proves that not only are the hydraulic forces transmitted to seals and bearing but with further research and optimisation, the model could be capable of accurately assessing the response to the hydraulic forces.
- Opportunities to optimise the present numerical model have been discussed

8 Conclusion and Further Work

The conclusions for this study are presented in this chapter. It has been separated into four sections. Firstly, concluding remarks are briefly summarised followed by the main conclusions drawn from the study. The industrial application of the numerical method investigated in this study is discussed and finally suggestions for further work that have been identified, that would enhance the methodology are presented.

8.1 Concluding Remarks

A detailed investigation of the transient interactions in a centrifugal pump has been carried out.

The pump chosen for the study was a single stage overhung pump. The pump was selected based upon a test pump being available for experimental testing, provided by the sponsor of this work.

The numerical method outlined in section 4 provided good guidance on CFD parameters for the purpose of capturing hydraulic excitation forces.

The experimental campaign set out to obtain the relevant vibration behaviour of the single stage pump for the purpose of comparing with the numerical results presented in chapter 6. This consisted of pressure pulsation measurements at specific locations within the sidewall of the volute and displacement vibration measuring direct shaft displacement at the mechanical seal location. In addition, pump performance characteristics were obtained

The numerical investigation involved simulating the single stage pump across five operating conditions providing visualisation of the fluid flow features at nominal flow, at low and high flow regions. The pump characteristics were obtained and compared with the experimental data. Utilising the same monitoring points as in

the experimental tests unsteady pressure fluctuations were captured and compared.

The hydraulic excitation forces were represented in a rotordynamic model and the corresponding displacements at specific locations were evaluated.

8.2 Conclusions

The main observations and conclusions from the investigation briefly described above are summarised as follows.

- A total of five transient analysis's have been successfully conducted representing approximately 1800hrs of continual analysis run time
- Velocity flow features generated by the CFD analysis are agreeable with published work for the range of operating conditions investigated including part load operating condition.
- Pressure pulsation data was collected experimentally and numerically. The results were generally found to be in reasonable agreement particularly for the nominal flow operating condition where estimations were within 15% and at "off design" conditions estimations were within a 23% range.
- The pressure pulsations estimations showed the highest unsteady fluctuation was found in the cutwater region. Within this region the pressure pulsation data was found to be in better agreement at nominal flow when compared to the data collected for lowest flow condition.
- The estimated normalised pressure pulsation at the BEP at the cutwater location which corresponded to the blade passing frequency was 503kPa. When operating at the minimum flow condition the estimated vibration was 70% greater than that at the BEP. At the maximum flow condition, the estimation was just 11% greater.
- Hydraulic excitation forces were obtained numerically and represented into a rotordynamic model. It was observed that the transient

displacement vibration followed a similar trend to the pressure pulsation results, as the highest vibration was estimated at the low flow region. However, when compared to the experimental data the results were not within an acceptable tolerance range. This could have been attributed by the experimental technique employed to measure the displacement at the seal location as well as restriction within the radial bearing clearance of the test pump. In addition, the rotordynamic numerical method requires optimisation to represent a continuous periodic hydraulic force rather than for one impeller revolution. This led to the estimated peak to peak values being effected as the transient response decayed over time.

- For indicative purposes the estimated displacement vibration (peak to peak), at the BEP was 2μm, which is considered negligible. However, the estimated displacement vibration at low flow was 23 μm. Although this is likely to be an overestimation as the experimental data approximates the displacement vibration to be 13 μm, it suggests hydraulic excitation forces could be significant when operating at low flow operating conditions.
- The investigation on the single stage pump did not uncover a potential vibration problem with the pump however this is a design that has been developed and tested many times and was an expected outcome.

8.3 Application of the Numerical Method for Assessing Pump Vibration Behaviour

Pumps are adaptable turbomachines; they can be operated at a range of flow points, not only at the “on-design” operating condition. The advancement in variable speed drives have led to an increase demand for pumps operating for range of running speeds. Pump manufacturers routinely generate bespoke hydraulic design to satisfy customer specific duty requirements. Generating these

new designs is both expensive and high risk. Industry standards specify limits to discrete frequency vibration which manufacturers must comply with during acceptance testing of a pump.

The numerical method investigated in this study could be employed as a design tool for new hydraulic designs and to advance existing pumping technology to meet the expectations of pump users. Modern lightweight machines combined with high efficiency are expected to perform reliably. These factors present a challenge for pump design engineer as efficiency can be compromised to ensure low vibration performance. The numerical method could also investigate the effect pumping medium has on the vibration behaviour of a pump and for multiple operating conditions. Therefore, it is possible to simulate field conditions and test stand conditions at the design stage, ensuring both test stand acceptance and optimum performance in the field. Importantly the geometrical features could be easily modified and the results evaluated for multiple operating conditions prior to manufacture, this provides a design engineer the opportunity to finely tune the pump design for a particular application. From a manufacturers point of view, the desired outcome is increasing market share and low cost manufacture by satisfying the needs of the customer whilst remaining profitable.

8.4 Further Work

Transient interactions are inherent in all centrifugal pumps due to the close proximity of rotating and stationary components. However, some pump designs are at greater risk of higher vibration levels than other designs, this is mainly high energy multistage pumps. It is foreseen that the application for this work would be most suited to multistage pumps

Firstly, the methodology for numerically predicting the transient interactions in a centrifugal pump requires optimising as discussed in section 7.2. This could be performed utilising the existing single stage pump model with inclusion of leakage flow passageways. Incorporating leakage flow passageways may not be

essential for single stage modelling as it has been demonstrated reasonable results can be obtained when compared with experimental data. However, when pump simulations of greater complexity are explored such as multistage pump studies, the inclusion of the leakage flow passageways would be required to achieve good conformity with experimental results due to interaction with recirculating the fluid and the main flow (Spence 2008).

The obvious next step would be to investigate the effect of geometrical features have on the hydraulic excitation forces. It is often a fundamental trade-off when designing for high efficiency and low vibration performance. Close running clearances provide high efficiency performance however this can lead to high levels of hydraulically induced vibration which is not easily overcome at the test stand and can lead to failures in the field. Pumps are expected to be capable of operating at many flowrates where good vibration behaviour is expected. As discussed in section 8.3 an increase towards multiple operating speeds means pump rotordynamics plays an important part in the advancement of pump technology. Another factor discussed above is the effect of fluid medium on the hydraulic excitation forces. It may be of interest to investigate low specific gravity operating conditions where it is not uncommon for the first dry critical speed for a given multistage pump to be below the running speed of the pump. Maintaining lightweight machines for this application would require a comprehensive rotordynamic investigation with inclusion of hydraulic excitation forces.

Ultimately it is foreseen that a comprehensive model, combining hydraulic interaction forces and rotordynamics contributions, could be capable of predicting the fluid borne destabilizing forces of new designs within an acceptable tolerance and the likely effects on the vibration characteristics of the machine. Estimating the response of the rotor to the hydraulically induced vibration and the bearing housing reaction will highlight any risk of the design. The ability to numerically re-design hydraulic components and predict vibration potential would be a revolutionary step to pump design

.

REFERENCES

Abramian M. and Howard J.H.G. (1998) “Experimental investigation of the steady and unsteady relative flow in a model centrifugal impeller passage” ASME Journal of Turbomachinery. Vol. 116, pg. 269-279.

Admas, M. and Dekker, M. (2009) “Rotating Machinery Vibration” CRC Press/Taylor & Francis

Adkins, D. R., and Brennen, C. E., (1988) "Analyses of Hydrodynamic Radial Forces on Centrifugal Pump Impellers," ASME Journal of Fluids Engineering, Vol. 110, pg. 20-28.

Agrati, G. and Piva, A. (1999) “Multistage horizontal boiler feed pump: rotor ynamic and structural advantages multistage horizontal boiler feed pumps: Rotor dynamic and structural advantages of the opposite versus equidirectional Impellers configuration”, Weir Gabbioneta, Sesto S. Giovanni, Italy

Alder D. and Levy Y. (1979). “A laser Doppler investigation of the flow inside a backswept, closed, centrifugal impeller” Imeche Journal Mechanical Engineering Science Vol. 21, No1, pg. 1-6.

Allaire, P. E., Branagan, L. A., and Kocur, J. A. (1982) "Aerodynamic Stiffness of an Unbound Eccentric Whirling Centrifugal Impeller with an Infinite Number of Blades," NASA CP. 2250, pg. 323-343.

Arndt, N., Acosta, A. J., Brennan, C. E. and Caughey, T. K. (1990). “Experimental Investigation of Rotor-Stator Interaction in a Centrifugal Pump with Several Vaned Diffusers.” ASME Journal of Turbomachinery Vol. 112, pg. 98-108.

Asuaje, M., Bakir, F., Noguera, R. and Rey, R. (2006) “Three Dimensional Quasi-Unsteday Flow Simulation in a Centrifugal Pump: Comparison with Experimental Results” IMECHE Journal of Power and Energy Vol. 220 Part A, pg. 239-256

Barrio, R., Blanco, E., Parrondo, J., González, J. and Fernández, J. (2008) “The Effect of Impeller Cutback on the Fluid-Dynamic Pulsations and Load at the Blade-Passing Frequency in a Centrifugal Pump” ASME Journal of Fluids Engineering Vol. 130.

Baun, D., Kostner, L. and Flack, R.D (2000) “Effect of Relative Impeller- to- Volute Position on Hydraulic Efficiency and Static Radial Force Distribution in a Circular Volute Centrifugal Pump” ASME Journal of Fluids Engineering Vol. 122, pg. 598-605.

Benra, F-K., Dohem, H.J. and Wan, B. (2006) “Determination of Pump Deflections:Compariosn of FSI Simulations to Measurements” Proceedings of FEDSM2006 ASME US-European Fluids Engineering Summer Meeting July 17-20 Maiami

Binder R.C. and Knapp R.T. (1958).“Experimental determinations of the flow characteristics in the volutes of centrifugal pumps.” Trans ASME Paper No. HYD-58-4.

Blanco-Marigorta E., Fernandez-Francos J., Gonzalez-Perez J. et al (2000). Numerical flow simulation in a centrifugal pump with impeller–volute interaction. In: FEDSM200-11297. Proceedings of ASME FEDSM’00. ASME 2000 Fluids engineering division summer meeting, June 11–15, Boston, Massachusetts; 2000

Brownell R.B., Flack R.D. and Kosrezewsky G.J. (1985). “Flow visualisation in the tongue region of a centrifugal pump.” The Journal of Thermal Engineering Vol. 4, pg. 35-45

Bolleter, U., Leibundgut, E. and Sturchler, R. (1989) “Hydraulic interaction and excitation forces of high head pump impellers”. ASME paper Vol. 81, pg. 187-193

Busemann A. (1928), Das Forderverhaltniss radialer Kreiselpumpen mit logerithmischspiraligen Schaufeln, Zeitschrift fur Angewandte Mathematik und Mechanik, Vol.8 October pp372-384 as cited in Tuzon J (2000) Centrifugal Pump Design.

Chamieh, D. S., Acosta, A. J., Brennen, C. E., Caughey, T. K. and Franz, R. (1985), ‘‘Experimental Measurements of Hydrodynamic Radial Forces and Stiffness Matrices for a Centrifugal Pump Impeller,’’ ASME J. Fluids Eng., Vol. 107, pg. 307–315.

Cheah, K.W., Lee, T.S., Winoto, S.H. and Zhao, Z.M (2007), “Numerical Flow Simulation in a Centrifugal Pump at Design and Off Design Conditions” International Journal of Rotating Machinery Vol. 2007, Article ID 83641

Chen and Liaw (1997) “The Flowfield calculation of a centrifugal pump with volute”. Proceedings of the International Gas turbine and Aerospace Congress and Exhibition. 97-GT-49. pg. 1-10

Childs, D. W. (1983a) "Dynamic Analysis of Turbulent Annular Seals Based on Hirs' Lubrication Equation," ASME Journal of Lubrication Technology, pg. 429-436.

Childs, D. W. (1983b) "Finite-Length Solutions for Rotordynamic Coefficients of Turbulent Annular Seals," ASME Journal of Lubrication Technology, pg. 437-445.

Childs, D. W. and Kim, C. H. (1985) "Analysis and Testing for Rotordynamic Coefficients of Turbulent Annular Seals with Directionally-Homogeneous Surface-Roughness Treatment for Rotor and Stator Elements," ASME Journal of Tribology, pg. 296-306.

Childs, D. W. (1993) Turbomachinery Rotordynamics, New York, New York: John Wiley & Sons, Inc.

Childs, D. W. (1994) "Annular Pump Seals and Rotordynamics," Proceedings of the Fourth International Conference on Rotordynamics, IFToMM, Chicago, Illinois, pg. 153-162.

Choi, J-S., McLaughlin, D.K. and Thompson, D.E. (2000) “Experiments on the unsteady flow field and noise generation in a centrifugal pump impeller” Journal of sound and vibration Vol.263, pg. 493-514

Chu, S., Dong, R. and Katz, J. (1995) “Relationship Between Unsteady Flow, Pressure Fluctuations, and Noise in a Centrifugal Pump – Part A: Use of PDV Data to Compute the Pressure Field.” ASME Journal of Fluids Engineering Vol. 117, pg. 24-29.

Chu, S., Dong, R. and Katz, J. (1995) “Relationship Between Unsteady Flow, Pressure Fluctuations, and Noise in a Centrifugal Pump – Part B: Effects of Blade-Tongue Interactions.” ASME Journal of Fluids Engineering Vol. 117, pg. 30-35.

Colding–Jorgensen, J. (1980) “Effect of Fluid Forces on Rotor Stability in Centrifugal Compressors and Pumps.” NASA CO-2133, pg. 249-266.

Cooper P. and Graf E. (1994) “Computational Fluid Dynamical analysis of complex internal flows in centrifugal pumps”. Proceedings of the eleventh annual international pump user’s symposium. pg. 83-94

de Jong, C.A.F. (1995) “Analysis of pulsations and vibrations in fluid-filled pipe systems” ASME, Design Engineering Division (Publication) DE Vol 84, Issue 3 Pt B/2, 1995, pg. 829-834

de Ojeda, W., Flack, R. D. and Miner, S. M. (1995) ‘‘Laser Velocimetry Measurements in a Double Volute Centrifugal Pump,’’ Int. Journal of Rotat. Mach., 1, Nos. 3–4, pg. 199–214.

Dean, R.C. (1959) “On the necessity of unsteady flow in fluid machines”, Journal of Basic Engineering, March 1959, pg. 24-28

Domm, U. and Hergt, P. (1970) ‘‘Radial Forces on Impeller of Volute Casing Pumps,’’ Flow Research on Blading, Elsevier, NY, pg. 305–321.

Dong R., Chu S. and Katz J. (1992a) “Quantitative visualisation of the flow within the volute of a centrifugal pump. Part A: technique.” ASME Journal of Fluids Engineering Vol. 114, No. 3 pg. 390-395.

Dong R., Chu S. and Katz J.(1992b). “Quantitative visualisation of the flow within the volute of a centrifugal pump. Part B: results and analysis.” Vol. 114, No. 3 pg. 396-403

Dong, R., Chu, S. and Katz, J. (1997) “Effect of Modification to Tongue and Impeller Geometry on Unsteady Flow, Pressure Fluctuations and Noise in a Centrifugal Pump,” ASME J. Turbomach., Vol. 119, pg. 506–515.

Dring, R.P., Joslyn, H.D., Hardin, L. W. and Wagner, J. H. (1982) “Turbine Rotor-Stator Interaction” ASME Journal of Engineering for Power, Vol 104, pg. 729-742

Dupont, P., Caignaert, G., Bois, G. and Schneider, T. (2005) “Rotor-Stator Interactions in a Vaned Diffuser Radial Flow Pump” Proceedings from the ASME Fluids Division Summer Meeting and Exhibition June19-23, Houston TX USA

Dyson, G. (2007), “Investigation of the closed valve head of centrifugal pumps” Cranfield University

Eckardt, E. (1976). “Detail Flow Investigation Within a High Speed Centrifugal Compressor Impeller.” ASME Journal of Engineering For Power, Vol 98, pg. 390-402.

Fischer K. and Thoma D.(1932) “Investigation of the Flow in A Centrifugal Pump” Presented at the meeting of ASME June27 1932

Fongang, R., Colding-Jorgenson, J. and Nordman, R. (1998), ‘‘Investigation of Hydrodynamic Forces on Rotating and Whirling Centrifugal Pump Impellers,’’ ASME J. Turbomach., Vol. 120, pg. 179–185.

Fowler, H. (1968). The distribution and stability of flow in a rotating channel. Journal of for Gas Turbine and Power, pg. 229-236.

Genta, G. and Gugliotta, A. (1988) “A conical element for finite element rotor dynamics,” Journal of Sound and Vibration, Vol. 120, no. 1, pg. 175–182, 1988.

Ghoneam, S, M,.Abdel-Rahman, S. and Gazzar, D. (2011), “Dynamic performance application of a variable speed Centrifugal pump” Fifteenth International Water Technology Conference, IWTC 15 2011, Alexandria, Egypt

Goulas A. and Truscott G. (1988) “The flow at the tip of an impeller at off-design conditions.”C336/88 Proc. IMechE Conf. “Part-Load Pumping operation, control and behaviour.”

González, J., Fernandez, J., Blanco, E. and Santolaria, C. (2002). “Unsteady Flow Structure on a Centrifugal Pump: Experimental and Numerical Approaches.” In 2002 Joint US-European Fluids Engineering Summer Conference, Montreal Canada, July 14-18, 2002. FEDSM2002-31182.

González, J., Parrondo, J., Santolaria, C. and Blanco, E. (2006), “Steady and Unsteady Radial Forces for a Centrifugal Pump with Impeller to Tongue Gap Variation,” ASME J. Fluids Eng., Vol. 128, pg. 454–462.

Goto, M. (1990) “Pressure pulsation in a centrifugal pump-piping system (experimental examination of characteristics of pressure pulsation)” JSME International Journal Vol 33, Issue 1, pg. 106-113

Graf, E. (1993) “Analysis of centrifugal impeller BEP and recirculation flows; comparison of Quasi-3D and Navier-Stokes solutions.” ASME FED – Vol. 154 Pumping Machinery

Guelich, J., Jud, W. and Hughes, S. F. (1986). “Review of Parameters Influencing Hydraulic Forces on Centrifugal Impellers.” In: Radial Loads and Axial Thrusts on Centrifugal Pumps: Papers Presented at a Seminar Organized by the Fluid Machinery Committee of the Power Industries Division of Mechanical Engineers on 5 February 1986.

Guelich, J. and Bolleter, U. (1992). “Pressure Pulsations in Centrifugal Pumps.” ASME Journal of Vibration and Acoustics, Vol. 114, pg. 272-279.

Gulich, J.F. (2007). “Centrifugal Pumps.” Berlin Heidelburg New York: Springer.

Guo, S., Okamoto, H. amd Maruta, Y. (2006) “Measurement on Fluid Forces Induced by Rotor-Stator Interaction in a Centrifugal Pump” JSME International Journal Vol. 49 No. 2

Hajem, M. El., Akhras, A., Champagne, J. Y. and Morel, R. (2001) “Rotor-stator interaction in a centrifugal pump equipped with a vaned diffuser,” in Proceedings of the 4th European Conference on Turbomachinery, Fluid Dynamics and Thermodynamics, Firenze, Italy, March 2001.

Ismaier, A. and Schlucker, E. (2009) “Fluid Dynamic Interaction Between Water Hammer and Centrifugal Pumps” Journal of Nuclear Engineering and Design Vol. 239, pg. 3151-3154

Ivanyushin, A.A., Nakonechnyi, L.P. and Ivanova, E.A. (1987) “Examination of Pressure Pulsations in a Single Stage Pump” AA110634 Trans FXBK99 Chemical and Petroleum Engineering Vol. 23, pg. 558-560

Iversen H.W., Rolling R.E. and Carlson J.J. (1960) “Volute pressure distribution, radial force on the impeller, and volute mixing losses of a radial flow centrifugal pump.”ASME Journal of Engineering for Power pg.136-144

Jei, G, Y and Lee, C. W. (1992) “Modal analysis of continuous asymmetrical rotor-bearing systems,” Journal of Sound and Vibration, Vol. 152, no. 2, pg. 245–262,

Jery, B., Acosta, A. J., Brennen, C. E. and Caughey, T. K. (1984) "Hydrodynamic Impeller Stiffness, Damping and Inertia in the Rotor dynamics of Centrifugal Flow Pumps," NASA CP 2338, pg. 137-160.

Kaupert, K and Thomas, B (1999) “The Unsteady Pressure Field in a High Specific Speed Centrifugal Pump Impeller Part1 – Influence of the Volute”. Journal of Fluids Engineering. Vol. 121, pg. 621-626

Kaupert, K. and Staubli, T. (1999). “The Unsteady Pressure Field in a High Specific Speed Centrifugal Pump Impeller – Part 2: Transient Hysteresis in the Characteristic.” ASME, Journal of Fluids Engineering, Vol. 121, pg. 627-632.

Kikuyama K., Minemura K., Hasegawa Y., Asakura E. and Murakami M. (1987) “Unsteady pressure distributions on the impeller blades of a centrifugal pump-impeller operating off-design.” ASME Gas Turbine Conf. And Exhibition Paper No. 87-GT-144.

Krain, H. (1981), “A Study on Centrifugal Impeller and Diffuser Flow.” ASME Journal of Engineering for Power Vol. 103, pg. 688-697.

Koumoutsos, A. (1999), “Unsteady Flow Interactions in Centrifugal Turbomachinery Configurations.” (Unpublished PhD Thesis) Cranfield University, Cranfield.

Kuiken, G.D.C. (1988) “Amplification of Pressure Fluctuations due to Fluid – Structure Interaction” Journal of Fluids and Structures 2, pg. 425-435

Launder, B., E, and Spalding, D.B. (1974) “The numerical computation of turbulent flows.” *Comp. Methods Appl. Mech. Eng.*, 3:269-289

Lennemann E. and Howard J.H.G. (1970) “Unsteady Flow Phenomena in Rotating Centrifugal Impeller Passages”. Journal of Fluid Engineering for Power. ASME Series A Vol. 92 No1, pg. 65-72

Lino, T. and Kasai, K. (1985) “An Analysis of Unsteady Flow Induced by Interaction a Centrifugal Impeller and a Vaned Diffuser” Trans. Jpn. Soc. Mech. Eng., (in Japanese), Vol.51, No.471, B pg.154-159.

Lorett, J. and Gopalakrishnan, S. (1986), “Interaction Between Impeller and Volute of Pumps at Off-Design Conditions.” ASME Journal of Fluids Engineering, Vol. 108, pg. 12-18.

Majidi, K. (2005) “Numerical Study of Unsteady Flow in a Centrifugal Pump,” ASME J. Turbomach., Vol. 127, pg. 363–371.

Miner S.M., Flack R.D. and Allaire P.E. (1992). “Two-dimensional flow analysis of a laboratory centrifugal pump.” ASME Journal of Turbomachinery Vol. 114, pg. 333-339

Miner, S. M. (2000), “Evaluation of Blade Passage Analysis Using Coarse Grids.” Journal of Fluids Engineering. ASME Vol. 122, pg. 345-348.

Morgenroth, M. and Weaver, D. S. (1998) “Sound Generation by a Centrifugal Pump at Blade Passing Frequency,” ASME J. Turbomach., Vol. 120, pg. 736–743.

Nelson, W. E. (1987) "Pump Vibration Analysis for the Amateur," Proceedings of the Fourth International Pump Symposium, Turbomachinery Laboratory, Texas A&M University, College Station, Texas, pg. 109-119.

Nordmann, R. and Massmann, H. (1984) "Identification of Stiffness, Damping, and Mass Coefficients for Annular Seals," Proceedings of the Third International Conference on Vibrations in Rotating Machinery, Institution of Mechanical Engineers, pg. 167-181.

Ohashi, H. and Shoji, H. (1987) "Lateral Fluid Forces on Whirling Centrifugal Impeller (2nd Report: Experiment in Vaneless Diffuser)," ASME Journal of Fluids Engineering, Vol. 109, pg. 100-106.

Ozguven, N and Levent Ozkan, Z. (1984) “Whirl speeds and unbalance response of multibearing rotors using finite elements,” Journal of Vibration, Acoustics, Stress, and Reliability in Design, Vol. 106, no. 1, pg. 72–79,

Pace, S. E., Florjancic, S. and Bolleter, U. (1986) "Rotordynamic Developments for High Speed Multistage Pumps," Proceedings of the Third International Pump Symposium, Turbomachinery Laboratory, Texas A&M University, College Station, Texas, pg. 45-54.

Parrondo-Gayo, J. L., Gonzalez-Perez, J. and Fernandez-Francos, J. (2002). “The Effect of the Operating Point on the Pressure Fluctuations at the Blade Passage Frequency in the Volute of a Centrifugal Pump.” ASME Journal of Fluids Engineering June 2002, Vol. 124, pg. 784-790.

Peck, J.F.(1950) “Investigations Concerning Flow Conditions in a Centrifugal Pump and the Effect of Blade Loading on Head Slip”. Proceedings of the ImechE Vol. 162, pg. 409

Pedersen, N., Larsen, P. S. and Jacobsen, C. B. (2003). “Flow in a Centrifugal Pump Impeller at Design and Off-Design Conditions – Part 1: Particle Image Velocimetry (PIV) and Laser Doppler Velocimetry (LDV) Measurements”. ASME Journal of Fluids Engineering, Vol. 125, pg. 61-72.

Rzentkowski, G. (1996) “Generation and control of pressure pulsations emitted from centrifugal pumps: A review” ASME, Pressure Vessels and Piping Division (Publication) PVP Vol. 328, pg. 439-454

Rzentkowski, G.a, Zbroja, S.b. (2000) “Experimental characterization of centrifugal pumps as an acoustic source at the blade-passing frequency” Journal of Fluids and Structures Vol 14, Issue 4, pg. 529-558

Shi, F. and Tsukamoto, H. (2001) “Numerical study of pressure fluctuations caused by impeller-diffuser interaction in a diffuser pump stage,” ASME Journal of Fluids Engineering, Vol. 123, no. 3, pg. 466–474

Simon, F. and Frêne, J. (1992) “Analysis for Incompressible Flow in Annular Pressure Seals” Journal of Tribology, Vol 114, Issue 3, pg. 431-438

Simpson,H.C., Clark, T.A. and Weir, G.A. (1966) “A Theoretical Investigation Of Hydraulic Noise In Pumps” Journal of Sound and Vibration Vol. 5 (3), pg. 456-488

Spence, R. (2006) CFD Analyses of Centrifugal Pumps with Emphasis on Factors Affecting Internal Pressure Pulsations, PhD Thesis, Cranfield University School of Mechanical Engineering Department of Power And Propulsion

Spence, R. and Amaral-Teixeira, J. (2007) “A CFD parametric study of geometrical variations on the pressure pulsations and performance characteristics of a centrifugal pump” Journal of Computers and Fluids Vol. 38, Issue 6, June 2009, pg. 1243-1257

Spence, R. and Amaral-Teixeira, J. (2008) “Investigation into pressure pulsations in a centrifugal pump using numerical methods supported by industrial tests” Journal of Computers and Fluids Vol. 37, Issue 6, July 2008, pg. 690-704

Spence, R. and Amaral-Teixeira, J. (2009) “A CFD parametric study of geometrical variations on the pressure pulsations and performance characteristics of a centrifugal pump” Journal of Computers and Fluids Vol. 38, Issue 6, June 2009, pg. 1243-1257

Timouchev, S. (2005) “Computational Study of Pressure Pulsation in a Medium Specific Speed Pump” Proceedings Of FEDSM2005 ASME Fluids Engineering Division Summer Meeting and Exhibition, June 19-23 Houston TX USA

Torbergsen, E. and White, M.F. (1997) "Transient Simulation of Impeller/Diffuser Interactions", Proceedings of the 1997 ASME Fluids Eng Division Summer Meeting, FEDSM97-3453,

Tsujimoto, Y., Acosta, A. J. and Brennen, C. E. (1988), "Theoretical Study of Fluid Forces on a Centrifugal Impeller Rotating and Whirling in a Volute," ASME Journal of Vibration, Acoustics, Stress, and Reliability in Design, Vol. 110, No. 3, pg. 263-269.

Versteeg, H.K. and Malalasekera, W. (1995) “An Introduction to Computational Fluid Dynamics the Finite Volume Method” Longman Scientific and Technical

Vetter, G; Seidl, B., (1989), “Pressure Pulsation Dampening Methods for Reciprocating Pumps.” Proc. 10th Pump Users Symp. Houston Texas 1993,

Warren Pumps, Pressure Pulsations Generated by Centrifugal Pumps, Available from:www.warrenpumps.com/resources/pressurepuls.pdf [Accessed 30 April 2009]

Wo, A. and Bons, J. (1994), “Flow Physics Leading to System Instability in a Centrifugal Pump.” ASME Journal of Turbomachinery, Vol. 116, pg. 612-620.

Worster R.C. (1963) “The Flow in Volutes and its Effect on Centrifugal Pump Performance”. Proc. ImechE Vol. 177, pg. 843-865

Young G.A.J. (1956) “Flow in the Rotating Passages of a Centrifugal Pump Impeller”. British Hydromechanics Research Association paper SP530

Yedidiah (1993). “The drooping curve of a centrifugal pump.” Proc. ROCON 93 Rotating Machinery Conf. And Exposition, Nov. 12-13 New England, USA

Zhang, M.-J. Pomfret, M. J. and Wong C. M. (1996) “Three dimensional viscous flow simulation in a backswept centrifugal impeller at the design point,” Computers and Fluids, Vol. 25, no. 5, pg. 497–507

Bibliography

Adams M.L (2001), *Rotating Machinery Vibration*. Marcel Dekker,Inc New York

Anderson, J, D, Jr. (1995) *Computational Fluid Dynamics – The Basics with Applications*, McGraw-Hill, Inc.,New York, ISBN 0-07-001685-2

API610 Standard 10th Edition (2004), *Centrifugal Pumps for Petroleum, Petrochemical and Natural Gas Industries*

Friswell, M.I (2010) *Dynamics of rotating machines*. Cambridge University Press

Gulich, J.F (2008), *Centrifugal Pumps*. Berlin Heidelburg New York: Springer.

Stepanoff, A. J., (1957) *Centrifugal and Axial Flow Pumps*, John Wiley & Sons, 2nd Edition, USA

Vance, J (2010) *Machinery Vibration and Rotordynamics*. John Wiley & sons, Inc., New Jersey

APPENDICES

Appendix A CFD Grid sensitivity study

A.1 Grid sensitivity study of an Impeller Passageway

An impeller passage has been meshed utilising CFX Turbogrid. A coarse, medium and fine mesh were investigated. Figure A-1 shows a view each mesh. Comparisons can be made of the velocity distribution through the impeller Figure A-2 shows an example, for the velocity distribution at the impeller outlet for varying grid density.

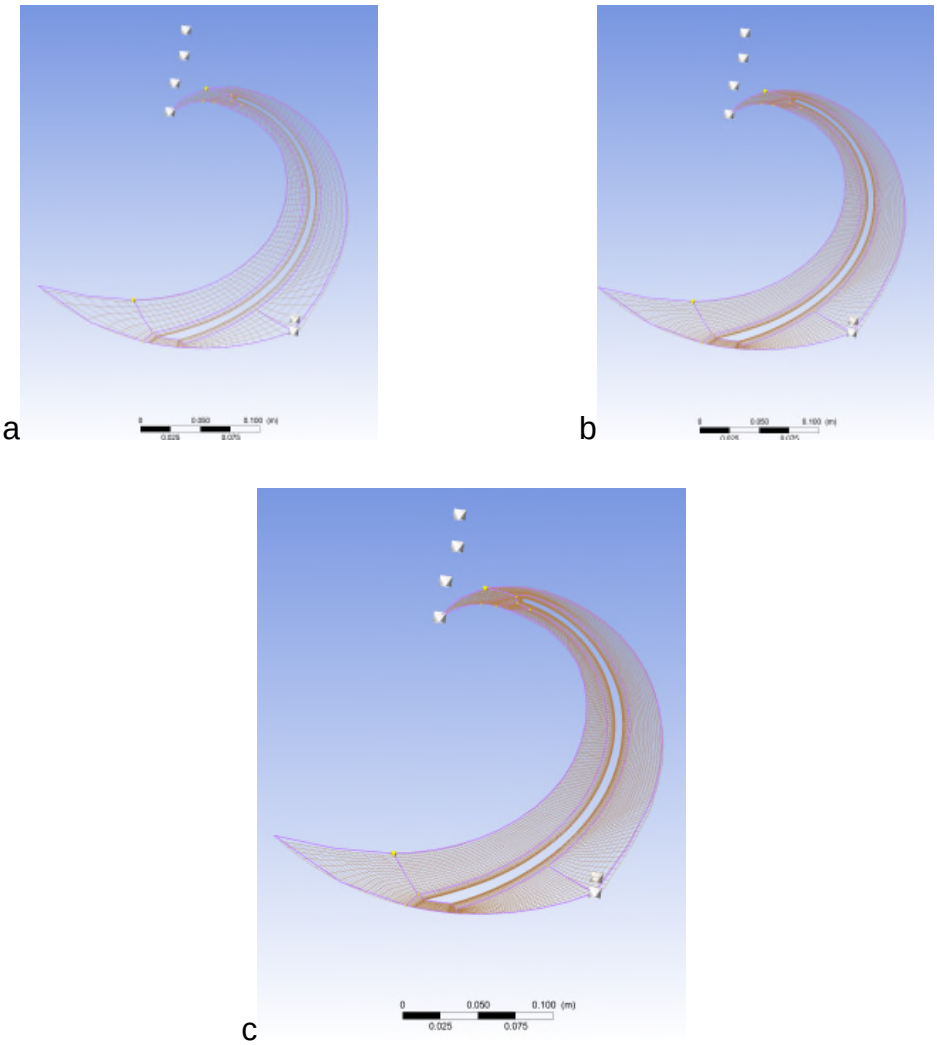

Figure A- 1 Impeller mesh for a) coarse b) medium and c) fine grid density

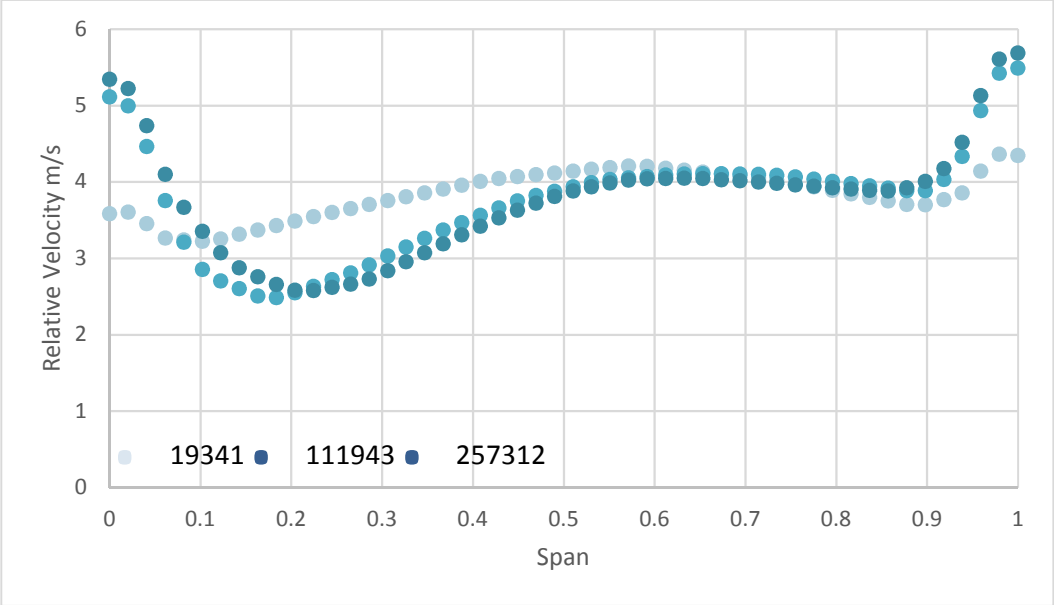

Figure A- 2 Comparison of outlet meridional velocity distribution

Appendix B Experimental Test 01 Vibration Report

In this appendix vibration average spectrum samples are provided for Test 01. Figure B-1 shows the bearing housing velocity vibration, Figure B-2 shows the pressure pulsation vibration and the Figure B-3 shows the displacement vibration.

a

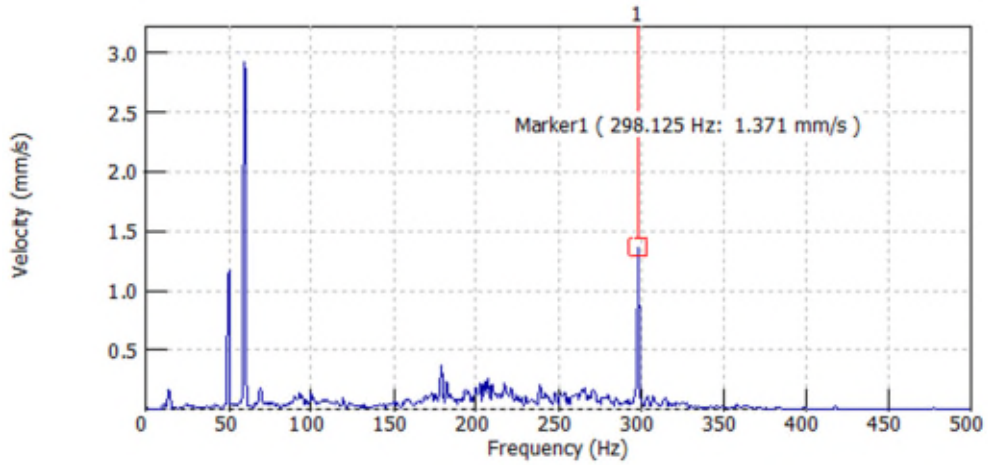

b

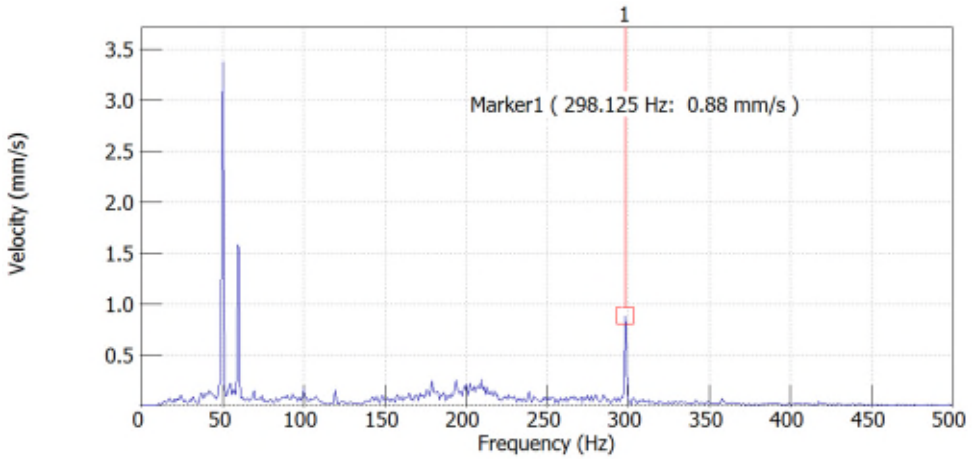

c

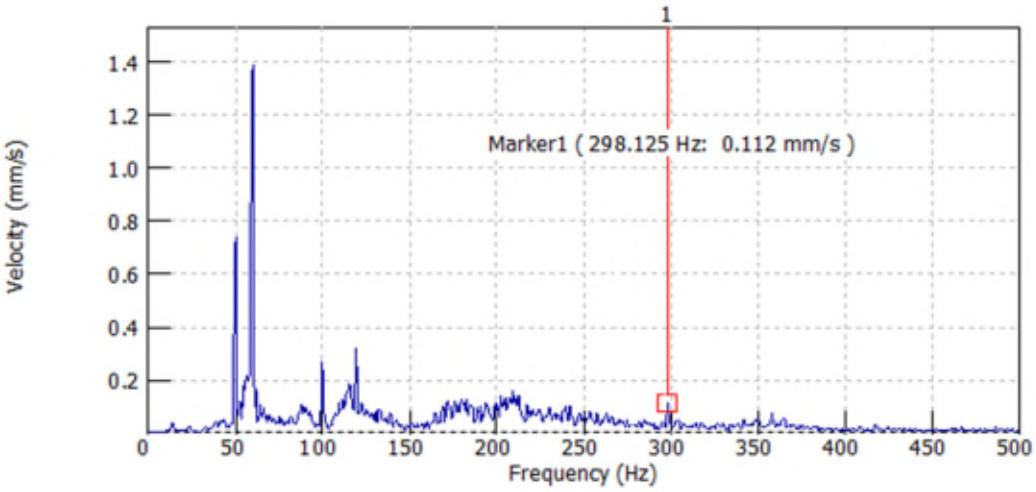

Figure B 1 Bearing Housing velocity measured in the a) vertical b) horizontal and c) axial positions respectively

a

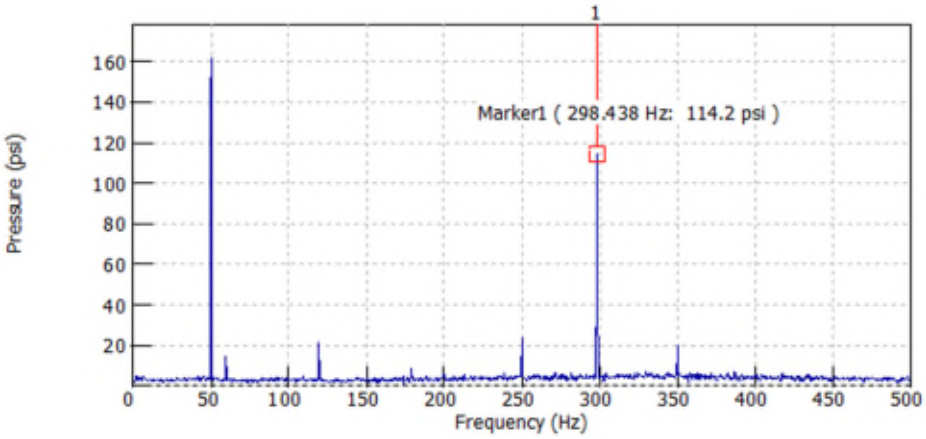

b

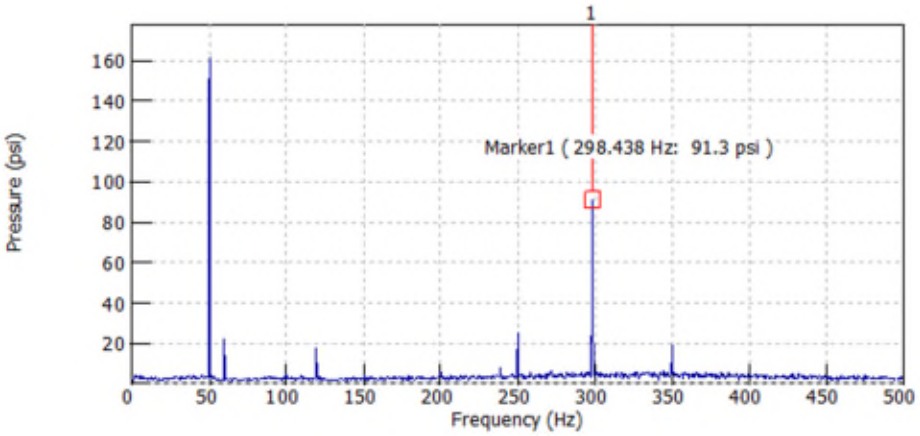

c

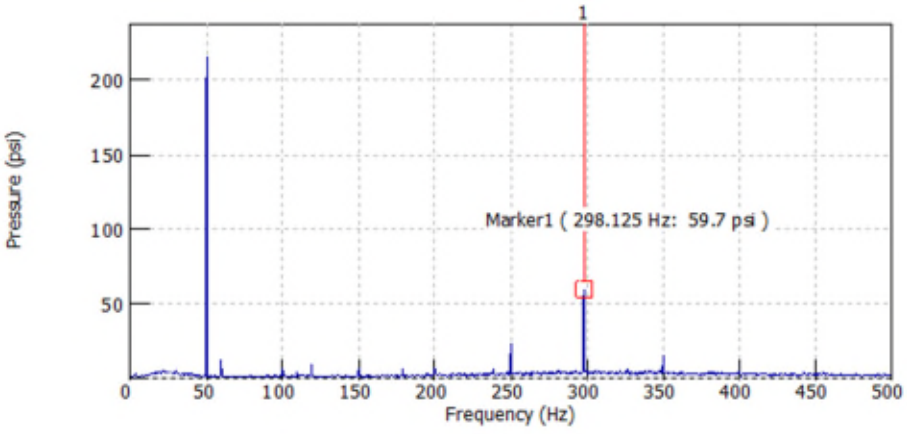

Figure B 2 Sample Unsteady pressure measurement at location C1, for a) 0.25Qn, b) 0.5Qn and c) 0.75Qn

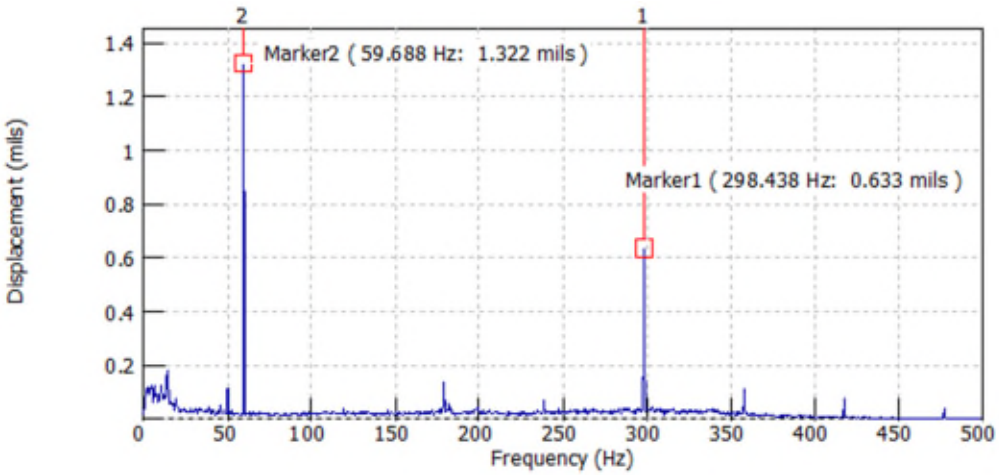

Figure B 3 Sample Displacement measurement for 0.25Qn

Appendix C Rotordynamic Lateral Analysis of a Single Stage Pump

C.1 Undamped Critical speed analysis

The free-free mode is the first assessment of the rotor. It is not connected with any bearings; this is the simplest model, shown in figure C-1. The rigid body modes are shown as natural frequencies at 0rpm. This analysis can be run with and without gyroscopic effects.

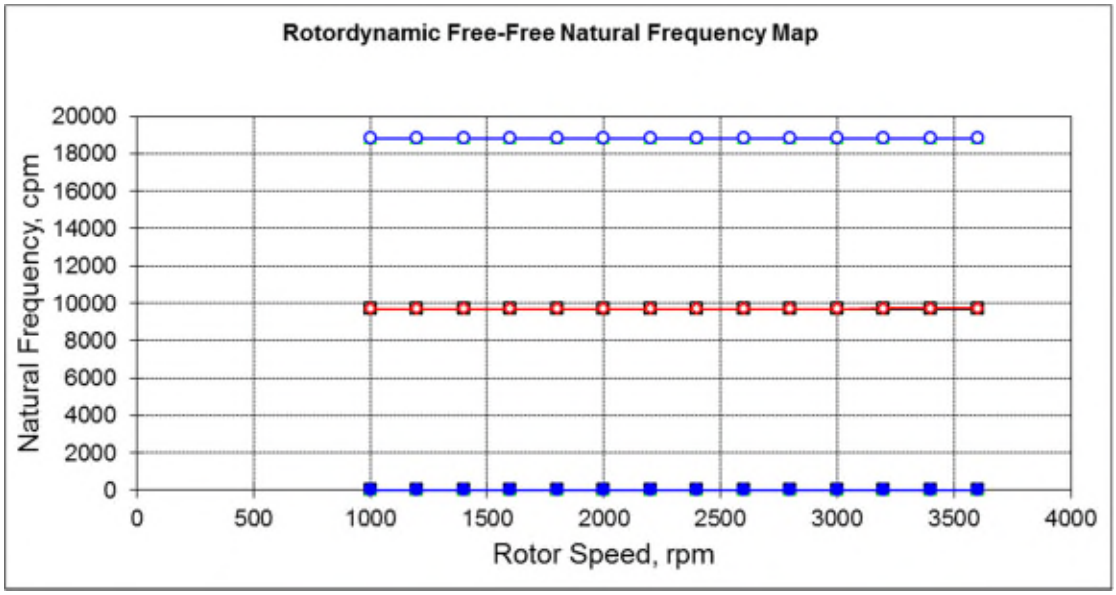

Figure C 1 Free-free natural frequency map with units cycles per minute (cpm)

The undamped critical speeds are produced by considering the direct stiffness of the bearings, figure C-2. The bearing stiffness has a significant effect on the first mode. By considering the first mode plot, figure C-3, it can be seen the highest deflection will occur at the impeller due to the heavier mass.

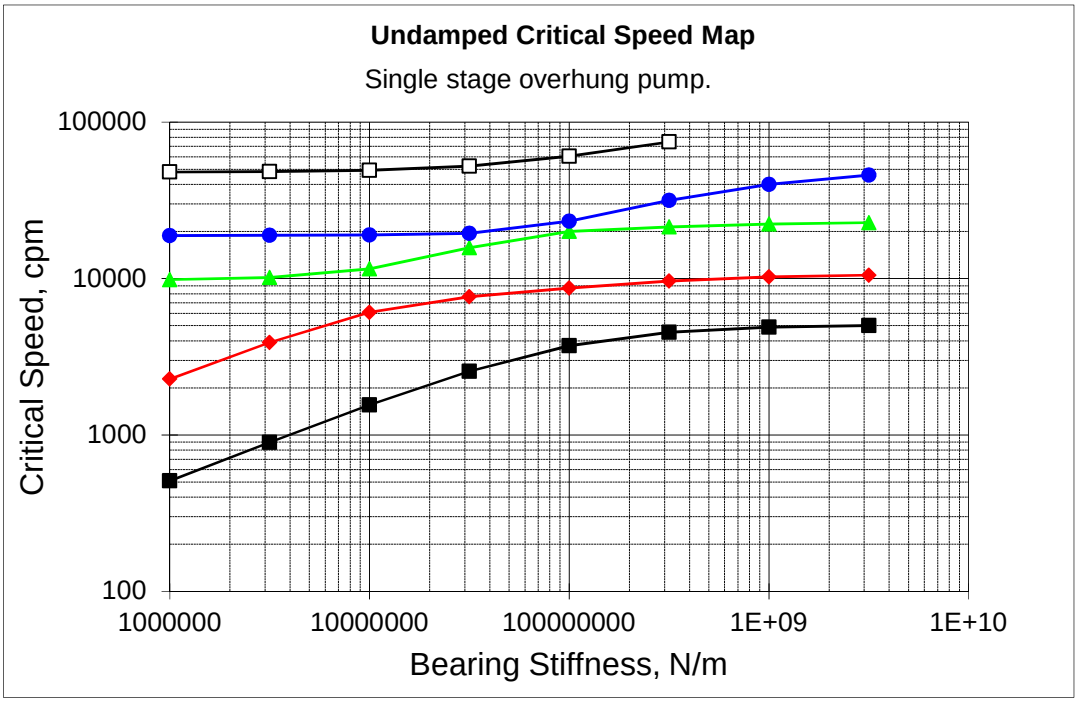

Figure C 2 Undamped critical speed map where bearing stiffness is 1E+09

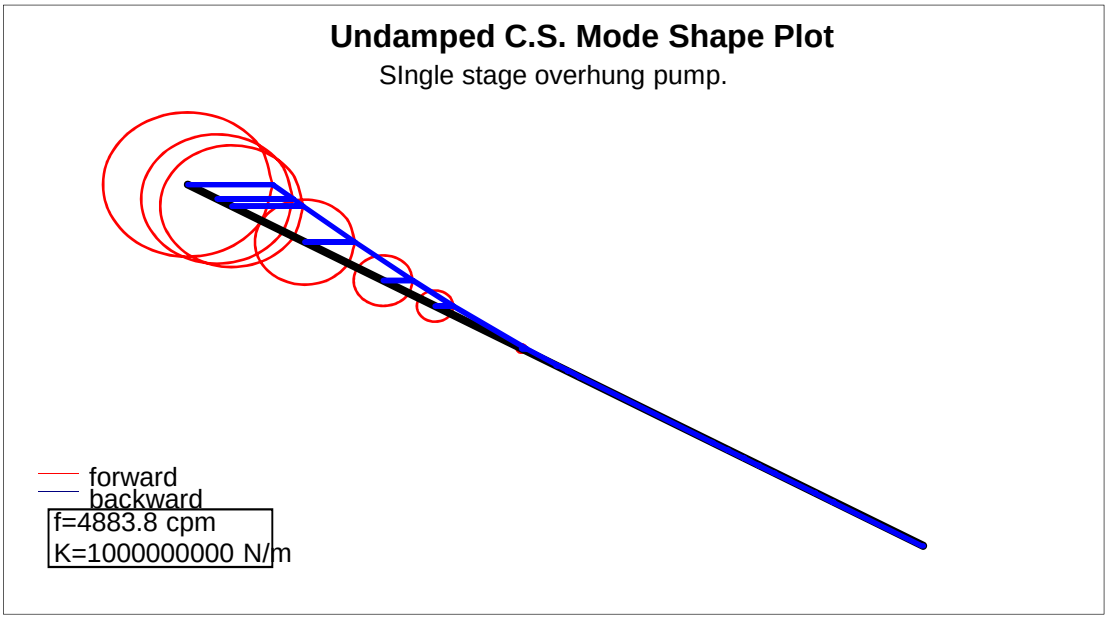

Figure C 3 Undamped mode shape plot

C.2 Damped natural frequency analysis

The damped natural frequency analysis is carried out for “dry” and “wet” operating conditions. Pump rotordynamics as outlined in Chapter 2 produce different results for the two conditions due to the density of the pumped fluid. It is observed from the damped natural frequency map shown in figure C-4, that for the single stage overhung pump is well damped and would not enter a critical speed region within the operating range. This was the expected result for this pump type

a

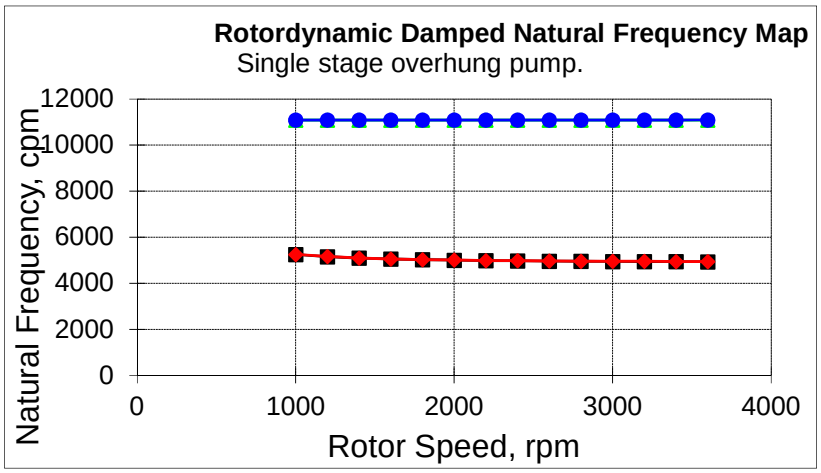

b

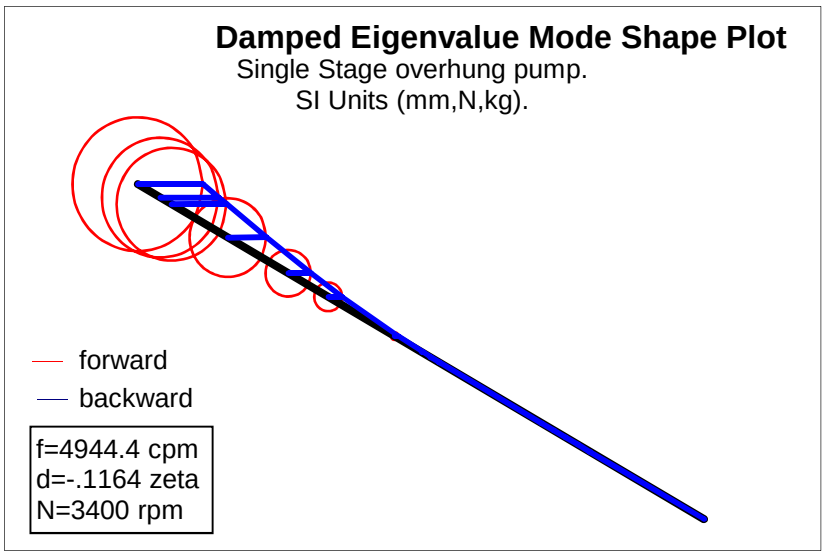

Figure C 4 damped natural frequency map for “wet” conditions b) corresponding mode plot